Exploring the influence of fractures and rock type on seismic velocity in volcanic rocks: A combined laboratory and field study of Tuawera / Cave Rock, Sumner New Zealand

A thesis submitted in partial fulfilment of the requirements for the Degree

of Master of Science in Geology

in the University of Canterbury

by

Callum Cleary

2020

Acknowledgements

I would like to thank my supervisors Ben Kennedy and Marlène Villeneuve for the opportunity to take on this project and for all their guidance and assistance over the past year. The range of scientific techniques you have helped me to understand have kept me interested and made the process highly enjoyable.

Massive thanks to Dave Prior, Hamish Bowman and Aleasha King from Otago University for the aiding in collection of field data in some seismic surveys that were unconventional to say the least. Thanks especially to Dave and Hamish for helping me to begin scratching the surface of geophysics.

Thanks to Mike Finnemore and Richard Mellis from Southern Geophysical for data processing, knowledge and discussions relating to picking and analysing seismic waveforms, along with the opportunity to use the cross hole logging equipment.

Thanks to the technicians at UC; Matt Cockcroft, Cathy Higgins, Sarah Pope and Sacha Baldwin for the help with the rock lab, GPS and other equipment. Special thanks also to Jonathan Davidson and Joe Struthers for help with the 3D modelling of Tuawera / Cave Rock, your knowledge of Agisoft and Leapfrog saved me on many occasions.

Finally, thanks to Jim Cole and my Dad for the final reviewing of my thesis.

Abstract

Seismic investigations have long been used to assess characteristics of rock masses, subsurface structures, magma, and areas of economic interest that are otherwise invisible at the Earth's surface. Here I show that assessing seismic velocity from picking arrival times of primary waves through above ground rock outcrops within such features as caves, tunnels and rock arches provides a simple method to assess the impact of rock masses on the speed of primary seismic waves. This research utilises geophone surveys using eight three – component geophones combined with field geotechnical modelling, 3D modelling and laboratory experiments. The aim is to evaluate the influence of lithology changes and discontinuities per metre on the velocity of primary and shear waves in volcanic rocks at Sumner Beach, Christchurch, New Zealand. Sumner lies on the northern portion of the Lyttleton Volcanic Complex and contains two coastal erosion features – Tuawera / Cave Rock and Cottage Rock. The different lithologies were mapped, using geologic mapping and scanlines to assess fracture characteristics, which were combined with drone created SfM images to create an outcrop scale 3D model. The results show that ultrasonic velocities of core samples in the lab recorded average Vp of 2872 m/s and Vs 1257 m/s for coherent lava; 2221 m/s (Vs) and 1104 m/s (Vs) for breccia; and 2080 m/s (Vp) and 1079 m/s (Vs) for volcanic tuff. This study documents Vp reducing by 38% in coherent lava cores by introducing up to three fractures perpendicular to energy propagation and recording velocities under each condition. When introducing sections of varying proportions of coherent lava, breccia and tuff into a single stack of core, p wave velocities ranged from 2113 m/s for stacks with the largest proportion of coherent lava and 1719 m/s for the stack with the least proportion of coherent lava.

Measured field velocities of primary waves range from 904 m/s – 4200 m/s for Cottage Rock (consisting of fractured coherent lava) and a small ridge on the edge of Cave Rock consisting of coherent lava, breccia and tuff. Cave Rock velocities over 9 – 25 metres are slower through varying proportions of lithologies ranging from 761 m/s – 2805 m/s, however at Cave Rock, coherent lava was found to have 1 - 3 discontinuities/m and breccia 0.2 - 0.3 discontinuities/m. Using a 3D model, cross sections were sliced through different shot paths and respective proportions of tuff, breccia and fractured coherent lava and correlated these

with Vp from each Cave Rock shot. No distinct relationship was found between lithology proportion and Vp, but using information calculated from the laboratory experiments and field mapping, it is likely that fractured coherent lava, with its higher discontinuity per metre value, may reduce the field velocities for the shots with higher proportions of coherent lava. This has implications for engineering geology as it has been shown that in the field, it is difficult to distinguish between breccia and fractured coherent lava, as the discontinuities in coherent lava can reduce the field Vp to be similar to breccia, despite having higher Vp and Vs properties in intact core samples measured in the laboratory.

Contents

List of Figures

Chapter 1: Introduction

Chapter 2: Methods

List of Tables

Chapter 2: Methods

Chapter 3: Results

Chapter 1: Introduction

1.1 Project Background

Seismic techniques can help to recognize different rock types, migrating magma, active faults and other structural features that are otherwise impossible to observe beneath the Earth's surface (Chiarabba et al., 2000; Lengliné et al., 2016). Seismic techniques are thus essential tools to explore for economic deposits (Badley, 1985), mapping of subsurface structures (Bruno & Castiello, 2009) and monitoring changes in the Earth's crust (Tolstoy et al., 2006).

Seismic tests on boreholes are an extremely important aspect of geotechnical engineering (Keys, 1979; McCann et al., 1975). Specifically, in Christchurch seismic tests were used for evaluating and developing a regional 3D seismic velocity model (i.e. Canterbury regions, e.g.; Lee et al. (2013). However, as highlighted by Lesage et al. (2018) there is currently little discussion or research that explores the link between large scale seismic data collected in the field and small scale laboratory data on rock properties. In particular, there is a dearth of data addressing the influence of small scale heterogeneities and discontinuities on the field scale data.

The following chapter reviews some of the techniques and results of previous studies of seismology of volcanic rocks and how seismic wave velocities have been measured.

1.2 Seismology, attenuation and anisotropy

Seismology is the area of science that focusses on the patterns and habits of elastic waves as they travel through the Earth (Stein & Wysession, 2009) and seismic waves can be broken into two main source categories; natural and artificial. Natural seismic waves are generated by either earthquakes or volcanic eruptions and artificial sources are generated by manmade methods, such as a controlled explosion or the hit of a sledge hammer (Stein & Wysession, 2009). Once a source generates a seismic wave, it will radiate from that source until the energy dissipates, a process called attenuation, through scattering, dispersion and internal reflection of the waves within the material. The rate of attenuation depends on the physical

characteristics of the surrounding material and can be calculated using relationship of the frequency of the seismic source to the material the wave has passed through (M. Toksöz et al., 1979; Tonn, 1989).

Seismometers measure seismic energy by recording the arrival and passage of seismic waves before the energy is attenuated and dissipates completely. If the source of the seismic wave time is known along with the time of arrival and distance to the seismometer, seismic velocity can be calculated for the medium the wave has passed through. However, this process becomes complicated rapidly by the separation of seismic waves into separate forms, such as primary (p) and secondary or shear (s) waves (Figure 1.1) (Castagna et al., 1985; Kuster & Toksöz, 1974; Savage, 1999). For some geologic sequences with alternating shale and sandstone layers, the ratio of p and s velocities can be analysed to differentiate between the two lithologies (Castagna et al., 1985; Dankbaar, 1985).

In a p wave, particle vibration is parallel to the shot source or propagation of energy (Figure 1.1) and these primary waves are generally the first to arrive at the receiver. S waves generate particle vibration that is perpendicular to the source of energy and can be broken down into different components such as vertical and horizontal s waves (Brune, 1970; Savage, 1999; Z. Wang, 2001).

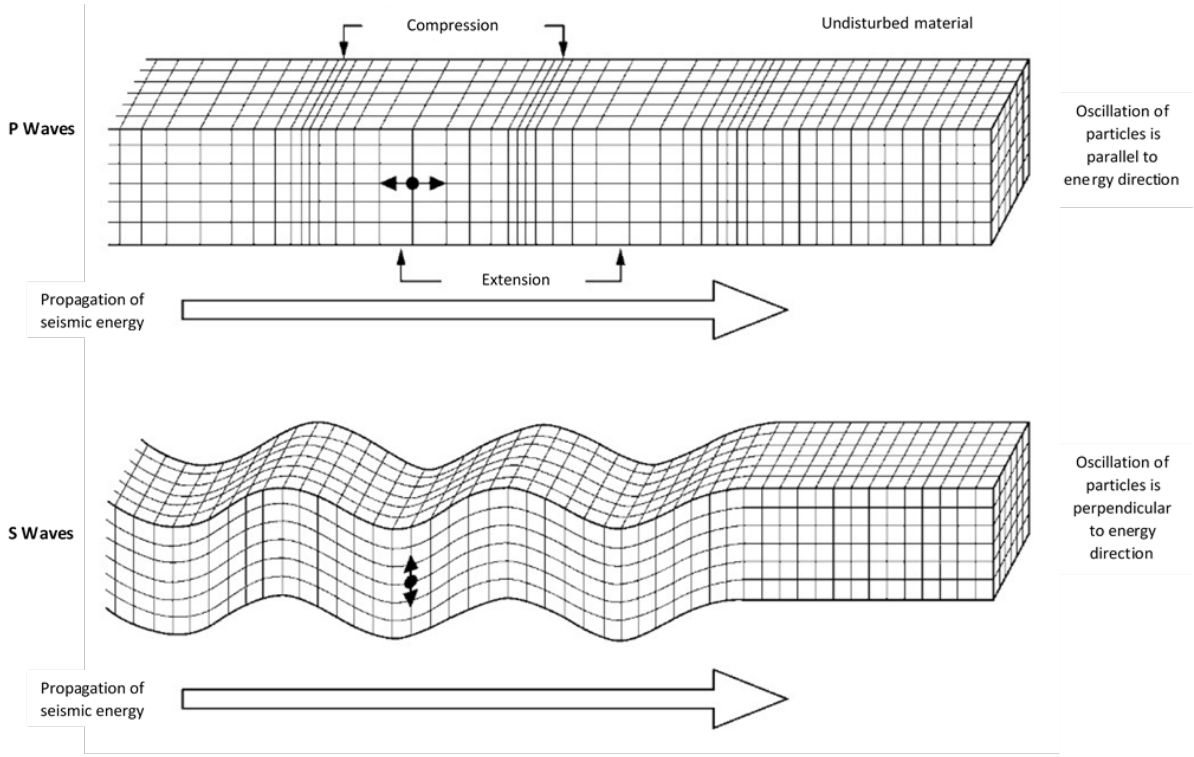

Figure 1.1: Diagram of p and s waves showing particle vibration direction and propagation of seismic energy. Modified from Borr (1982) and Barton (2006).

Anisotropy

When seismic waves have particles vibrating in different directions to the source, i.e. parallel vs perpendicular, the velocities of the different waves can vary, resulting in seismic anisotropy (Savage, 1999). Anisotropy refers to materials having varying properties in multiple directions and seismic anisotropy develops due to numerous rock properties such as crack orientation, lineations and bedding (Helbig, 1984; Schubnel & Guéguen, 2003). Anisotropy is only one characteristic of the overall rock mass but can be a significant factor influencing seismic velocity (Arts et al., 1996). Nur (1971) found that cracks initiating from increases in pressure are effective mechanisms for creating anisotropy in rock, with micro fractures opening causing either the velocity increase or decrease of seismic waves. The findings of Nur (1971) have been further evaluated through various studies including Vilhelm et al. (2010) who characterised p wave anisotropy through circular samples with varying orientations of fractures. Generally, anisotropy affects seismic velocity negatively when internal rock 'fabric' is perpendicular to the particular wave, thus slowing the wave down (Figure 1.2) and anisotropy affects waves less when internal rock fabric is parallel to the propagation of waves

(Castagna et al., 1985; Dankbaar, 1985; Savage, 1999). Anderson and Spetzler (1970) and Anderson et al. (1974) also show that reductions to velocity are greater when flat cracks are present rather than spherical pores.

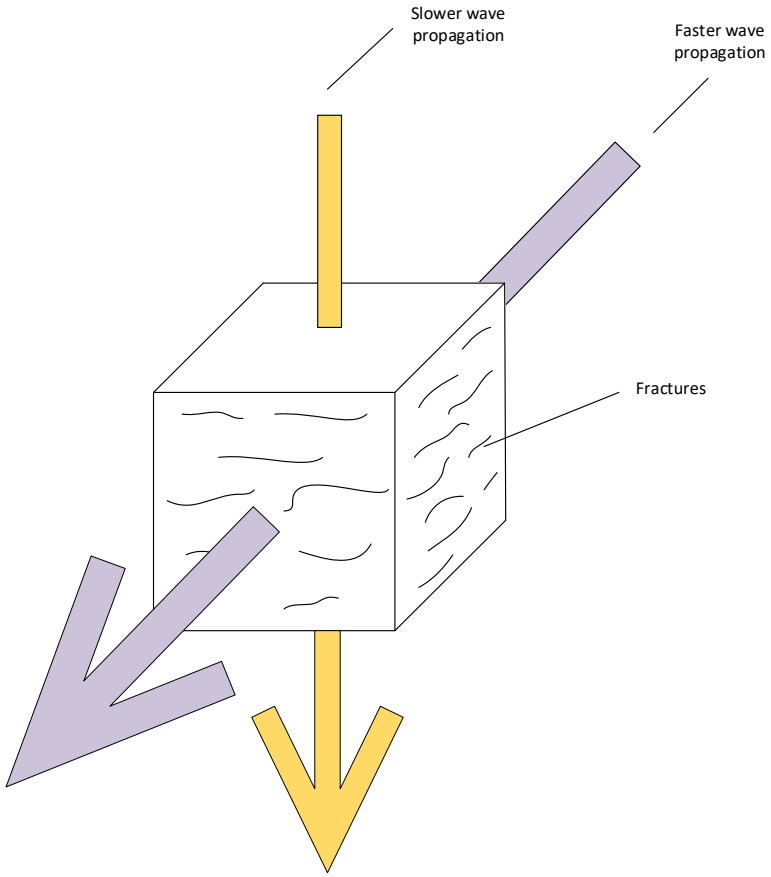

Figure 1.2: Diagram showing wave propagation parallel and perpendicular to internal material fabric. The larger purple arrow is faster through the block as it parallel while the smaller yellow arrow is slower due to the perpendicular angle to the fractures and discontinuities

1.3 Seismic velocities of volcanic rocks in the field

Many seismic studies of rocks in the field have been undertaken to model and map the subsurface structures of volcanoes and freestanding rock masses using the velocity of p and s waves (e.g.; Bruno and Castiello (2009); Lesage et al. (2018); Liberty et al. (2015); Moore et al. (2018)). Field seismic studies of volcanic systems often include survey lines numerous kilometres long that penetrate several kilometres into the earth such as the Bruno and Castiello (2009) study of onshore volcanoes and the Ferrazzini et al. (1991) survey of tremors in Hawaii. Further studies of wells up to 3km deep in the Campi Flegrei volcanic system have

been sampled and established anisotropy and velocity increase of p and s waves with depth in another relatively large scale survey (Zamora et al., 1994). Seismic surveys are also valuable in determining seismic velocity structures of continents such as in the Zhao et al. (1992) survey of North East Japan and the even larger scale study of continent/mantle coupling by Silver (1996). Liberty et al. (2015) show that heterogeneity, such as interbeds of sedimentary rocks in a volcanic sequence, correlate to low seismic velocities in a seismic profile.

On a smaller scale, the resonance study of freestanding rock arches by Moore et al. (2018) using small seismometers placed on rock arches to determine elasticity of the rock mass proved to be an effective passive method to measure seismic properties. Cross hole sonic logging is another seismic technique typically used in concrete pile testing (Li et al., 2005) but has also been shown in larger, rock studies (Hayles et al., 1994; Urosevic et al., 1995). Although these geologic surveys (Hayles et al., 1994; Urosevic et al., 1995) occur over hundreds of metre scales in large well holes, employment of small scale concrete pile equipment may be used to attain high resolution seismic data of rock mass at a small (metre) scale. Cross-hole sonic logging tests used to evaluate the strength and integrity of concrete pile using boreholes (Li et al., 2005) use a source and receiver that are lowered into two water filled holes (e.g. Figure 1.3, a setup used in the cross hole sonic logging experiment on Mt Pleasant, Christchurch). The water acts as a coupler to the material being measured and the transmitter sensor uses piezometric crystals to vibrate at high frequencies (55 or 66 kHz), which when used in concrete gives a high frequency arrival wave, resulting in high accuracy picking of wave arrivals. However, piezometric sources have also been used in sedimentary basin inter-well evaluations to attain high frequency and high resolution data on reservoir properties (Harris, 1988). Piezometric sources, as used by Harris (1988) to measure reservoir characteristics between wells in sedimentary basins provides high frequency source and receiver capabilities, enabling the capture of high resolution data.

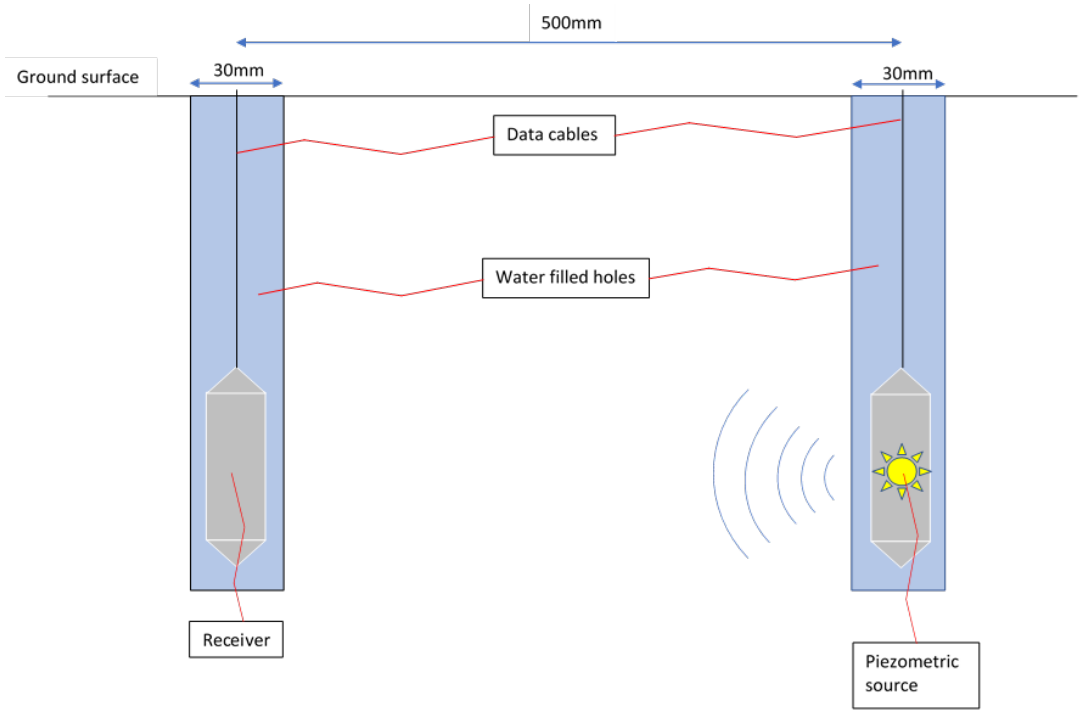

Figure 1.3: Schematic cross section of piezometric source and receiver setup used at Mt Pleasant in basalt basement rock.

Seismic velocity experiments in the field are typically large scale surveys of volcanoes but are becoming smaller and more focussed as seen in the studies of Vilhelm et al. (2010) and Moore et al. (2018). One factor that is important for smaller scale seismic surveys is the evaluation and selection of the source of seismic waves.

Seismic techniques can prove difficult to record and interpret accurate data in volcanic environments due to effects such as attenuation, scattering, wavelength issues and scaling problems (Bruno & Castiello, 2009; Lesage et al., 2018). While some of these studies are reviews of other findings or generic models for specific volcanoes, a recurring problem is the gap between laboratory scale experiments and field measurements and how to accurately model p and s wave velocities given this disconnect.

Seismic sources and geophone coupling

Selection of seismic source can play an important role in the quality of seismic data, especially in shallow surveys as seismic source selection can influence wavelength. Lesage et al. (2018) state that often, seismic waves cannot accurately determine volcanic structures because of wavelengths that are too long. Miller et al. (1986) document 15 seismic sources including

ANFO explosives, Buffalo guns and sledge hammers and show a range of magnitudes and frequencies between the different sources along with stating that choosing the right seismic source may be one of the most important decisions when conducting a seismic investigation. Furthermore, the quality and strength of data can be greatly influenced by belowground conditions at the geophone and source locations (Herbst et al., 1998).

A recent approach to seismic sources for shallow land surveys has been used by GNS Science by dropping bags full of sand and or rock boulders from a helicopter in the Tongariro National Park (Jolly et al., 2014) and on Whakaari / White Island, New Zealand (Jolly et al., 2012). The high velocity impact weights were around 700kg and were concluded to be effective sources of seismic energy in both cases, although depth of survey penetration is not accurate deeper than a few hundred metres.

Schmidt Hammer testing

One way to quickly assess rock properties in the field is to use a Schmidt hammer, a spring loaded mechanism that records rebound or 'R' value for the location where the hammer hits. Schmidt rebound number has been used in a variety of situations for engineering purposes and can also gather a large amount of data in geologic environments quickly. Schmidt rebound has been analysed and associated with seismic velocity, rock strength and how jointed a rock mass is (Çobanoğlu & Çelik, 2008; Dinçer et al., 2004; Kahraman, 2001).

1.4 Seismic velocities of volcanic rocks in the laboratory

The measurement of rock properties in the laboratory is both helpful for understanding internal rock properties and also rock behaviours under certain experimental conditions such as deformation patterns and strength testing (Dinçer et al., 2004). Laboratory experiments are also important for understanding rock properties at a small scale and many methods have been used and adapted from engineering disciplines over the last 50 years (Hoek, 2000). Studying rock properties in the lab is an effective and sometimes non-destructive way of measuring and analysing internal rock properties under ranges of simulated conditions such as strength under confining pressure (destructive) (Arts et al., 1996) and variable fracture content (non-destructive) (Nara et al., 2011). Some of the main influencers on lab seismic velocity have been shown to be hydrothermal alteration and porosity (Schubnel & Guéguen,

2003; Wyering et al., 2014), pressure changes simulating varying confining pressures at depth (Jones & Wang, 1981; M. Toksöz et al., 1979; M. N. Toksöz et al., 1976), fracture roughness (Kahraman, 2002) and fracture density as a proportion of the overall core sample size (H. Wang et al., 2015).

Numerous laboratory experiments of volcanic rocks such as basalt, andesite, trachyte and pyroclastics from Whakaari / White Island NZ, Mt Etna and Campi Flegrei (Fortin et al., 2011; Heap & Kennedy, 2016; Vanorio et al., 2002; Zamora et al., 1994) have analysed rock properties and measured p and s wave velocities.

Previous lab studies on basaltic rocks have found p wave velocities of 5000-6000 m/s (Mavko, 2005), and of 4380-5520 m/s for Hawaiian olivine basalts (Manghnani & Woollard, 1965). Mavko (2005) also defines that increased porosity decreases both p and s wave velocities and increases dispersion and attenuation, which is consistent with other studies (Schubnel & Guéguen, 2003; Wyering et al., 2014). There are also several models and laboratory studies that simulate confining pressures for rocks buried at varying depths (Jones & Wang, 1981; M. N. Toksöz et al., 1976), which evaluate the effect of porosity on seismic velocity. Wyering et al. (2014) show that shallow, hydrothermally altered rock cores with higher porosity have lower ultrasonic p (around 900 m/s less) and s (around 700 m/s less) wave velocities than deeper rock cores from the same hydrothermal zone. Fortin et al. (2011) and Nara et al. (2011) document that increases in pressure (to 190 MPa) result in the closure of microfractures in core samples and an increase in seismic velocity. Schubnel and Guéguen (2003) show that dispersion, or the separation of low and high frequency waves, can increase by 30% depending on microfracture density. From the studies that have been conducted, heterogeneity, porosity, confining pressure and dispersion seem to be the major factors that play a key role in the change in velocity and concentration of seismic waves. However, there are few studies that directly compare seismic velocities between small field scale (10 m to 20 m) and laboratory samples from the same field location and analyse properties and relationships of the wave velocities between the two scales.

1.5 Upscaling of Laboratory data to field scale data

The effects of upscaling must be considered when comparing lab measurements (such as p wave velocity) of core samples of rock to field scale surveys.

Vilhelm et al. (2010) analysed p wave anisotropy and how the distribution of cracks effected seismic velocities in peridotite in samples both in the field and in the lab. Experiments done in the field over four metres showed anisotropy of 25% while laboratory samples showed anisotropy of less than two percent. This study (Vilhelm et al., 2010) begins to show that the number of mappable fractures over different shot lengths is far more significant when measuring p wave velocities in the field than in the laboratory, which is an important factor to consider when upscaling lab data to compare to field measurements. Lesage et al. (2018) compile data from numerous studies on volcanoes, core samples and well logs, showing that p and s waves in volcanic settings vary greatly between samples, and the large variability in Vp (p wave velocity) and Vs (s wave velocity) in volcanic rocks e.g. Hornby (2001).

To make these field scale and laboratory tests relevant to engineering or geological problems, full understanding of any effects that may affect seismic waves must be understood.

1.6 Aims

This study aims to quantify the role of lithological heterogeneity (changes in rock type) and discontinuities (fractures) when comparing the velocity of primary (p) and secondary (s) seismic waves in laboratory experiments to small, field scale measurements of p and s wave velocities. As a part of this study, a 3D geotechnical model will be created to create sliced cross sections through seismic shot paths in the field, constraining the proportions of lithology in each shot and the correlating p wave velocity.

This research aims to close the gap between seismic velocities from laboratory experiments to the larger field scale (outcrop or borehole data). This variation is then used to discuss upscaling p and s wave measurements from laboratory experiments to field scale seismic surveys of outcrops. This research framework of seismic velocity comparisons of p waves between laboratory experiments and field scale measurements would be transferrable to study well log data from boreholes in the surrounding Banks Peninsula area, such as the

Takamatua Borehole, Akaroa, and boreholes nearby Sumner such as Clifton Hill and Richmond Hill. This research also fills a research gap to gather seismic velocity data in volcanic rocks at a scale that lies between laboratory core sample size and kilometre, volcano scale.

Aim 1: Evaluate the influence of lithology and microfractures on p and s wave velocity in the lab

Aim 2: Develop methodology for gathering seismic p wave arrivals, geological and geotechnical data in 3D volcanic outcrops and create a 3D model of Tuawera / Cave Rock to generate cross sections.

Aim 3: Evaluate the influence of lithology and fractures on p wave velocity on outcrop scale.

Aim 4: Establish volcanological setting and interpretation for Tuawera / Cave Rock, Sumner

1.7 Study site and local geology

The location for this combined geological, geotechnical and geophysical study is Sumner, New Zealand (Figure 1.4). Sumner is situated in the Canterbury Region of the South Island of New Zealand, 10 km South East of Christchurch City Central Business District. At Sumner there is a beach with a number of coastal erosion exposures which lie on the northern portion of the Lyttelton Volcanic Complex, Banks Peninsula (Ring & Hampton, 2012). This site provides a well constrained site of variable volcanic material within a confined area (2500m^2) and contains predominantly basaltic volcanic rocks such as basalt, trachyte and pyroclastic deposits (Sewell, 1988). The main coastal exposure feature on Sumner Beach is Tuawera / Cave Rock, a large rock outcrop 15 m tall and 60 m long with a tunnel, Cave Rock cave, running approximately north-south through the underside of the outcrop (Figure 1.5). Cottage Rock, another volcanic rock outcrop is 20 metres away from Cave Rock and is a freestanding rock outcrop mostly composed of coherent lava and a two small blobs of breccia. These two coastal exposures and the open-ended cave allows the three-dimensional mapping and measuring of lithological variabilities alongside numerous discontinuities, which can be recorded with scanlines (Chaminé et al., 2015).

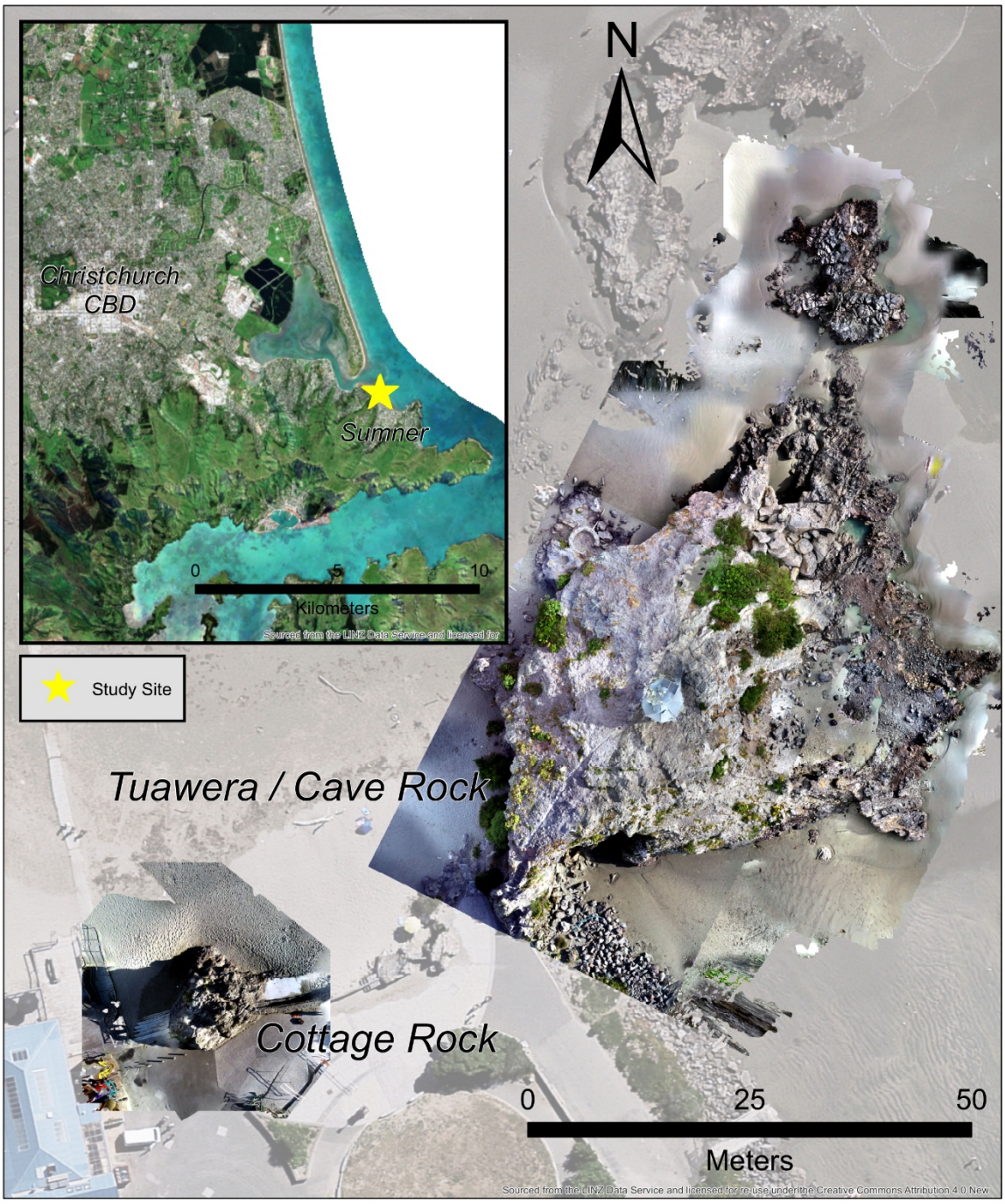

Figure 1.4: Location map of Tuawera / Cave Rock and Cottage Rock at Sumner Beach, New Zealand. A 1 m high man-made stone wall with blobs of rock outcropping join Cottage Rock to Cave Rock.

Tuawera / Cave Rock is a location where this study can be carried out as Cave Rock cave, effectively a tunnel, runs approximately north-south underneath the rock outcrop. This tunnel allows the placement of the seismic source along varying locations inside the cave,

enabling the path of the waves to pass through varying thicknesses and lithology in the rock above (Figure 1.5).

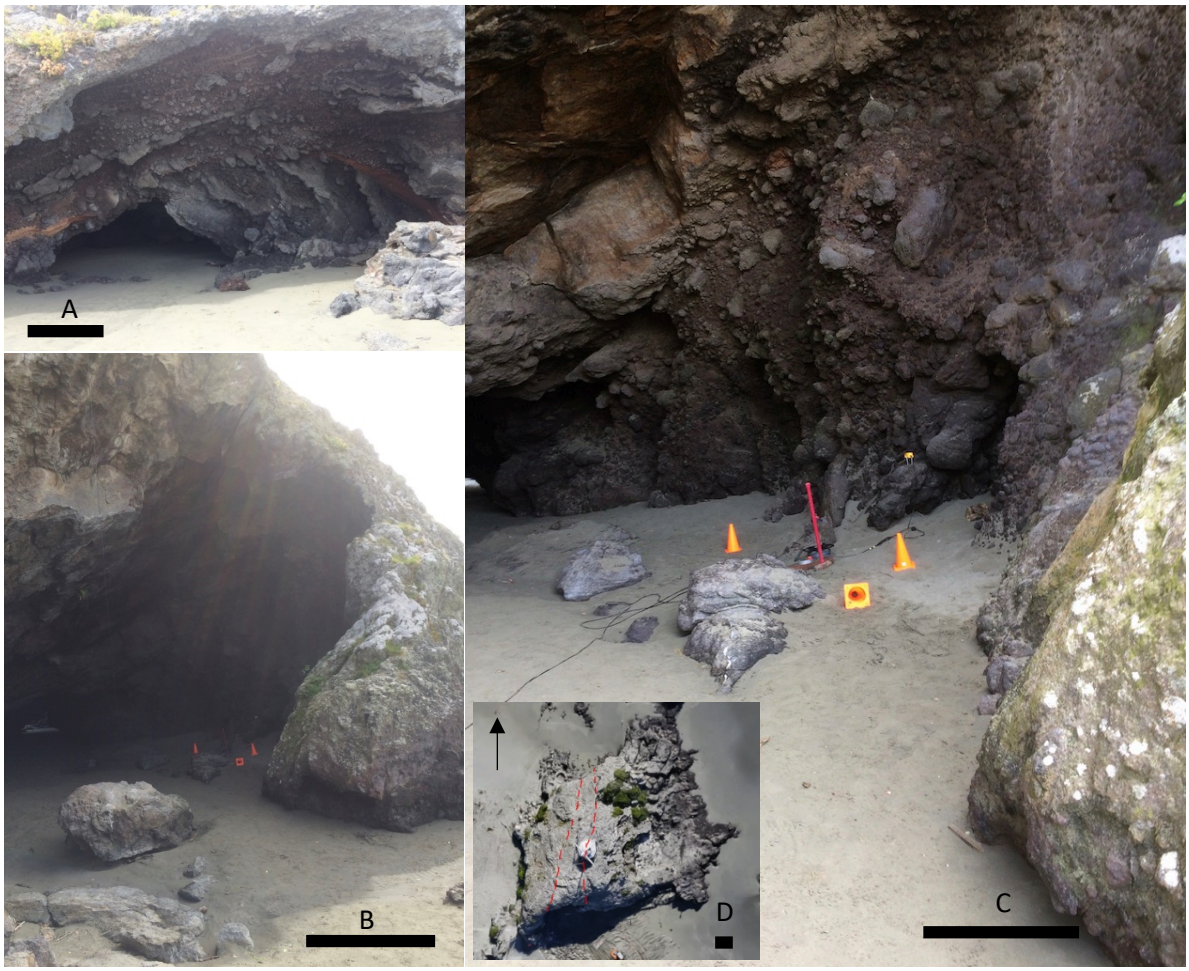

Figure 1.5: A. North entrance to cave, variable lithology visible with orange tuff layer noted in middle of outcrop. B. South entrance. C. Inside south entrance, variable lithology visible. D. Aerial view of Cave Rock, cave tunnel outlined in red. Black bars underneath letters indicate a length of 2 m relative to each image.

The velocity results from Cave Rock are expected to vary between individual layers and also show variation through different portions of the cave due to heterogeneity in lithology i.e. changes from lava to ash (Liberty et al., 2015) and the presence of fractures (Schubnel & Guéguen, 2003), and one of the research objectives is to quantify this. Accurately mapping the variations in lithology and the discontinuities present at Cave Rock allow geological data to be paired with seismic p and s wave travel times through different parts of the cave. By coupling this information together, the effect of heterogeneity and discontinuities on seismic

velocity can be picked apart and analysed to determine the role these variations play in affecting seismic travel time.

Local Geology

Cave Rock and Cottage Rock lie on the Northern portion of the Lyttelton Volcanic Complex, one of the two main volcanoes of Banks Peninsula, which erupted from 12.4– 9.7 Ma (Sewell, 1988) producing volcanic deposits 2 – 3 km thick (Ring & Hampton, 2012) of mostly basalt, trachyte, breccia and pyroclastic deposits such as ash and tuff (Sewell, 1988). Outcrops at Cave Rock and Cottage Rock show three main geological units, which have been split into 5 geotechnical units similarly to del Potro and Hürlimann (2008) and Mordensky, Villeneuve, Kennedy, et al. (2018) consisting of volcanic breccia, low, medium and highly fractured coherent lava and volcanic tuff. The orangey red tuff layer can also be seen elsewhere in the Port Hills and locally in the coastal cliff erosion exposures immediately to the South of Sumner Beach.

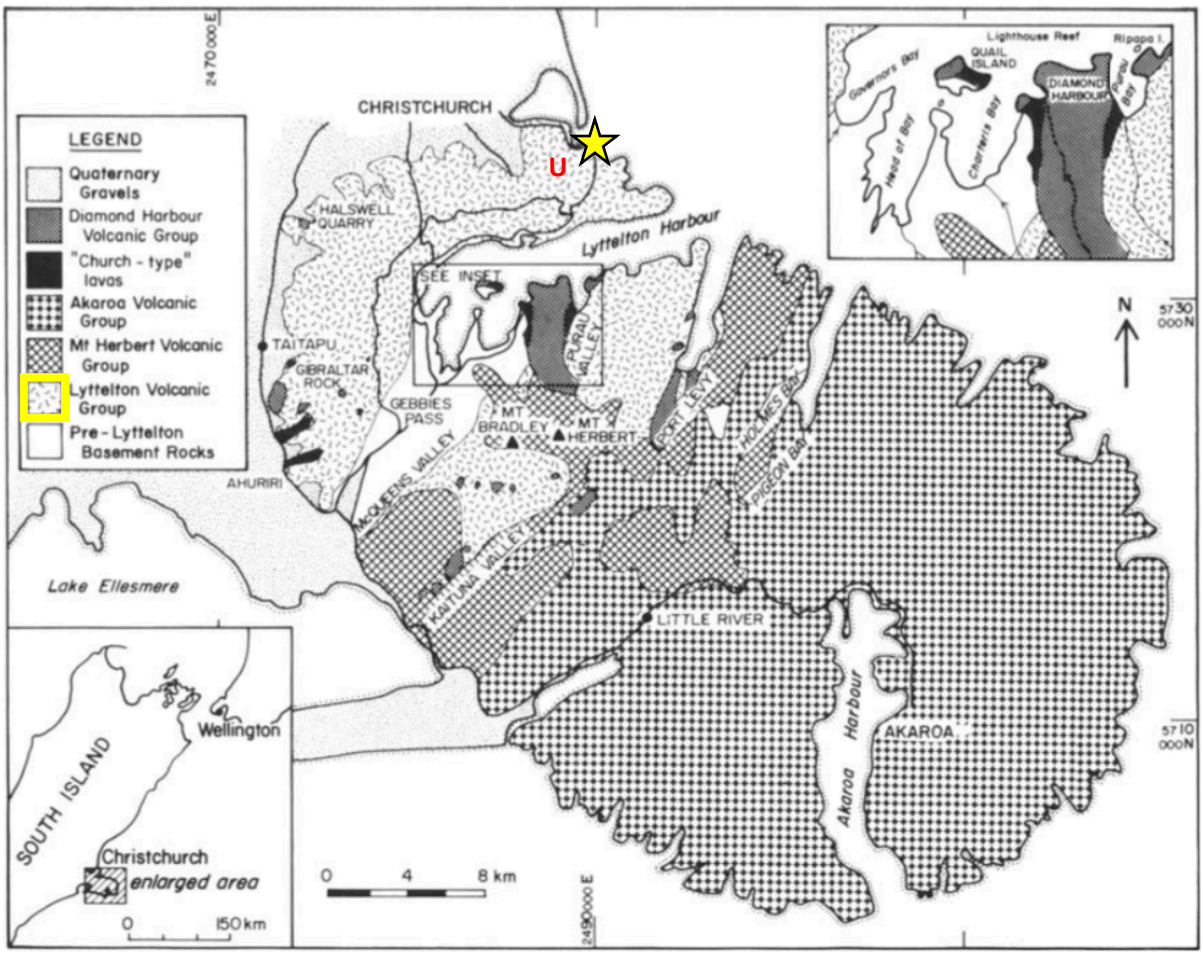

Figure 1.6: Geologic map of Banks Peninsula showing main volcanic units adapted from Sewell (1988). Cave Rock location is shown with a yellow star. The red U is the location from cross hole sonic logging experiment on Mt Pleasant.

1.8 Basaltic lava flow morphology

As the rock types present at Sumner Beach are primarily basaltic volcanic rocks, basaltic lava flow controls and morphology have been examined to aid in developing a lava flow history of Sumner Beach, primarily Cave Rock. The findings of Hampton and Cole (2009) show that by projecting dyke, ridge and valley orientations, 15 volcanic centres can be deduced for the Lyttelton volcanic complex. Sumner Beach lies in the overlapping zone between eruptive centres 9 and 10, on the north eastern extent of the complex. The nature of these overlapping volcanic landforms (Hampton & Cole, 2009) is likely to produce complex overlapping lavas and pyroclastic deposits, with multiple phases of deposition and erosional processes proximal and distal to the eruptive centres.

Features observed are likely to include radial valleys originating from the eruptive centres, lava flows and tuff layers interbedding with varying dip angles and thicknesses, planezes (flat dip slope ridge surfaces) (Cotton, 1944). As Cave Rock is an island of rock on the beach, field observations are also made in the coastal cliff exposures nearby at the foot of the eruptive flanks of the Lyttelton Volcanic Complex to aid in interpreting the volcanic setting of Cave Rock.

1.9 Māori significance

Tuawera / Cave Rock is one of many natural sites in New Zealand that bears Māori significance and must be treated with due respect. Cave Rock, or Tuawera, is said to be the remains of a great whale that was stranded by a tribe as a means to eliminate another tribe (Christchurch City Libraries, 2019). Prior to the start of the project, Rapaki tribe was contacted for permission to conduct research and agreed that no direct damage would occur to the coastal erosion outcrops present on Sumner Beach.

Chapter 2: Methods

This chapter outlines the laboratory, mapping and geophysical methods for the combined lab and field study of p wave velocities in volcanic tuff, breccia and coherent lava with variable fracture densities at Cave Rock, Sumner, New Zealand.

2.1 Laboratory experiments

The laboratory experiments carried out as a part of this project are used to evaluate the influence of fractures and lithology on primarily p wave velocity but will also touch briefly on relationships between fractures and s wave velocity.

To measure ultrasonic velocities of the rocks present at Sumner Beach, cores were drilled from respective samples of the three main geotechnical units collected from the ground on Cave Rock; coherent lava, breccia and tuff. Due to Cave Rock being culturally significant to Māori, samples were not hit or broken off the outcrop but collected from parts of the outcrop that were already broken off after consulting with Andrew Scott of Ngāi Tahu. Cores were drilled using a drill press at the University of Canterbury, then cut and ground to be cylinders with parallel ends. Cores were then dried at 65^{o}C for at least 48 hours then removed for 10 minutes to cool before laboratory ultrasonic tests were conducted. Sample geometries were aimed to be at least 2.5 times length to diameter however, a minimum of two times length to diameter was accepted when there was no alternative. Standard core sample dimensions ranged from 130.46 mm to 83.26 mm length and 40 mm to 40.49 mm for diameter.

To measure p and s wave velocities, cores were smeared on each end with ultrasonic gel, placed in a CMT rig with CGS CATS collecting data under load of 1000 N with piezometric crystals producing wave frequencies of 900 kHz. This set up was used for measuring intact core sample velocities with various lithologies and increasing core break number experiments under conditions as recommended by the ISRM Standard (Ulusay, 2014). Picking of velocities was done manually on CGTS CATS software by using first significant change of energy for p wave arrival and bottom of first trough for s wave arrival. Wave forms were stacked at least 10 times to obtain a clear wave signal to give the clearest and most accurate pick, which were done five times resulting in a manual pick error of 100 m/s.

Porosity measurements were conducted using a pycnometer at the University of Canterbury, where porosity was obtained by measuring the volume of cores then subtracting the volume of nitrogen gas when the pycnometer chamber was full after the sample had equilibrated. Gas pycnometers provide a quick, non-destructive method for measuring intact rock properties at a high precision of around 0.003 – 0.004 units (variability calculated from repetitive samples e.g.; McIntyre et al. (1965)).

The influence of fractures on p and s wave velocity

To analyse the effect of fractures on p and s wave velocities, intact cores of coherent lava were incrementally cut up to four times horizontally (Figure 2.1a) and one time vertically (Figure 2.1b) to simulate fractures or discontinuities in the field. Samples with vertical cut were held together with a piece of masking tape wrapped around the centre of the core. After each cut the cores were dried then placed back together as a stack and p and s wave velocities were measured in the same manner as the uncut cores. Similar studies of discontinuities and p wave relationships have been analysed in the lab on sample of coal using cores with variable fracture densities under ultrasonic conditions (H. Wang et al., 2015).

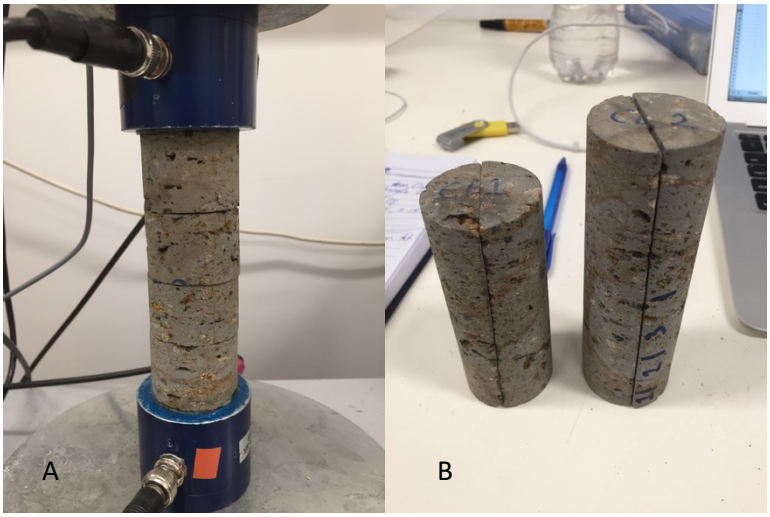

Figure 2.1: Close up images of sample with three horizontal cuts (A) and two samples with one vertical cut (B) experiments for simulating fractures in the lab. Cores were too thin for more than one vertical cut. Note that coherent lava samples have numerous semi spheroidal vesicles throughout.

The influence of lithology on p wave velocity

To evaluate the influence of changes in lithology on p wave velocity a makeshift 'lithology stack' was formed using varying thicknesses of breccia and coherent lava with a consistent slice of tuff in the middle (Figure 2.2). This experiment was designed to serve as a model for variations in lithology and presence of fractures/bedding discontinuities in the field and to try to simulate the approximate ratios of coherent lava to breccia present in the field at Cave Rock. For this experiment stack height was kept as close to 2.5 times the width as possible. Stacks consisted of alternating lava, breccia and tuff with the proportions of breccia and coherent lava changing in each test. Overall length of the stack ranged from 103.04 mm to 118.27 mm (Table 2.1) and loading stress was 1000 N as in all lab tests. Samples were coded with respect to amounts of coherent lava and breccia as a ratio as tuff thickness stayed uniform, for example BL 8-1 had 8 cm of breccia, 1 cm of lava and 1 cm of tuff.

Table 2.1: Table of sample dimensions for ultrasonic lithology stack experiment. Percentage of breccia decreases through tests while percentage of coherent lava increases.

Test No.	% Lava	% Breccia	% Tuff	Height (mm)	Mass (g)	Diameter (mm)	Volume (mm3)	Density (g/mm3)
BL 8-1	10.10	78.31	11.59	106.39	287.18	40.28	135571.88	0.00212
BL 7-2	19.68	68.32	12.00	103.04	282.64	40.35	131759.76	0.00215
BL 6-3	30.66	57.87	11.47	107.67	302.08	40.24	136930.61	0.00221
BL-5-4	35.93	44.33	19.74	118.27	312.69	40.37	151384.70	0.00207

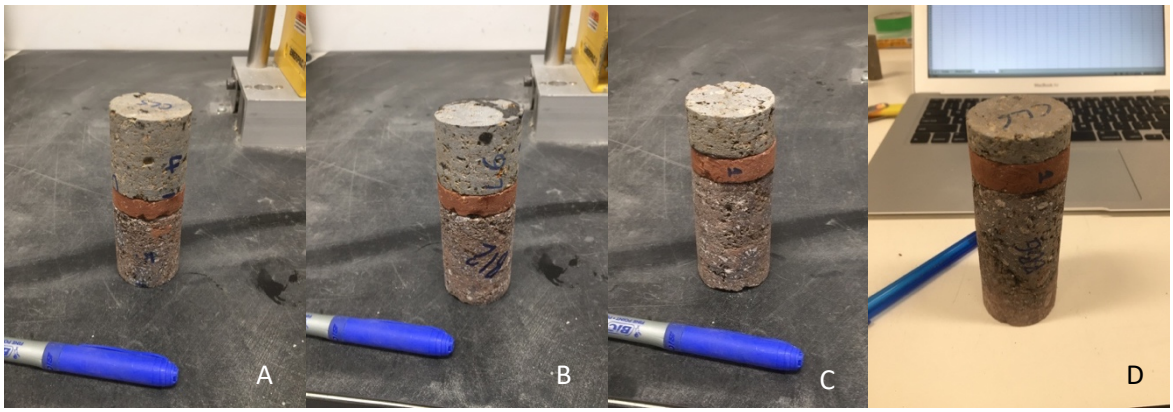

Figure 2.2: Images of the varying lithology experiment conducted showing progressively decreasing amounts of coherent lava and progressively increasing amounts of breccia from A - D. Stack height was kept as close to 2.5x width as possible. From left to right samples are BL 5-4, BL 6-3, BL 7-2, BL 8-1.

2.2 Mapping

Lithologic and structural mapping was conducted at Cave Rock to gather data which would help evaluate relationships between lithology, discontinuities and seismic wave arrival times.

Scanlines

Scanlines were used to gather unbiased structural data by laying out a tape measure along a batter surface or flat wall section of outcrop and recording each discontinuity along a chainage length. Geologic mapping was conducted with a map board, mylar and compass approach to gather information and data on unit boundaries. To quantify the discontinuities present at Cottage Rock, two scanlines were undertaken along the orientation of the two geophone lines. Data was collected following methods of other volcanic geotechnical studies (e.g. stratocone crater walls and volcanic ridges (Moon et al., 2005; Mordensky, Villeneuve, Farquharson, et al., 2018) and included dip and dip direction of discontinuity, Schmidt rebound, trace length, rock type, aperture, type of discontinuity, infilling, weathering and alteration using a joint roughness gauge, ruler, schmidt hammer and compass (Figure 2.3). Whilst scanlines are primarily used on quarry batter slopes, equivalent uniform flat surfaces that exceed several metres are not common in volcanic rock outcrops at Sumner Beach, so the tape measure line was pulled as tight and close to the undulating and rough rock surfaces as possible along the two geophone lines (Figure 2.4). I classified discontinuities as either joints, fractures or bedding surfaces, with fractures being a mappable crack up to 1 m long, while joints occurred in sets of two or more that were traceable for more than one metre and typically were wider in aperture than fractures.

Figure 2.3: Equipment used for scanlines. Clockwise from top left; joint roughness gauge, ruler, tape measure, Schmidt hammer and geologic compass.

Figure 2.4: Tape measure lines for the two scanlines Sc2 (A) and Sc3n (B) at Cottage Rock. Image B is on the right hand side of A, note small stone wall in bottom right corner of both photos. B is taken looking south east and A, south west.

Scanlines were conducted at Cave Rock in the same manner as Cottage Rock, using the same equipment and methods to obtain non-biased quantitative data on the fracture characteristics and densities of discontinuities in the coherent lava and breccia present. Scanlines at Cave Rock proved impossible along direct shot points as they went up through the roof of the cave but it was possible to get data for individual units along the walls of the

tunnel and outcrop for breccia and the central coherent lava unit. Two scanlines were conducted in coherent lava, one in breccia and one along a section of outcrop consisting of both breccia and coherent lava (Figure 2.5). These scanlines would help to evaluate how discontinuities vary between the two main rock types present at Cave Rock.

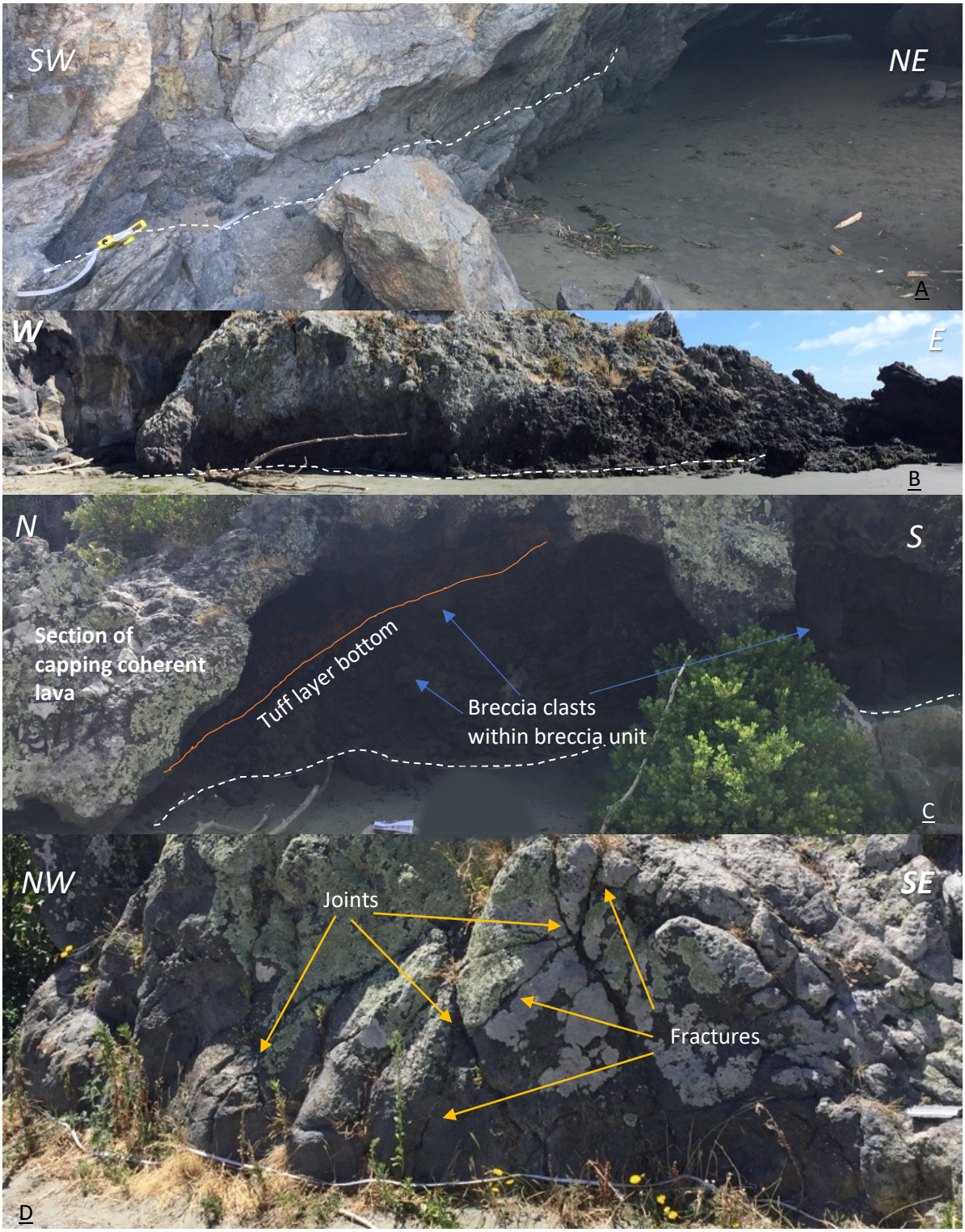

Figure 2.5: Scanlines conducted at Cave Rock in central lava (A), breccia on outside edge of outcrop (B), combined breccia and coherent lava scanline (C) and the section of coherent lava at the south west tip of Cave Rock (D). White dotted line follows tape measure line when difficult to see and labels in top left corners refer to scanline orientations.

Mapping

The geologic mapping of Cave Rock was first done to establish geologic boundary constraints and then to create a 3D geologic model of Cave Rock. Geologic mapping was conducted using the traditional mylar and aerial photo on map board with a geologic compass to measure dip and dip direction of layers present. Cave Rock is an exposed volcanic coastal erosion feature, and has many nooks and small overhangs that reveal important outcrop locations that are necessary for constraining the unit location and thickness (commonly the orangey red tuff layer was often obscured by a small lip of coherent lava or breccia in many locations). These obscure sections of outcrop (invisible from aerial view) become an important part of the Leapfrog geotechnical model later in the project. The technique used to get around this was to take screengrabs from the Structure from Motion Photogrammetry image generated of Cave Rock and supplement the geologic mylar map with additional mapping onto these images from sides of the outcrop that are not visible from above (Figure 2.6). Strike and dip data was collected as often as possible for input into Leapfrog Geothermal so the units could be constrained as much as possible. Mapping, SfM creation and leapfrog modelling was thus an iterative process.

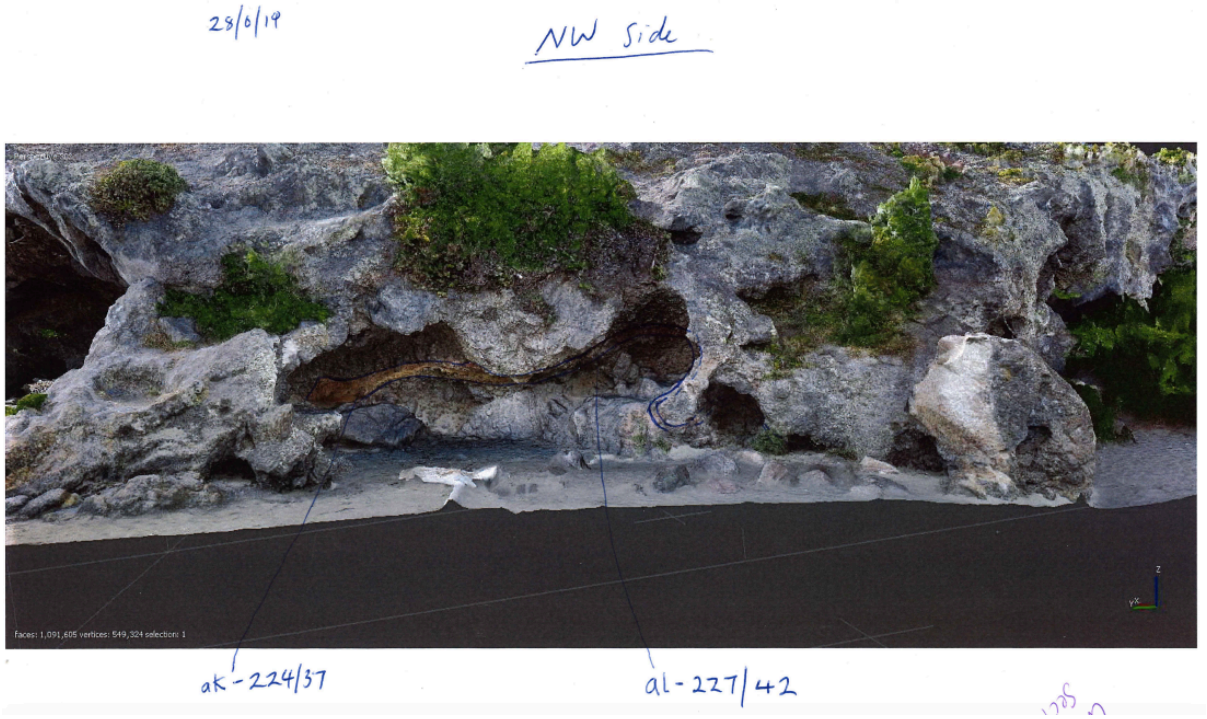

Figure 2.6: Example of Agisoft screengrab showing the orangey - red tuff layer obscured by an overhang. Coded strike and dip symbols are locations where data was collected and exposure is mapped in pen. Note colour is not true, but each pixel has been assigned an average colour based on the overlapping photos associated with creating the model

The geologic map created over several days of field work splits the rock units present into five geotechnical units; breccia, tuff and coherent lava with high, medium and low fracture density. On the south – east side of the outcrop there is lots of lichen and the orangey – red tuff layer was obscured, however from outcrops on both sides of the lichen section it is likely the layer either pinches out or continues but is obscured. Once the geologic map was completed, unit boundaries and structural information were inputted into the 3D model of Cave Rock.

Constructing a 3D leapfrog geologic model

To analyse the proportion of each geotechnical unit present in each seismic ray path, a three dimensional model was created using geological and geotechnical data collected from Cave Rock. As Cave Rock is effectively an island of rock with a tunnel running through, geotechnical units were able to be well constrained on both the top and the inside cave walls of the outcrop

which left leapfrog, a 3D geological modelling programme, to predict the structure of the units within the rockmass.

The first step in creating a 3D geologic model of Cave Rock / Tuawera was to create a 3D model using structure from motion photogrammetry (SfM). This method involves taking a multitude of photos of an object (Figure 2.7) with around two thirds overlap (Westoby et al., 2012) and loading them in to a photogrammetry software which compares pixels of similar constitution and overlaps them, matching images similar to a 3D panorama. Similar to previous studies (e.g. rhyolite intrusions in Iceland (Saubin et al., 2019)), Agisoft Photoscan (Metashape) was used for 3D modelling where around 4000 photos from a hand held camera and drone both around Cave Rock and inside Cave Rock Cave were captured. These photos were geo-located with a GPS to an accuracy of 10 cm and referenced in the software that then created a 3D model based entirely of 2D photos (Figure 2.8).

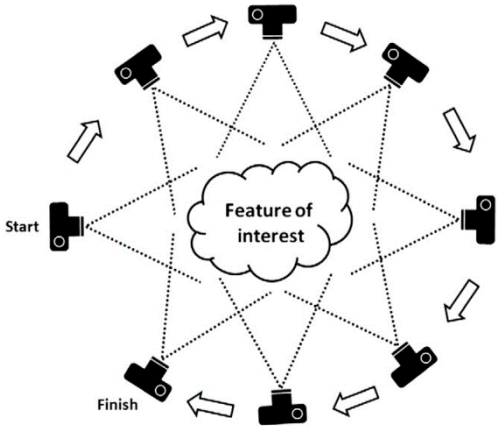

Figure 2.7: Overview of the SFM photogrammetry technique involving multiple photos taken of a single object from Westoby et al. (2012).

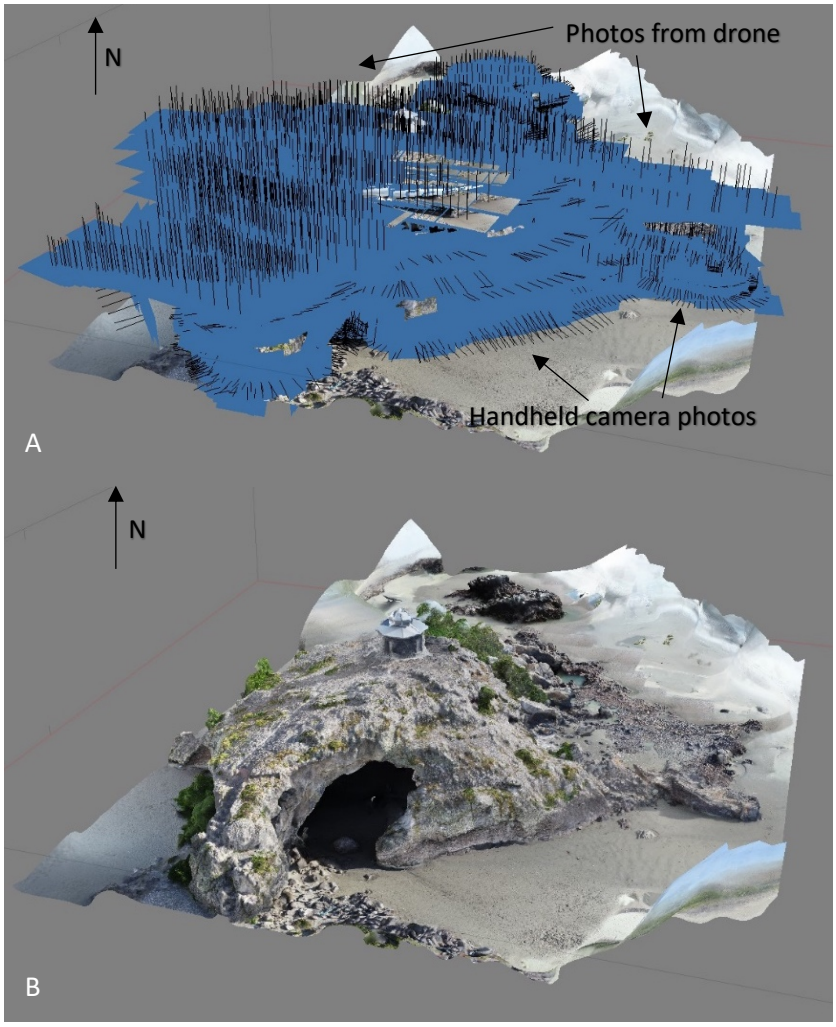

Figure 2.8: Comparison of models showing model with photos used for SfM modelling (A) and without (B). In A, each black line represents a photo taken which is attached to a blue polygon but due to the density of photos the individual polygons are mostly indistinguishable.

Once the 3D models of Cave Rock and Cottage Rock were created in Agisoft, turning these into geotechnical models was the next step of the process using geotechnical modelling in Leapfrog Geothermal, developed by Seequent. The process involved inputting features from the Agisoft model and then adding geologic and geotechnical data to the model. The process is outlined in Figure 2.9.

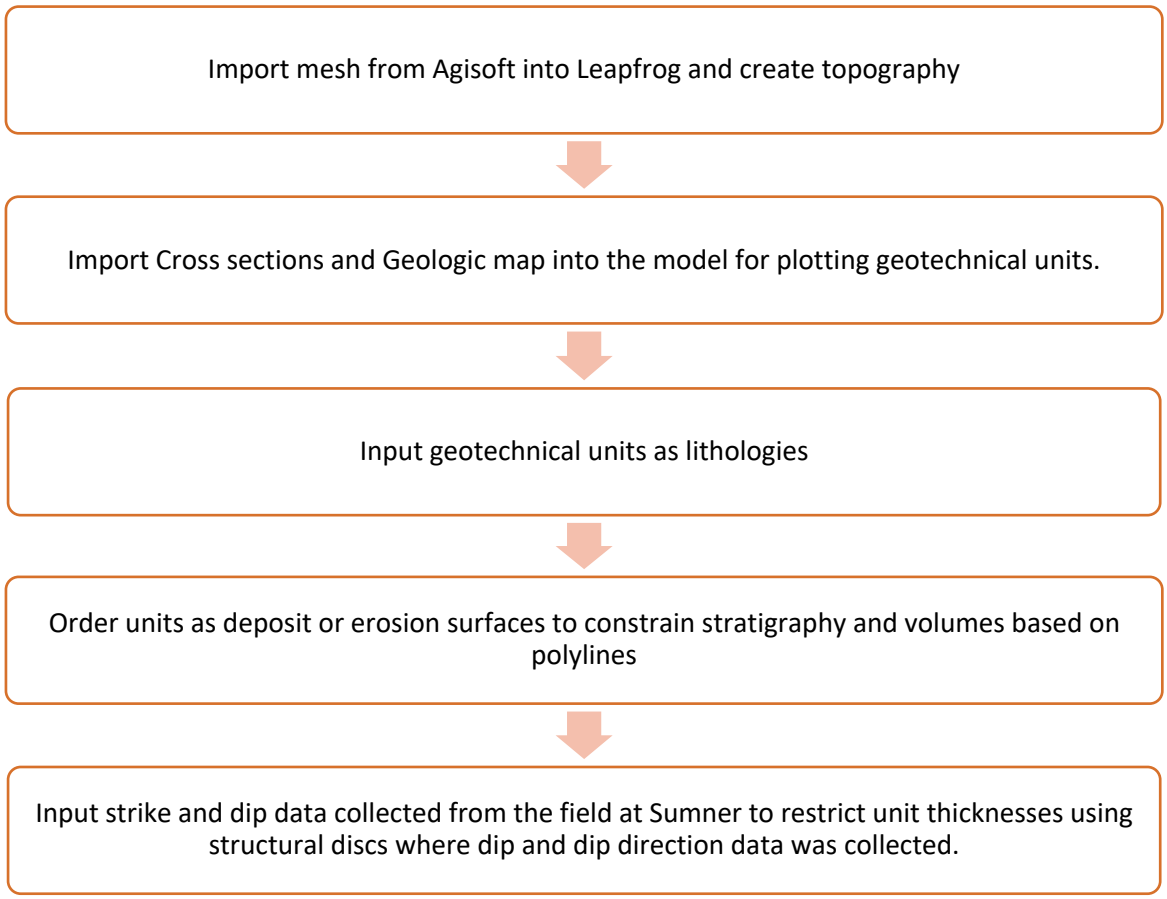

Figure 2.9: Flow chart of Leapfrog Geothermal processes taken to model geotechnical units at Cave Rock

The resulting model uses the inputs from fieldwork and structural data both in and on the cave and predicts the behaviour of these layers within the rockmass, with manual adjustments of thickness or orientation if a boundary does not obey geologically reasonable scenarios. To calculate the proportion of different lithologies in each shot path, vertical slices were taken between each shot to geophone and the cross sections were then measured using a ruler to gather percentages of tuff, breccia and coherent lava present (Figure 2.10). In the geologic model green represents breccia (split into upper and lower for modelling purposes), purples represent lava and orange is the tuff layer. Summary tables of p wave arrival velocities can be found in Online Appendix 1.

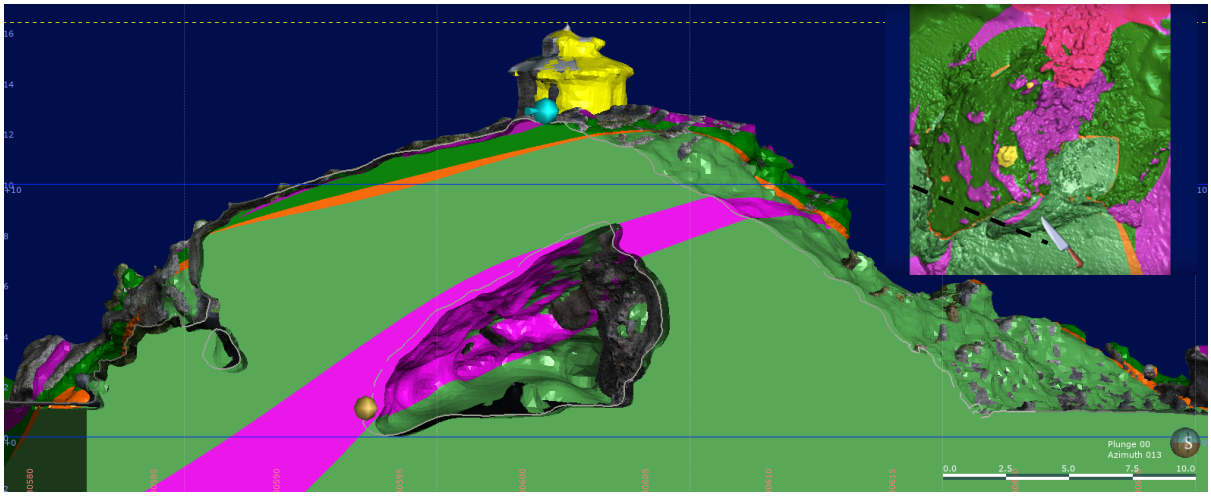

Figure 2.10: Example cross section showing shot R (yellow orb) to geophone 2 (blue orb). The edge of the tunnel (shown in the light grey line) varies slightly to the edge of the coloured model due to different 3D models created from the SfM software. Inset shows orientation of slice from aerial perspective.

Volcanic setting, history and interpretation of Cave Rock

The Lyttelton Volcanic complex consists of many eruptive centres that formed many phases of overlapping basaltic and trachytic lavas and pyroclastics up to 1km thick (Hampton & Cole, 2009; Ring & Hampton, 2012; Sewell, 1988). These overlapping sequences have been formed, weathered and eroded into many forms and features that have been previously categorised into constructional, hypabyssal and erosional features (Hampton & Cole, 2009).

This section uses past studies, observations and measurements taken in the field at Cave Rock to interpret the volcanic history and structure of the coastal exposures present at Sumner Beach. Structural data, geologic models, literature and observations from cliff faces nearby to Cave Rock will assist in the reconstruction of the area.

2.3 Geophysical surveys

The first survey was carried out on the South East Ridge of the main Cave Rock outcrop (Figure 1.4), the second survey occurred on Cottage Rock, to the south west of the main Cave Rock outcrop and the third and largest survey took place on Cave Rock itself. The South East Ridge and Cottage Rock tests were initially used as equipment testing locations, but aspects of the

data collected at the two sites is beneficial to the project aims so results will be discussed regardless.

Along with the geophone survey, another, smaller, ultrasonic experiment in basalt bedrock on Mt Pleasant (Figure 1.6) was conducted to compare coherent lava velocities from the coastline to the hills surrounding the area.

Geophysical equipment

To measure seismic velocity on the field scale at Sumner Beach, NZ, a kit of geophones from Otago University was used. This kit consisted of a trigger, eight three-component (3C) geophone seismic receivers, an Octobox, a Geometrics geode box and a field laptop (Figure 2.11). Once the geophones had recorded seismic information, each of the eight output cables transfers the data to the 'octobox' which collates all the 24 different seismic sensors (three per each of the eight geophones) into one output cable. The octobox then feeds into the Geometrics geode which converts the geophone information to digital format to be logged on the field laptop.

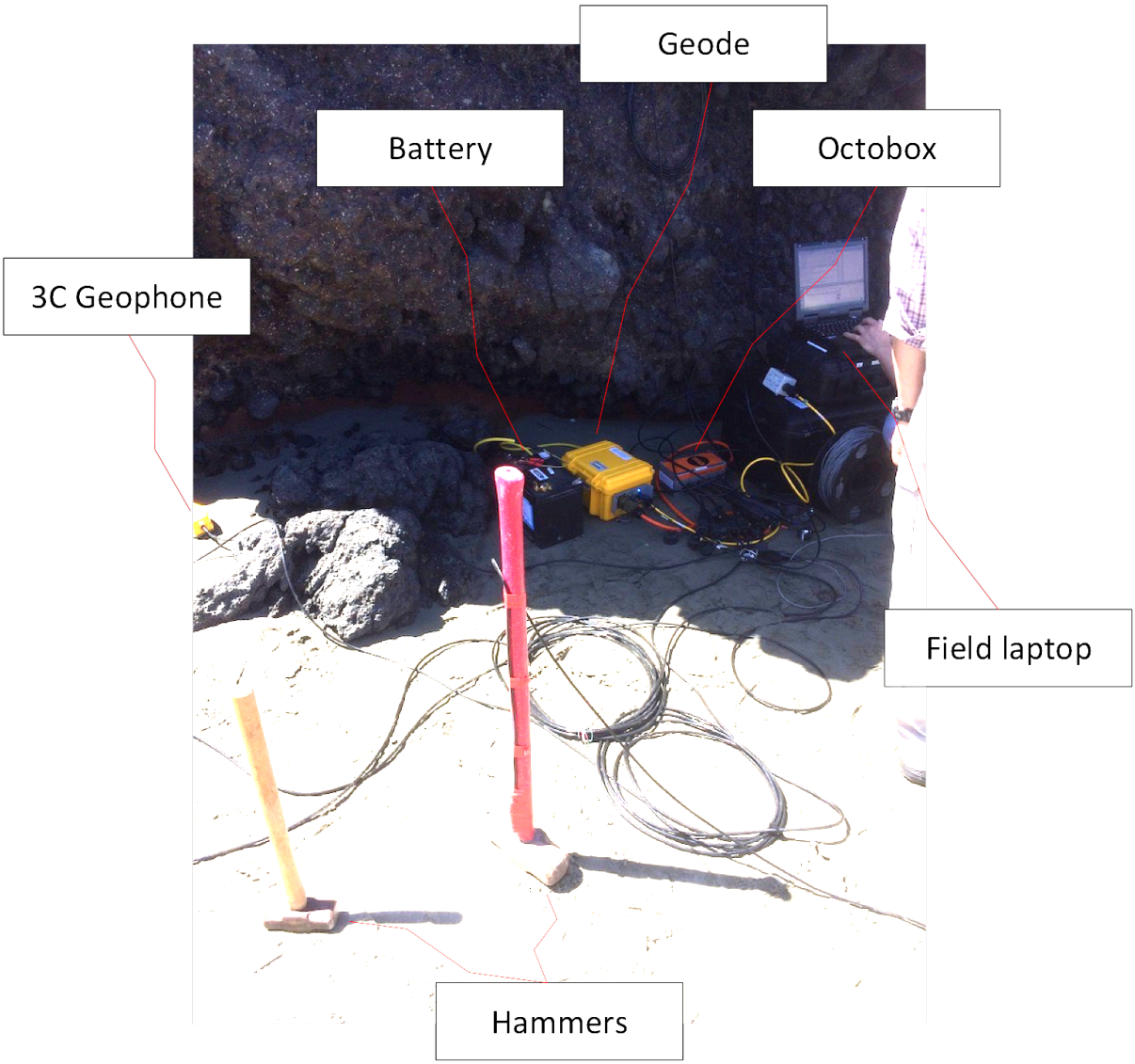

Figure 2.11: Brightness enhanced image of kit used showing hammers, geophones, geode, Octobox, battery and field laptop. Location: SE Ridge

Geophones and trigger system

The 3C geophones measure motion in three orientations, which when oriented to North and level are north-south, east west and vertically up and down (Figure 2.13). The trigger consists of a metal pipe with a bar in the centre which attaches to a hammer or another seismic source. When the hammer strikes a rock or material the inner bar touches the pipe and closes the circuit, initiating the start of data recording for the geophones for that hit (Figure 2.12).

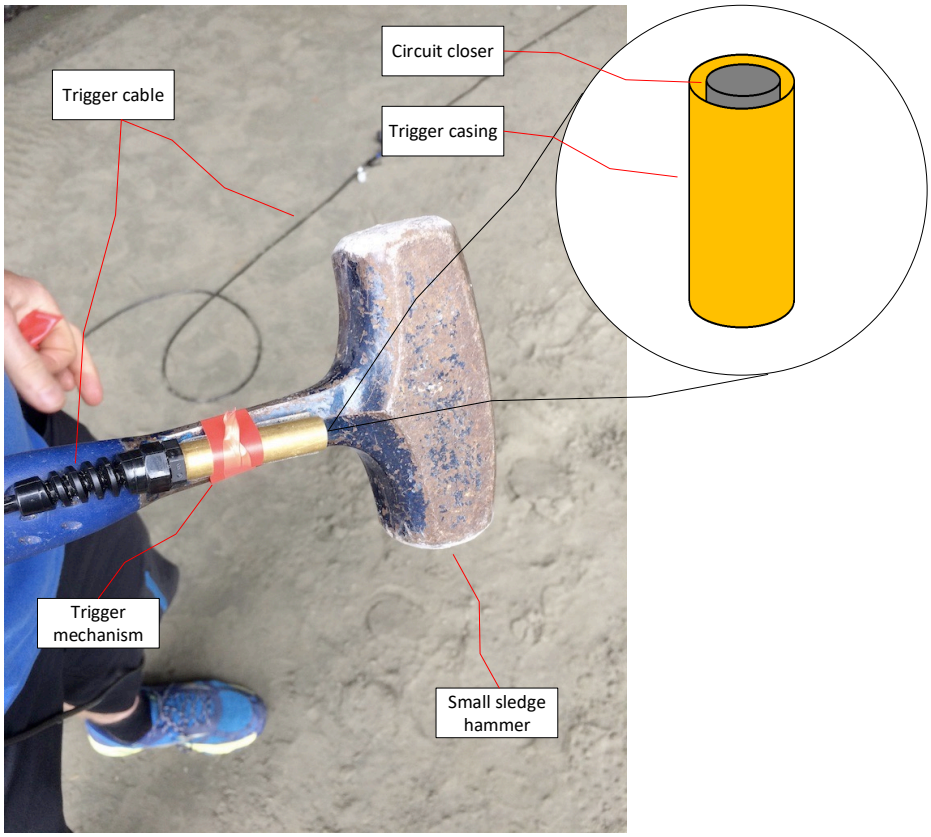

Figure 2.12: Trigger mechanism attached to small sledge hammer. Gold coloured cylinder houses rod which closes circuit, initiating geophone array recording for each hit.

Because Cave Rock has local and Māori significance, geophones were attached in a way that did not destroy the rock mass - small sand piles were built (Figure 2.13) at each geophone location that were deep enough for the long geophone spikes. The sand also allowed the body of the geophone to be appropriately orientated horizontal and north. Krohn (1984) explores coupling techniques and how to couple geophones to the ground in ways to get accurate seismic data and recommends either burying the geophones completely or using long spikes to attain good coupling. Krohn (1984) also states that the condition of the soil does not significantly affect the data collected by the geophones.

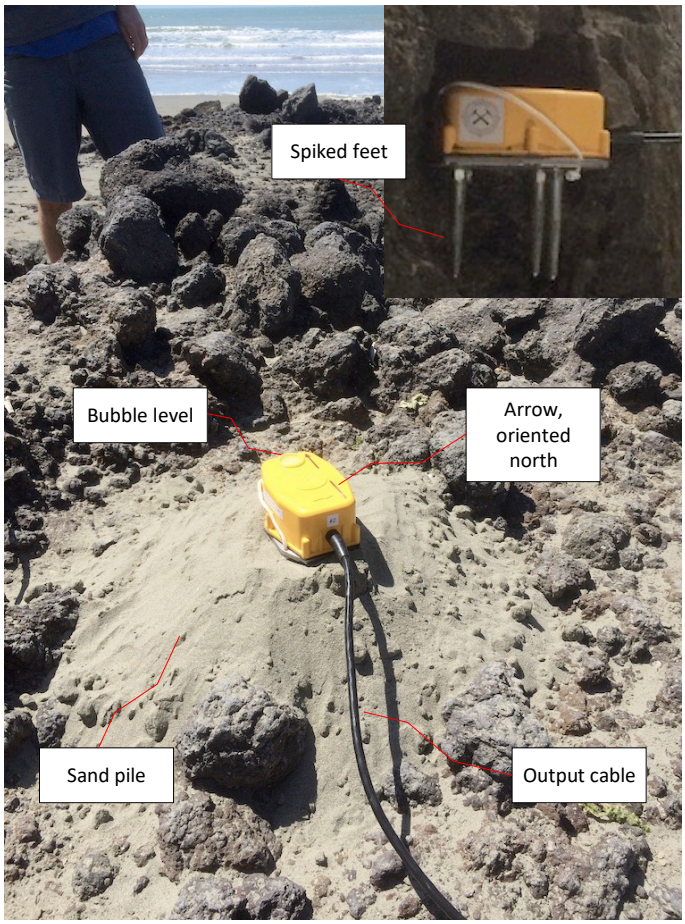

Figure 2.13: Image showing one of the eight 3C geophones. Geophone is oriented level and pointing north using the bubble level and north arrow. Spiked feet are shown which are inserted into sand piles. Spiked feet can be removed when the geophone has to fit in small spaces. Output cable transfers each of the three motion components to the Octobox from Figure 2.11.

Seismic data collection methods

Seismic data was collected in the field on the 6th and 7th of November 2018 using Claritas software from the Otago University. The files were imported to ReflexW as .dat files and loaded up to show each of the eight geophones with their respective three components (x, y and z) showing as separate graphs, giving 24 plots for each hit performed (Figure 3.11). These plots were analysed by picking the arrival of the first major significant divergence of energy, which is to be interpreted as the arrival of the p wave in milliseconds. The resulting .PCK files were imported into Microsoft excel as a text file. Each shot location with its five hits was collated into an individual table and then sorted first by geophone number and then by arrival time. The arrival times were then picked for each geophone by selecting the fastest time that

was the first time in a cluster as to remove outliers from incorrect picks. If a value was completely different, such as a value of 0.02 ms^{-1} within a cluster of 1.1, 1.14 and 1.2 ms^{-1} the 0.02 value was ignored. If a value was not clearly an outlier, an excel formula determined whether the number was outside the average plus two times the standard deviation minus the average of the first five values, minus the value of the suspect outlier. This method was used to keep the same criteria for selecting time values based on the picks from ReflexW. A table of all shots, .dat raw wave signature files and corresponding data file numbers can be found in Online Appendix 2 and Online Appendix 3.

Stacked vs. Unstacked data

Stacking of seismic data can increase signal and reduce noise, greatly improving data quality and acquisition (Klemperer, 1987). In some cases however, data does not need to be stacked as wave arrivals are clear and easily picked on geophone recordings. In this study, multiple stacked velocities were compared to un-stacked ones to see if there is a difference when calculating p wave velocities through the rock. At all of the survey shot points, shots were stacked by hitting in the same location 5 times before moving on to the next shot location, these shots could then be stacked later in processing steps to compare to individual shots.

GPS equipment

A Trimble Geo 7X with differential correction was used to record the location of the seismic geophones and shot locations. Trimble GPS Pathfinder Office Software was used for processing and downloading the GPS files, which were then differentially corrected to a horizontal precision of 10cm. The processed outputs were then saved in an excel spreadsheet for further analysis.

For the geophone locations in the cave, the laser rangefinder on the Trimble Geo 7X was used which recorded distance, bearing and inclination from a site visible to GPS satellites out of the cave to the shot points inside the cave. Because it was dark inside the cave and bright and sunny outside, it was sometimes difficult to see the small red laser dot on the shot locations, so a sweet navel orange was placed where the shot locations had been, the laser reflecting brightly on the shiny skin of the fruit. The bearing, inclination and distance from the location of the GPS then calculated the projected GPS location of the laser rangefinder. GPS points

were used to calculate straight line distances between geophones using trigonometry and calculated in excel. The formula (Equation 2.1) used easting, northing and elevation above sea level.

$$D = \sqrt{(x_2 - x_1)^2 + (y_2 - y_1)^2 + (z_2 - z_1)^2}$$

Equation 2.1: Formula for determining straight line distance between geophone and shot point locations where x is easting, y is northing and z is metres above sea level.

Survey Locations

The first location for the geophysical test was on a small ridge on the south east side of Tuawera / Cave Rock. The ridge consists of the orange red tuff layer and breccia underlying a cap of coherent lava. The ridge is 2m high and 10m long with sand on both sides (Figure 2.14). South East Ridge was the first location for testing the seismic kit from Otago due to time and tide constraints and rising tides also meant that two geophones were moved partway through the survey and re-located using the GPS.

3C geophones were arranged in two lines at this site with one line running approximately north-south and the other east-west (Figure 2.14). Shots at this location were performed with sledgehammers on a wooden plank and directly on rock (Figure 2.15) to see if there was any effect of hammer and source direction on wave attenuation and energy loss.

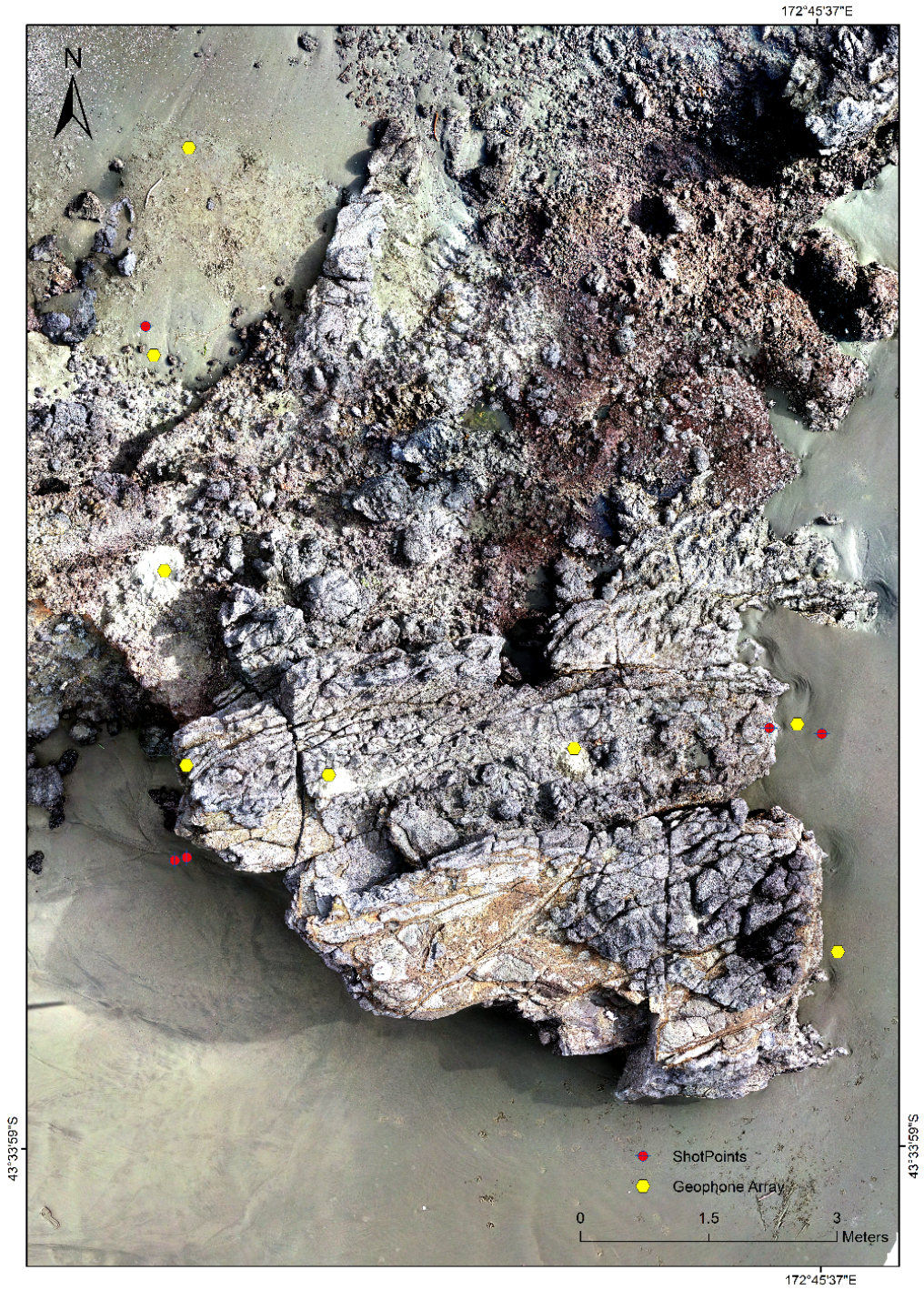

Figure 2.14: Close up image of the first geophysical survey at Cave Rock, South East Ridge. Geophones are shown in yellow and shot locations in red.

Figure 2.15: Direct rock hit at South East Ridge location. Wooden plank present is what was used for plank hits. First geophone of the line is also shown.

The second location for equipment testing was on Cottage Rock, a 7 m high blob of coherent lava to the south west of Cave Rock (Figure 2.16). This site provided another good opportunity to test the equipment at outcrop scale and also a chance to see the influence of fractures on p wave velocity as Cottage Rock is predominantly coherent lava riddled with fractures and joints (Figure 2.4).

As in the South East Ridge test, two rough geophone lines (Figure 2.16) were used to measure seismic velocities through different sections of the rock mass, with one being shorter and to the top of Cottage Rock and the other longer and around the face of the outcrop. At Cottage Rock a large variety of shot types, orientations and strike materials were again used to try and see which methods gave the clearest signal on the field laptop, which then would be the method used for the larger Cave Rock survey. The shot combinations used at Cottage Rock were sledge hammers and Estwing geologic hammers both upwards and sideways directly on the rock surface and also on metal plates and wooden planks on the sand (Figure 2.17).

Figure 2.16: Map and image showing geophone array and shot point locations for Cottage Rock. Note two rough lines of geophones up and over and around the front.

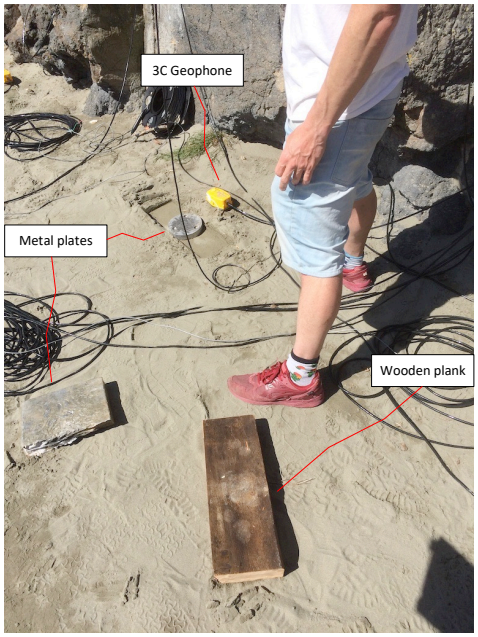

Figure 2.17: Image showing base of Cottage Rock and materials used to hit onto. Plank and plates were placed in the sand a short distance from the outcrop.

At Cave Rock, the geophone array was positioned on top of the outcrop and the shot locations were inside the cave moving firstly north along the eastern side of the tunnel and then back along the western side, with shots being directed either sideways or upwards into the rock mass. The geophone array for this test was placed on the top surface of the outcrop overtop of the tunnel running through the outcrop, with the approximate even spacing of geophones limited by sites that were appropriate for sand piles (Figure 2.18).

As a result of the equipment testing on SE Ridge and Cottage Rock, it was decided that a small sledgehammer using shots striking directly on the rockmass returned the best arrival wave signature and was the most optimal method available to use as the source for the larger Cave Rock survey.

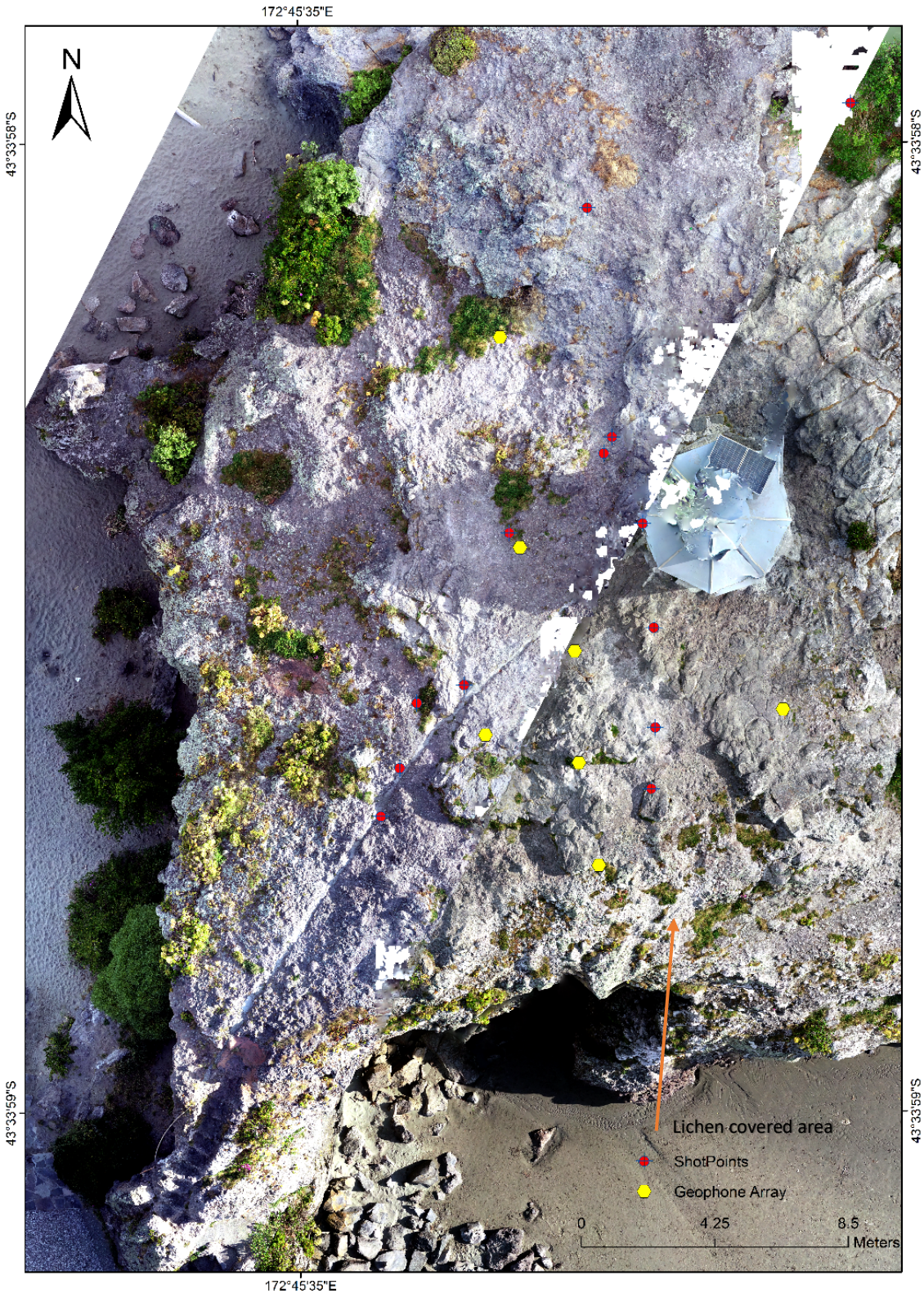

Figure 2.18: Map of the Cave Rock survey location. Yellow dots are once again geophone locations and shot points are red dots. It is important to note that these shot points are actually inside the cave and not on the top surface where the geophones are. Bottom right corner of outcrop shows paler grey colour, and is typical of areas of rock covered with more lichen.

Cross hole sonic logging

Another way sonic velocities were measured to compare to the Cave Rock velocities was using cross-hole sonic techniques (Figure 2.19) at a property at Mt Pleasant in basaltic bedrock (Figure 1.6). We drilled two water filled holes 30 mm wide at 500 mm intervals (Figure 1.3) and piezometric sources were lowered into the water and connected to a field computer.

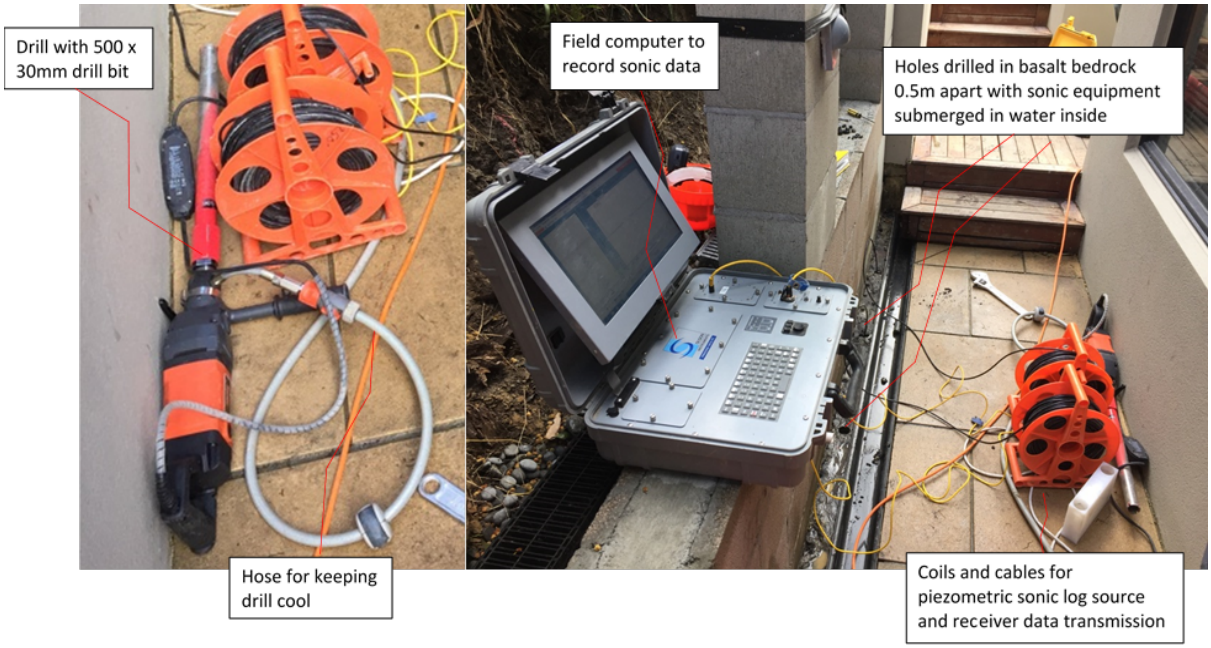

Figure 2.19: Set up of equipment used in sonic logging test showing laptop, data cables and drill. Piezometric sources are in the holes.

Chapter 3: Results

3.1 Laboratory experiments

Results from laboratory testing show distinct p and s wave velocities for tuff, breccia and coherent lava in ultrasonic experiments. Vp in coherent lava samples ranged from 2670 - 3075 m/s (2827.5 m/s average), tuff ranges 2029 - 2197 m/s (2080.4 m/s average) and breccia 2057 - 2470 m/s (221.8 m/s average. Vs in samples ranged from 1137 - 1594 m/s for coherent lava (1257.5 m/s average), 877 – 1367 m/s for breccia (1104.2 m/s average) and 1016 – 1121 m/s for tuff (1079.8 m/s average). Densities ranged from 0.00248 g/mm^3 for coherent lava, 0.00208 g/mm^3 for breccia and 0.00187 g/mm^3 for tuff. Average porosity for coherent lava was found to be 38.6 % while the breccia samples were found to be 50.6 % and tuff 53.4% (Table 3.1, Figure 3.1), however only one core for breccia and tuff were small enough to fit in the pycnometer while still adhering to the 2 times length to width minimum dimensions. A summary of average p and s wave velocities, porosity, and density for the three geotechnical units of breccia, ash and coherent lava is shown in Table 3.1.

It is noted that all samples are weathered and especially the coherent lava which has many vesicles and holes compared to a perfect unweathered core of unfractured unaltered basalt or basaltic andesite (see Figure 2.1A, B).

Table 3.1: Summary of p and s wave velocities, porosity and density of three geotechnical units that were experimented on in the laboratory at University of Canterbury.

Rock Type	Vp avg. (m/s)	Vp range	Vs avg. (m/s)	Vs range	Porosity avg. (%)	Porosity range	Density average (g/mm3)
Coherent Lava	2872.5	2670 - 3075	1257.5	1137 - 1594	38.6	11.3 - 52.6	0.00248
Breccia	2221.8	2057 - 2470	1104.2	877 - 1367	50.6	—	0.00208
Tuff	2080.4	2029 - 2177	1079.8	1016 - 1121	53.4	29.8-53.5	0.00187

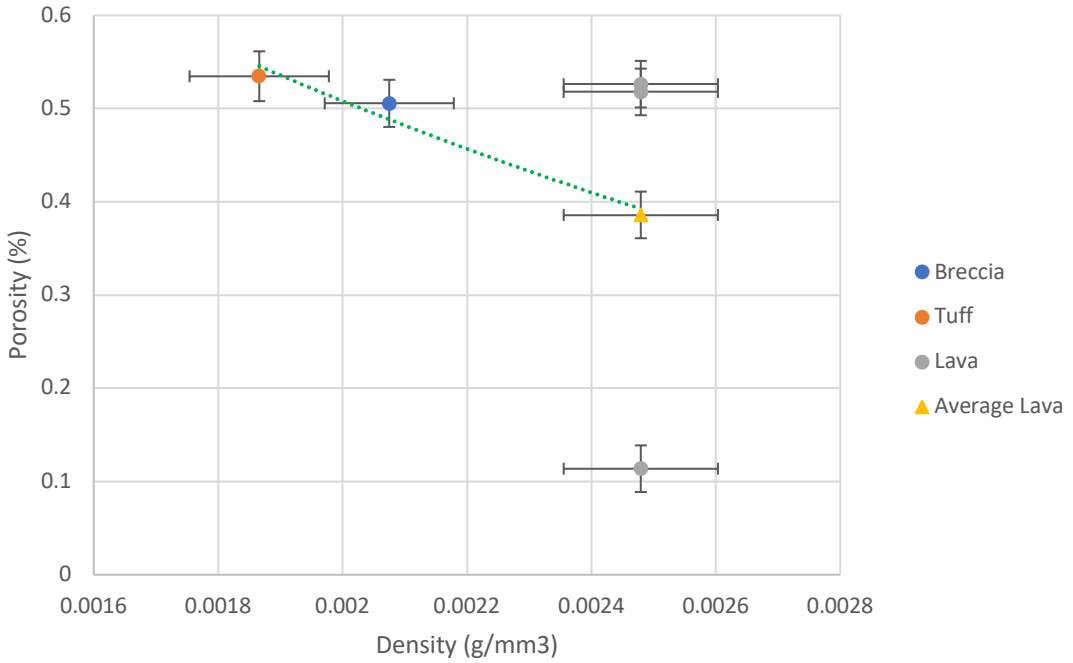

Figure 3.1: Plot of density vs porosity for laboratory samples of tuff, breccia and coherent lava. The green line is the line of best fit through the average porosity and density points of each rock type. Horizontal error bars were calculated from the range of density measurements from the larger cores used for ultrasonic testing.

When plotted against density, seismic p wave velocity shows a strong positive correlation. P wave velocity increases with increasing sample density. Tuff and breccia have similar p wave velocities despite the higher density of the breccia. The coherent lava has distinctly higher p wave velocity and density (Figure 3.2).

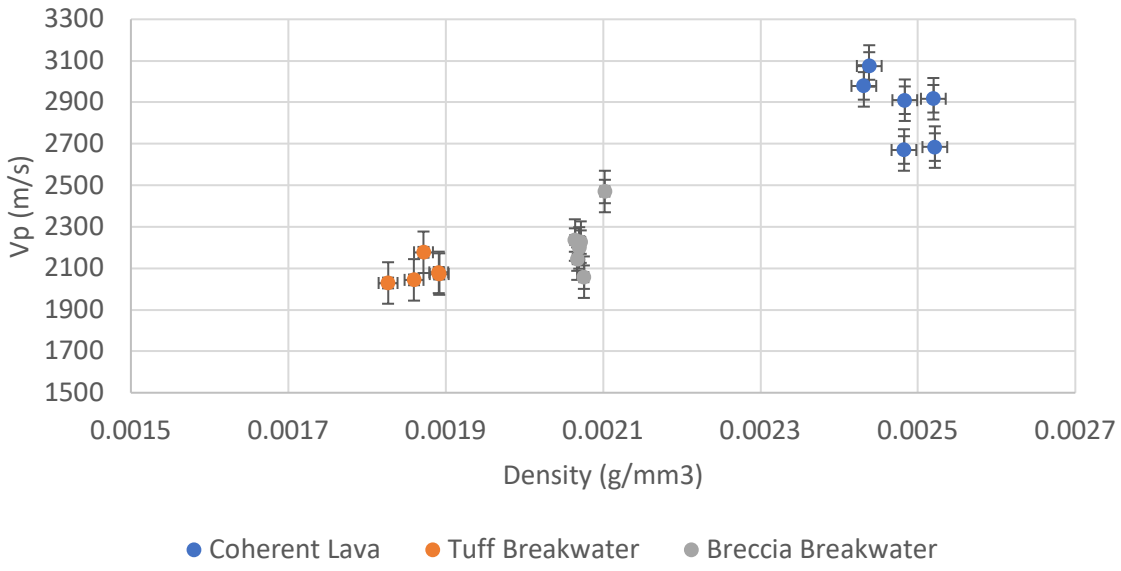

Figure 3.2: Plot of density vs p wave velocity for all the samples collected for the three geotechnical units at Cave Rock, Sumner. Error bars have been calculated from measurement error and manual pick error.

Influence of fractures on p and s wave velocity

The results from the cutting experiments on coherent lava cores show large changes (nearly 2000 m/s) in p wave velocity when increasing the fracture content from one to four fractures over the same length of core (Table 3.2, Figure 3.3). For the horizontal cut experiment simulating fractures perpendicular to energy propagation, p wave velocity decreased from 2979 m/s for the uncut core to 1136 m/s for the core with 3 horizontal cuts, a velocity drop of 38 %. S wave velocities were harder to pick after the experiment with more than one horizontal cut but there was a reduction from 1594 m/s to 1251 m/s from uncut to the sample with one cut.

Table 3.2: Summary of Vp and Vs for horizontal and vertical cut experiments for cores of coherent lava.

Test No.	Height (mm)	Mass (g)	Diameter (mm)	Volume (mm3)	Density (g/mm3)	Vp (m/s)	Vs (m/s	Cuts
CL3 - Uncut	120.49	377.2	40.49	155144.51971	0.00243	2979	1594	0
CL3 1 h cut	120.01	376.688	40.49	154526.46536	0.00244	2255	1251	1
CL3 2 h cuts	118.75	372.825	40.38	152074.40603	0.00245	1621		2
CL3 3 h cuts	118.22	368.68	40.35	151170.80108	0.00244	1136		3
CL1 - Uncut	96.5	309.215	40.24	122725.02770	0.00252	2917	1137	0
CL1 - 1 v cut	96.5	298.691	39.08	115751.41395	0.00258	2761	1516	1
CL2 - Uncut	121	383.4	40	152053.08440	0.00252	2684	1205	0
CL2 - 1 v cut	121	371.184	39.47	148050.37252	0.00251	2716	1563	1

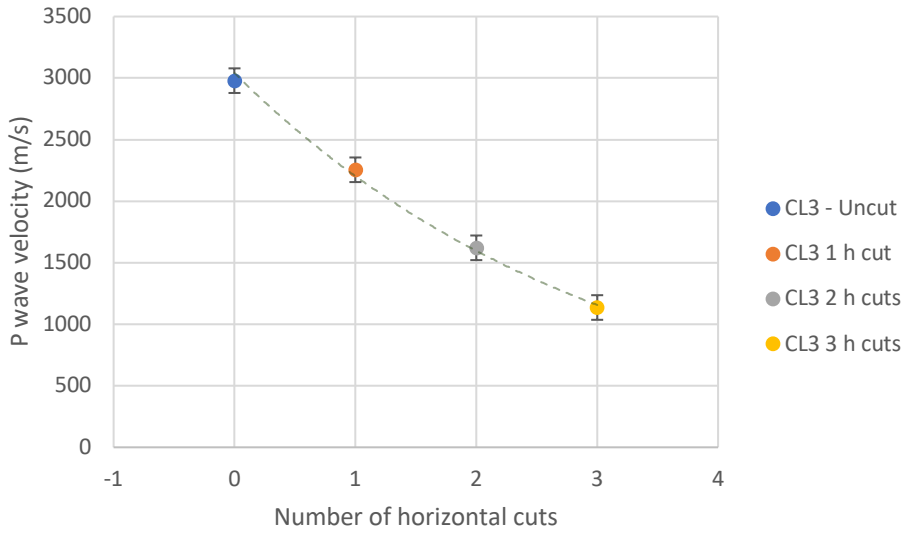

Figure 3.3: Plot of Vp for coherent lava sample with increasing amount of horizontal fractures. Approximate decrease between uncut and three horizontal cuts is 38%.

For the vertical cut experiments simulating fractures parallel to wave propagation there was no distinct increase or decrease in p wave velocity with an increase from 2684 m/s to 2715 m/s for one sample and a decrease from 2914 m/s to 2761 m/s in the other. Vs increased with one vertical cut in this experiment with both samples measured showing an increase from 1137 m/s to 1516 m/s and 1205 m/s to 1563 m/s (Figure 3.4, Table 3.2).

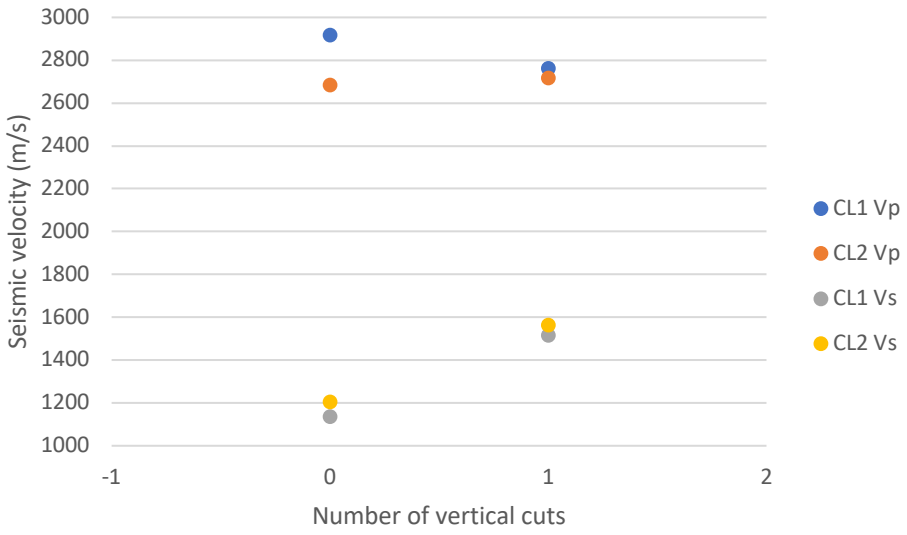

Figure 3.4: Plot of Vp and Vs for two samples comparing velocities through uncut coherent lava core and coherent lava core with one vertical cut. Vp shows both a slight decrease for one sample and slight increase for the other of 300 m/s. Vs in both samples increased from 1200 m/s to just over 1500 m/s.

Influence of lithology on Vp and Vs

The lithology stack experiments were designed as a way to simulate varying proportions of lithology over the same distance with the same fracture amounts, similar to the field study of upwards and sideways shots at Cave Rock, Sumner. The stacks used decreasing percentage of breccia and increasing percentage of coherent lava to see the influence of the cracks and lithology changes on Vp and Vs. Comparing the sample with the least proportion of coherent lava to the most proportion of coherent lava shows a decrease in p wave velocity from 2113 m/s (BL 5-4) to 1797 m/s (BL 8-1) (Figure 3.5, Table 3.3). However, there is a slight drop in Vp from BL 8-1 to BL 7-2 from 1797 m/s to 1719 m/s before the velocity increases again through BL 6-3 to BL 5-4. While the sample with the most coherent lava had the fastest p wave velocity (BL 5-4, 2113 m/s) the sample with the slowest p wave velocity did not have the least coherent lava, but second least (BL 7-2, 1719 m/s). Sample BL 5-4 has a different tuff proportion due to the lava and breccia slices being shorter than aimed for.

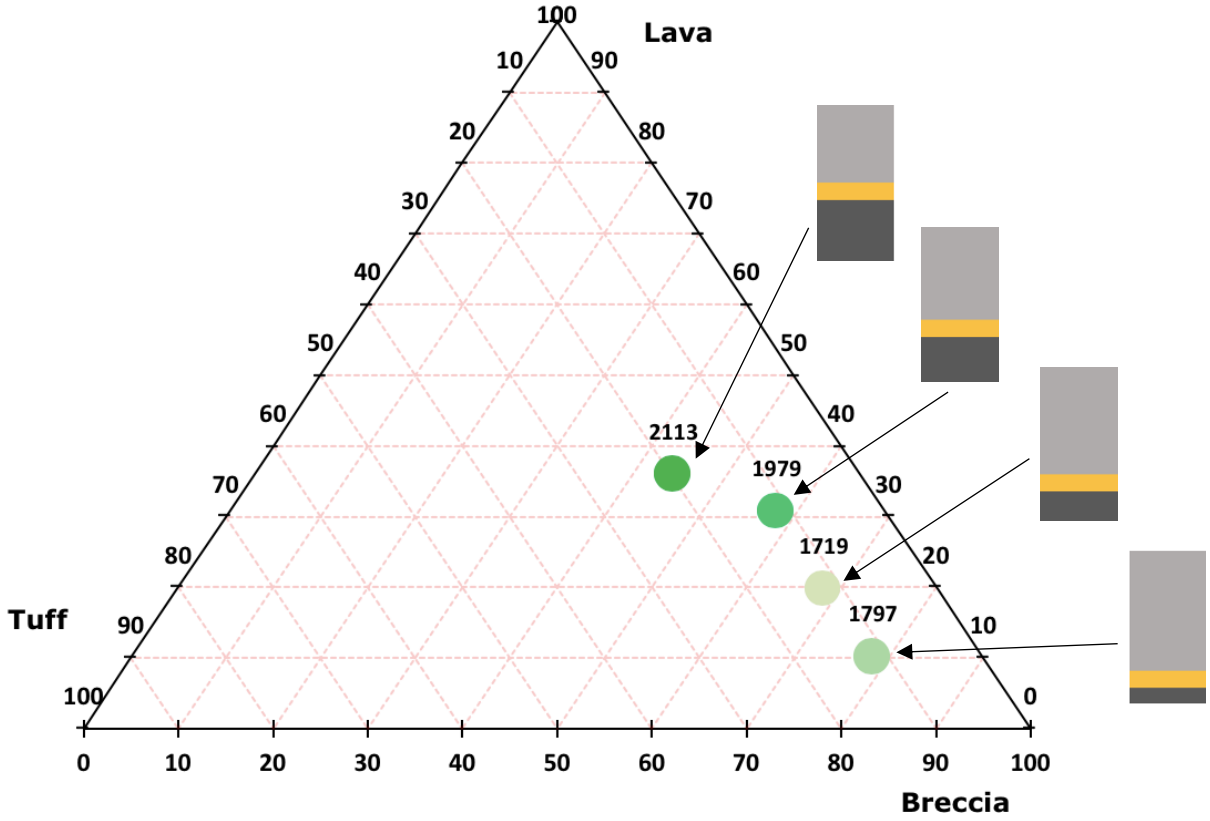

Figure 3.5: Ternary diagram displaying percentage of breccia, coherent lava and tuff samples from lithology stack experiment and Vp of each test. Data points are coded so darker green correlates to faster Vp and pictorial representations of cores correlate to lab experiments with tuff orange, breccia light grey and coherent lava dark grey. Ternary diagrams were created using template downloaded from Aps (2020).

Table 3.3: Summary of sample p wave velocities from the lithology stack experiment. Fastest Vp is in the 4 cm lava 5 cm breccia stack (BL 5-4, 2113 m/s) and slowest in the 7 cm breccia 2 cm lava stack (1719 m/s, BL 7-2).

Test No.	% Breccia	% Lava	% Tuff	Vp (m/s)
BL 8-1	78.3	10.1	11.6	1797
BL 7-2	68.3	19.7	12.0	1719
BL 6-3	57.9	30.7	11.5	1979
BL-5-4	44.3	35.9	19.7	2113

3.2 Mapping

Scanlines

The results from scanlines and geologic mapping show distinct relationships between lithology and discontinuity frequency between the different geotechnical units present at Sumner Beach.

The scanlines at Cottage rock were constructed as close as possible to the two geophone lines, one up and over the centre of the outcrop and one along the front – middle of the outcrop (Figure 2.4). The results from the scanlines showed many small fractures with an aperture of less than 1 cm to large fractures and joints that trace for several metres with an aperture of more than 1 cm (Table 3.4, Table 3.5). There are also many areas of red spheroidal type weathering where either side of a pre-existing crack the rock has altered to a red colour and sticks out more than the rest of the surrounding rock (Figure 3.6). The red weathering alteration has an average schmidt rebound number of 27.8 while the intact rock read an average value of 32.3, which gives a quick analysis of strength or material (Çobanoğlu & Çelik, 2008; Dinçer et al., 2004), showing that the intact rock is stronger than the hard red weathering altered fractures. Fractures and joints at Cottage Rock typically had roughness of undulating or stepped at the m scale and rough and smooth at the cm scale.

Table 3.4: Scanline 2 at Cottage Rock in coherent lava with fracture spacing, orientation, length, roughness, strength and infilling. Schmidt rebound numbers are the average of 10 tests. Scanline correlates to Figure 2.4A.

Location: Cottage Rock, Sumner, New Zealand. GP line 4-8 Nov Test. Scanline running diagonally up and across the rock outcrop
Date: 16/05/19 Photos: Photo in CC phone. Cottage rock w tape. 11:30am
Rock Type: Coherent lava w spheroidal weat Batter orientation: - Scanline Number: 2 Length: 9m

		Orientation					Roughness				Strength (MPa) or			
Scanline chainage	Feature Type	Dip	Dip Direction	Spacing (m)	Trace length/ persistence (m)	Aperture (mm)	m scale	cm scale	Asperity amplitude (mm)	Infilling/ alteration type	Infilling / alteration	Intact Rock	Water	Weathering
0.8	SW	52	132	-	0.3	3	Undulating	Rough	5	Red Weather	27.8	32.25	Dry	Red
1.05	Fracture	70	220	0.5	2	4	Undulating	Rough	5	Open	-	24.7	Dry	-
1.5	SW	86	340	0.005	0.6	6	Undulating	Rough	12	Red Weather	-	-	Dry	Red
1.55	SW	80	150	0.005	0.6	10	Undulating	Smooth	4	Red Weather	-	-	Dry	Red
1.6	Fracture	85	146	-	0.9	2	Stepped	Smooth	4	Open	-	-	Dry	-
1.69	Fracture	24	328	0.3	0.5	2	Undulating	Rough	5	Open	-	41	Dry	-
2.08	Fracture	30	327	0.25	0.6	2	Undulating	Smooth	8	Open	-	-	Dry	-
2.2	Fracture	8	350	0.25	0.4	4	Undulating	Smooth	6	Open	-	-	Dry	-
2.5	SW	73	318	0.15	1.3	2	Undulating	Smooth	6	Red Weather	-	-	Dry	-
2.7	SW	81	338	0.2	1.5	7	Undulating	Smooth	4	Red Weather	-	-	Dry	Red
2.9	Fracture	72	163	-	4	30	Undulating	Smooth	13	Open	-	-	Dry	Sand/gravel s
3.3	Fracture	74	340	-	1.8	10	Undulating	Rough	7	Open	-	-	Dry	-
3.6	Joint	65	310	-	6	23	Undulating	Smooth	17	Open	-	30.2	Dry	-
4.65	Fracture	64	328	0.4	1.3	10	Undulating	Rough	12	Open	-	-	Dry	Some minor r
5	Fracture	60	132	0.4	1.4	8	Undulating	Smooth	5	Open	-	-	Dry	-
5.4	Fracture	12	65	-	2	1	Undulating	Rough	10	Closed	-	-	Dry	-
5.7	Fracture	69	332	0.2	3	15	Undulating	Smooth	11	Open	-	33.2	Dry	-
6.8	Joint	84	286	-	3.5	29	Undulating	Rough	9	Open	-	-	Dry	-
7.6	Fracture	84	328	0.12	2	15	Undulating	Rough	8	Open	-	-	Dry	-
7.8	Fracture	71	171	0.15	2	8	Undulating	Rough	18	Open	-	-	Dry	-
8.1	Fracture	74	343	0.15	3	10	Stepped	Rough	12	Open	-	-	Dry	-
8.7	Fracture	30	317	-	0.5	2	Undulating	Smooth	10	Closed	-	-	Dry	-

Table 3.5: Scanline 3 at cottage rock in coherent lava with fracture spacing, orientation, length, roughness, strength and infilling. Schmidt rebound numbers are the average value of 10 individual tests. Scanline correlates to Figure 2.4B.

Location: Cottage Rock, Sumner, New Zealand. GP line 1-3 Nov. Straight up rock outcrop face
Date: 22/05/19 Photos: 11:28am CC phone
Rock Type Coherent lava Batter orientation: ESE-WNW Scanline Number: 3 Length: 7m

Scanline chainage	Feature Type	Orientation		Spacing (m)	length/ persistence (m)	Aperture (mm)	Roughness		Asperity amplitude (mm)	Infilling/ alteration type	Strength (MPa) or		Water	Weathering
		Dip	Dip Direction				m scale	cm scale			Infilling / alteration	Intact Rock		
0.65	Fracture	31	78	0.04	0.4	2	Undulating	Rough	9	Open	-	-	Dry	-
0.68	Fracture	58	210	0.06	0.04	1	Undulating	Rough	5	Open	-	-	Dry	-
0.7	Fracture	24	63	0.04	0.6	3	Undulating	Smooth	6	Open	-	-	Dry	-
0.75	Fracture	18	46	-	0.7	1	Stepped	Smooth	4	Open	-	-	Dry	-
0.8	Fracture	28	128	-	0.3	2	Undulating	Smooth	4	Open	-	-	Dry	-
0.85	Fracture	32	161	-	0.4	1	Undulating	Smooth	2	Open	-	30.05	Dry	-
0.97	Fracture	64	140	-	0.4	3	Undulating	Smooth	8	Closed	-	38.9	Dry	-
1.17	Fracture	55	136	-	0.2	2	Undulating	Smooth	5	Closed	-	-	Dry	-
1.22	Fracture	24	342	-	0.6	2	Undulating	Smooth	4	Open	-	-	Dry	-
1.32	Fracture	27	118	-	0.7	1	Undulating	Smooth	5	Closed	-	-	Dry	-
1.35	Fracture	35	132	-	1.5	3	Undulating	Smooth	6	Open	-	-	Dry	-
1.39	Fracture	42	85	-	0.9	2	Undulating	Smooth	2	Closed	-	-	Dry	Some RW
1.5	Fracture	26	98	-	1	1	Undulating	Smooth	10	Closed	-	-	Dry	-
1.75	SW	24	126	-	0.4	0	Undulating	Smooth	4	Closed	-	-	Dry	-
1.85	Fracture	20	318	-	0.7	1	Stepped	Smooth	10	Open	-	-	Dry	-
2.1	Fracture	28	270	-	1	2	Undulating	Smooth	8	Open	-	23.6	Dry	RW
2.4	Fracture	24	286	-	0.4	1	Undulating	Smooth	12	Open	-	-	Dry	-
2.9	Fracture	26	330	-	1	2	Undulating	Smooth	6	Open	-	-	Dry	-
3.4	Fracture	55	100	-	0.4	3	Undulating	Smooth	4	Open	-	-	Dry	-
4.8	Joint	80	120	-	5	28	Undulating	Smooth	15	Open	-	-	Dry	-
5.7	Fracture	55	11	-	2	25	Undulating	Smooth	20	Open	-	-	Dry	-
6.13	Fracture	65	355	-	1.5	15	Undulating	Smooth	15	Open	-	35.5	Dry	-
6.5	Fracture	70	340	-	1	18	Undulating	Smooth	13	Open	-	-	Dry	-
6.7	Fracture	58	100	-	0.8	1	Undulating	Rough	8	Closed	-	-	Dry	-

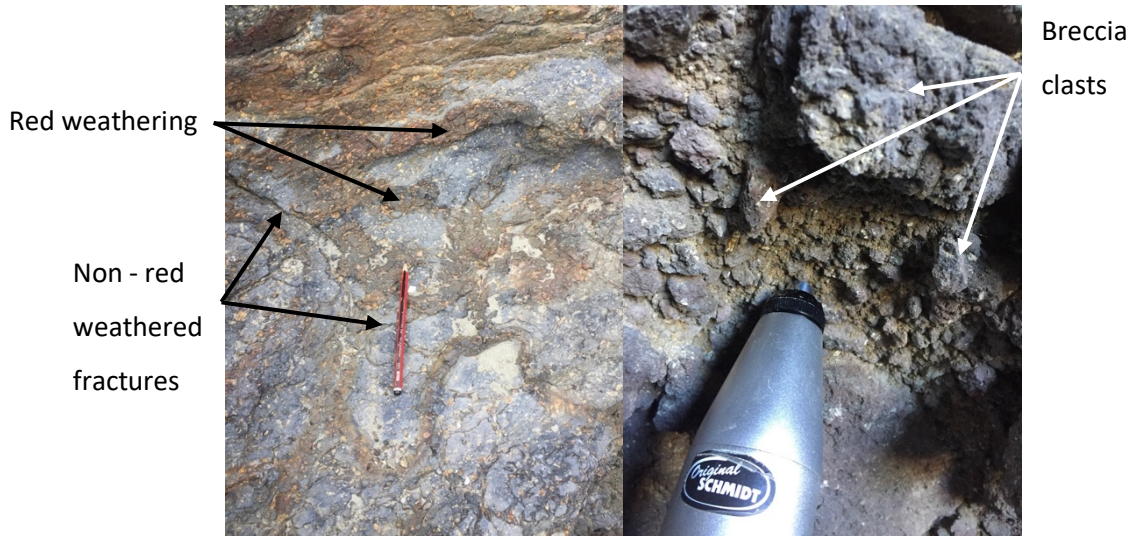

Figure 3.6: Left – Close up photo of typical red weathering fractures in coherent lava. Red sections stick up out of the rock face slightly but schmidt rebound value is larger on the intact rock rather than

the red fractures. Right – Close up of breccia has been included for fracture comparison, far fewer fractures are evident with many weathered clasts.

The scanlines undertaken at Cave Rock were in the two dominant rock types; breccia and coherent lava. The two breccia scanlines encountered very few discontinuities, one being 20.79 m long with four fractures (Table 3.6) and one bedding plane and the other 7.25 m long with two fractures and one bedding plane (Table 3.7). Compared to the breccia, the coherent lava has significantly higher discontinuity density with one scanline having four fractures and two joints over 2.34 m (Table 3.7), a second having nine fractures and five joints over 11.29 m (Table 3.8) and a third having seven fractures and three joints over 4.2 m (Table 3.9).

Table 3.6: Scanline 3, breccia on the outside south east edge of Cave Rock. Scanline is 20.79 m long with five discontinuities.

Location: Cave Rock, SE outside edge Date: 14/01/20 Photos: 10:36 cc phone
Rock Type Breccia Batter orientation: NE/SW Scanline Number: 10 Length: 21m

		Orientation					Roughness				Strength (MPa) or			
Scanline chainage	Feature Type	Dip	Dip Direction	Spacing (m)	Trace length/ persistence (m)	Aperture (mm)	m scale	cm scale	Asperity amplitude (mm)	Infilling/ alteration type	Infilling / alteration	Intact Rock	Water	Weathering
0.45	Fracture	70	6		3	3	Stepped	Rough	10	Sand			Dry	SW
10.38	Bedding	41	327		1	2	Undulating	Smooth	6	RW			Dry	SW
16.69	Fracture	63	250		0.75	Closed	Undulating	Rough	7	None			Dry	SW
19.84	Fracture	74	240		0.3	30	Undulating	Smooth	4	Open			Dry	SW
20.79	Fracture	61	310		0.3	5	Undulating	Rough	4	None			Dry	SW

Table 3.7: Scanline 4, joint scanline of breccia and coherent lava. Breccia at this location has only three fewer discontinuities than coherent lava, but is over 7.25 m compared to the 2.34 m of coherent lava.

Location: Cave Rock, Stalactites of Lava, Date: 14/01/20 Photos: cc phone 11:27
Rock Type: Breccia, Tuff, Lava Batter orientation: NW/SE Scanline Number: 11 Length: 12m

		Orientation					Roughness				Strength (MPa) or			
Scanline chainage	Feature Type	Dip	Dip Direction	Spacing (m)	Trace length/ persistence (m)	Aperture (mm)	m scale	cm scale	Asperity amplitude (mm)	Infilling/ alteration type	Infilling / alteration	Intact Rock	Water	Weathering
1.2	Bed	36	56		Metres	0	Undulating	Rough	60	none			Dry	SW
2.54	Bed	36	56	1.34	Metres	1	Undulating	Rough	61	none			Dry	SW
7.1	Vein(?)	26	208		1.1	0	Undulating	Smooth	7	Vein			Dry	SW
7.25	Fracture	60	160		0.6	1	Undulating	Rough	9	None			Dry	SW
NOW BECOMES A SECTION OF COHERENT LAVA														
9.36	Fracture	71	123	0.1	0.45	2	Undulating	Smooth	6	Open			Dry	SW
9.75	Fracture	70	192	0.15	0.8	3	Undulating	Smooth	10	OPen			Dry	SW
10.08	Joint	78	30	0.6	0.38	3	Undulating	Smooth	3	Open			Dry	SW
10.77	Joint	69	33	0.6	0.46	1	Undulating	Rough	5	Open			Dry	SW
11.6	Fracture	44	139		1.2	4	Undulating	Smooth	12	Open			Dry	SW
11.7	Fracture	80	98		1	3	Undulating	Smooth	3	None			Dry	SW

Table 3.8: Scanline 5, coherent lava inside western edge of Cave Rock cave with 14 discontinuities over 11.29 m.

Location: Cave Rock, Inside cave, centr Date: 14/01/20 Photos: 12:45 cc phone
Rock Type: lava, coherent Batter orientation: N/S Scanline Number: 12 Length: 12m

		Orientation					Roughness				Strength (MPa) or			
Scanline chainage	Feature Type	Dip	Dip Direction	Spacing (m)	Trace length/ persistence (m)	Aperture (mm)	m scale	cm scale	Asperity amplitude (mm)	Infilling/ alteration type	Infilling / alteration	Intact Rock	Water	Weathering
0.1	Fracture	84	200		Metres	4	Planar	Rough	3	None			Dry	SW
0.2	Fracture	22	283	0.27	8	6	Undulating	Rough	6	Sand			Dry	SW
1.56	Joint	73	238	0.45	1.5	2	Planar	Rough	4	Sand			Dry	SW
2	Joint	77	237	0.45	1.5	2	Undulating	Rough	9	Closed			Dry	SW
2.9	Fracture	67	345		0.5	3	Undulating	Rough	5	None			Dry	SW
3.09	Fracture	68	204		1	2	Undulating	Rough	12	Open			Dry	SW
4.72	Joint	90	54	2.72	1.7	7	Planar	Rough	12	Closed			Dry	SW
4.9	Fracture	53	331	0.001	0.4	0	Planar	Rough	4	RW			Dry	SW
5.15	Fracture	60	185		0.3	1	Undulating	Rough	11	None			Dry	SW
5.6	Joint	0	246	1	2.5	4	Planar	Rough	2	OPen			Dry	SW
6.04	Fracture	42	340	0.1	0.38	1	Undulating	Rough	7	Closed			Dry	SW
8.07	Joint	80	216	2	5	7	Undulating	Smooth	2	Open			Dry	SW
8.84	Fracture	72	34		0.6	4	Undulating	Rough	11	Open			Dry	SW
11.29	Fracture	36	214		0.4	3	Undulating	Smooth	3	None			Dry	SW

Table 3.9: Scanline 6, coherent ava at the south western tip of Cave Rock, near start of steps up to top of the outcrop. Scanline is 4.2 m long and crosses 10 discontinuities over the length of the line.

Location: Cave Rock, SW Tip, Steps up p Date: 14/01/20 Photos: 1:53 cc phone
Rock Type: Coherent lava Batter orientation: N/S Scanline Number: 13 Length: 5m

		Orientation					Roughness				Strength (MPa) or			
Scanline chainage	Feature Type	Dip	Dip Direction	Spacing (m)	Trace length/ persistence (m)	Aperture (mm)	m scale	cm scale	Asperity amplitude (mm)	Infilling/ alteration type	Infilling / alteration	Intact Rock	Water	Weathering
0.25	Fracture	80	20	0.1	0.3	1	Planar	Rough	3	Closed			Dry	SW
0.45	Fracture	80	40	0.1	0.5	1	Undulating	Smooth	2	Closed			Dry	SW
0.78	Fracture	54	350		0.3	3	Planar	Rough	4	Closed			Dry	SW
1.4	Joint	68	325	2	4	60	Undulating	Rough	6	Open			Dry	SW
1.6	Fracture	60	134	0.5	1	2	Undulating	Smooth	2	Closed			Dry	SW
1.9	Fracture	70	346	0.3	1.2	3	Undulating	Rough	4	Open			Dry	SW
2.6	Fracture	34	310	0.2	1	3	UNdulating	Smooth	6	Closed			Dry	SW
3.35	Joint	56	170	0.35	1	5	Undulating	Smooth	11	Open			Dry	SW
3.9	Joint	72	98	0.35	1.2	18	Undulating	Smooth	9	Open			Dry	SW
4.2	Fracture	80	36		0.3	1	Undulating	Smooth	10	Open			Dry	SW

In both rock types, discontinuity roughness is planar or undulating on the metre scale and smooth or rough on the centimetre scale, with apertures ranging from closed to up to 10 mm for fractures and up to 18 to 60 mm for the larger joints. Dips range from 30 to 90 degrees and dip directions are in all directions. All discontinuities are dry and slightly weathered.

Using the scanline data it is possible to gain a value of discontinuities per metre for the coherent lava unit and the breccia unit. The breccia has a range of 0.19 to 0.27

discontinuities/m and the coherent lava unit has 1.24 to 2.38 discontinuities/m which equates to the coherent lava having 6 – 8 times more fractures per metre than the breccia.

Geologic Mapping

The mapping results from fieldwork at Cave Rock are a 2D geologic map that influenced the modelling and creation of a 3D geologic model of Cave Rock. The rock mass has been split into 3 main units of breccia, tuff and coherent lava with medium, low and high fracture amounts. While there are three variable levels of fracturing in the coherent lava around the outcrop, the area of the geophysical survey encountered medium fractured lava only.

The grey coherent lava present at Cave Rock is vesicular with abundant white crystals up to 1.5 cm long, likely to be plagioclase feldspar. The coherent lava is very weathered in places showing spheroidal weathering, with orange/red staining along semi-circular fracture planes, especially at the base of Cottage Rock (Figure 3.6). It is also noted that the coherent lava that Cottage Rock is made of also outcrops in a line of multiple small 1-3m outcrops in between Cottage Rock and the most South Westerly edge of Cave Rock. A small stone wall has been erected along this line of outcrops which continues towards where the central lava sheet begins at the South West end of Cave Rock (Figure 1.4).

The red brown volcanic breccia also has a high amount of white crystals present and is highly vesicular. Clast size ranges from 5 cm to 1 m and the sorting of clasts is very poor. In some places around the cave, especially those south facing and covered in moss, it is difficult to distinguish between different clasts and matrix.

The tan brown to orangey red tuff layer traceable throughout Cave Rock and visible in the hills to the south, has grainsize predominantly of fine sand size with clasts of larger white crystals and basaltic scoria ranging from 0.5 – 20 cm but mostly lapilli sized - less than 3 cm. The tuff is matrix supported and poorly sorted with 20 – 40 % clasts. There are also areas that are small lenses of scoria clasts (> 5 cm) that are clast supported.

The structure of Cave Rock consists mainly of breccia, which has been separated into upper and lower breccia in the 3D model for plotting purposes (green). Within the lower breccia is the central lava unit, with medium fracture density (light purple). This central lava unit forms

the western wall and ceiling of the cave and can be seen at both the north and south ends of the outcrop (Figure 3.7). Sitting above the top of the lower breccia and central coherent lava is the orange tuff layer (orange), which drapes the lower breccia and central coherent lava. Atop the tuff is the upper breccia and the stratigraphically highest unit is a layer of coherent lava (purple) that increases in thickness and prevalence on the northern side of the outcrop (Figure 3.8). Online Appendix 4 is a link to a YouTube video showing spinning and slicing of the leapfrog 3D model.

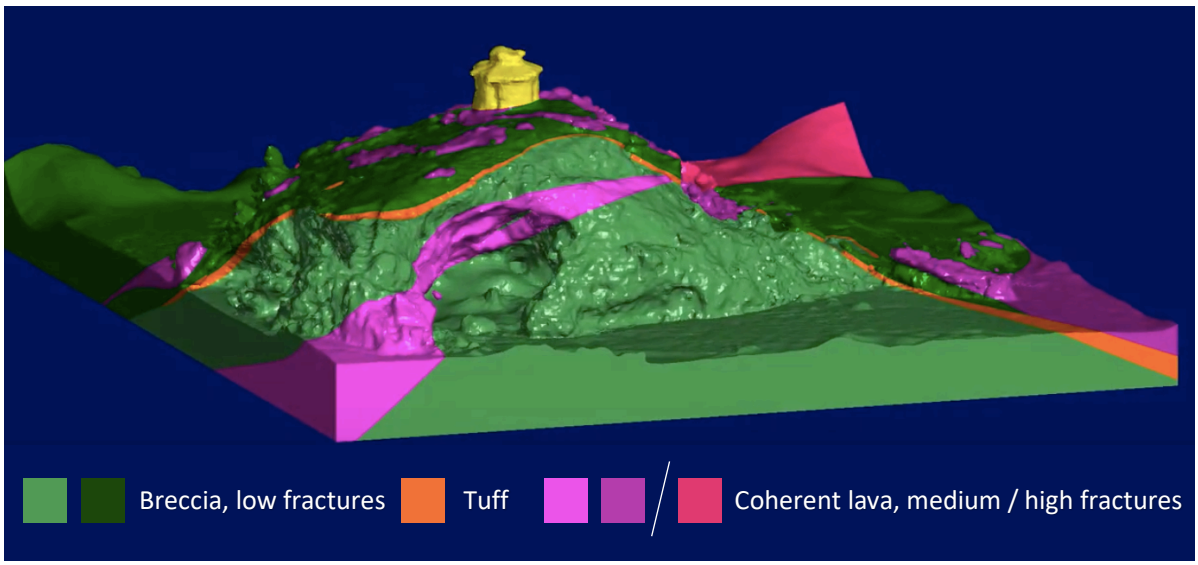

Figure 3.7: Oblique view of the leapfrog geothermal model looking north. Coherent lava with medium fractures is coloured purple, breccia upper and lower in green and tuff in orange. The man - made mast tower has been coloured yellow. Front and centre is the central coherent lava sheet with medium fractures (pink) that forms the ceiling of the cave tunnel.

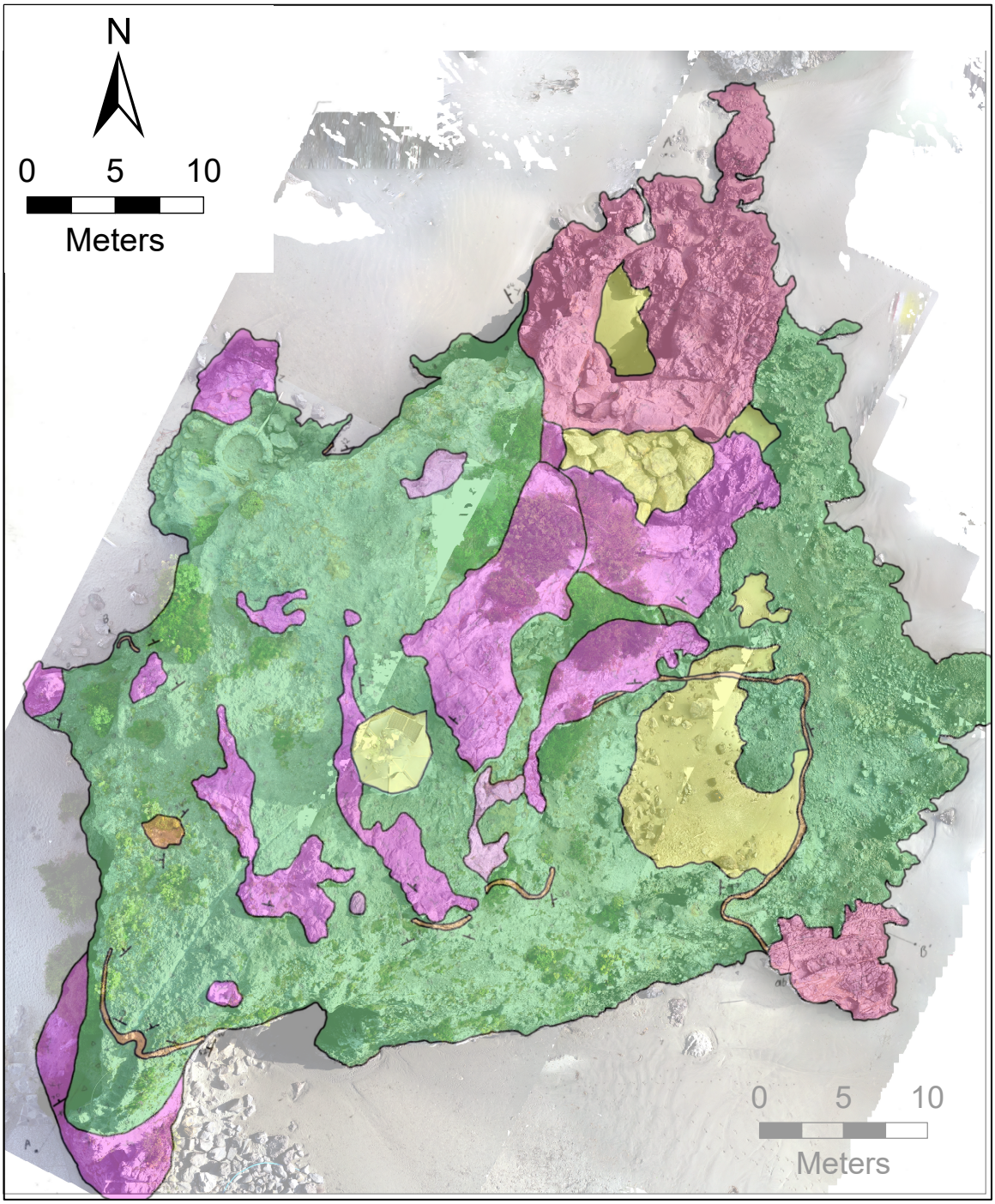

Figure 3.8: Geologic map of Cave Rock used for constructing the 3D geologic model. Purple is lava, pale green is breccia and orange is tuff.

Structural measurements and lithologic relationships

Overall, the structural patterns present at Cave Rock fall into two main dip directions. Below the orangey – red tuff layer the lower breccia and central coherent lava layer with medium fractures has lithological boundaries that dip between 45 and 70 degrees to the north west.

Comparatively, the tuff, upper breccia and capping coherent lava with varying fractures generally dip northwards with angles between 10 degrees and 40 degrees. The difference between structural trends above and below the tuff layer is seen distinctly in the northern end of the cave tunnel (Figure 3.9), where dipping bands of coherent lava and breccia clasts have clearly different habits. The tuff, upper breccia and capping coherent lava also show a draping habit where the tuff has blanketed the underlying units and then the upper breccia and coherent lava lie stratigraphically above. In the cliff face of Richmond Hill (Figure 3.10), lithologies appear to be mostly breccia with a layer of tuff above and stratigraphically highest is a layer or of coherent lava. The lithologies in the cut off ridge that forms the Richmond Cliff face trend north – north east and dip an estimated 20 – 40 degrees.

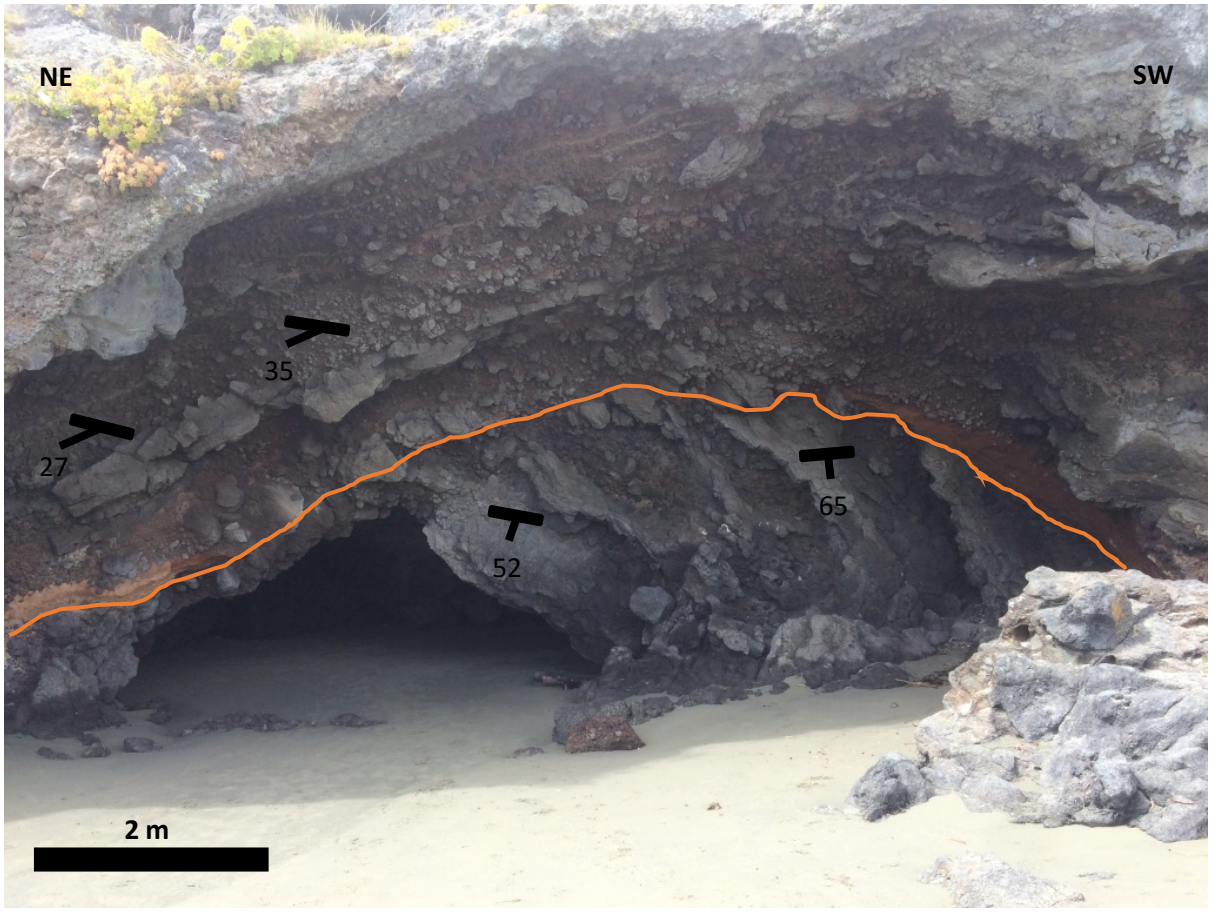

Figure 3.9: Image of layers displaying varying structural patterns at the north end of the Cave Rock tunnel entrance. Below the tuff layer, marked in orange, the units dip north west whereas above the tuff the units are dipping more north.

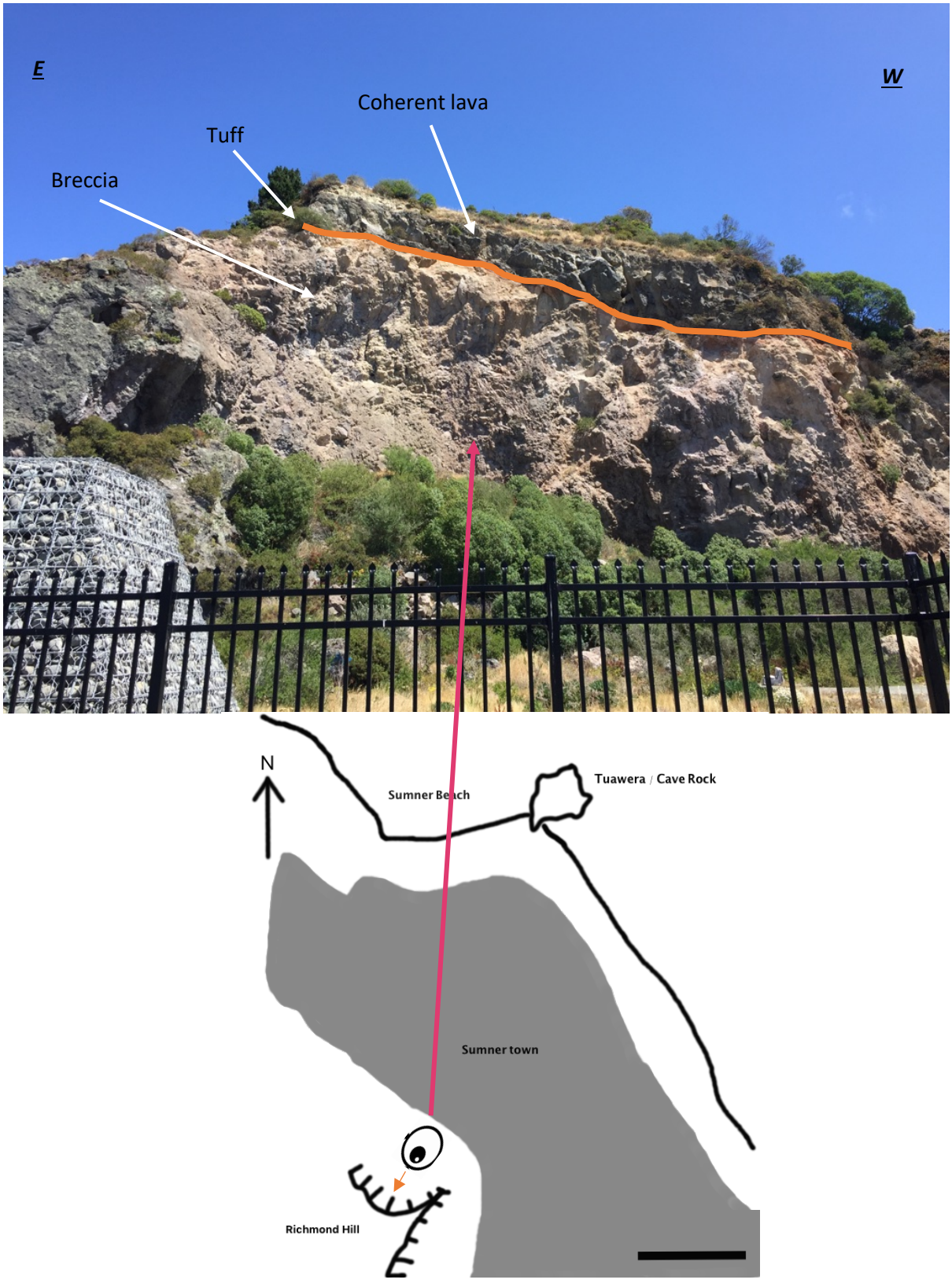

Figure 3.10: Map and photo showing Richmond Hill cliff face to the south of Cave Rock. The cut off ridge trends north – north east and dips an estimated 20 – 40 degrees.

3.3 Geophysical surveys

The results from the geophysical surveys show a range of velocities and frequencies of recorded waves through varying lithologies and orientations for each shot type.

Seismic signal of different sources

With each shot, each 3C geophone records a wave arrival for each of the x, y and z components (Figure 2.13) which then is converted and displayed as 24 individual traces when opened in ReflexW (Figure 3.11). From here, picking the first significant arrival of energy was done manually for each of the shots at each location. These pick files were loaded into excel and sorted and then used to work out velocities once the distance between each shot and geophone had been calculated. Different sources were explored to find the most appropriate seismic source for the experiments.

The geophone traces shown in Figure 3.11 compare wooden plank (a) and direct rock hit (b) and both hit types from South East ridge show clear wave arrival signatures with small red x's marking the manual first arrival pick however, there is a slight difference in frequency of recorded wave visible when examining the frequency spectrum plots of each hit. The average of the frequencies recorded varies slightly between hit types at the South East Ridge site, with wooden plank recording 187.3 Hz and direct rock hits 198.6 Hz (Figure 3.12).

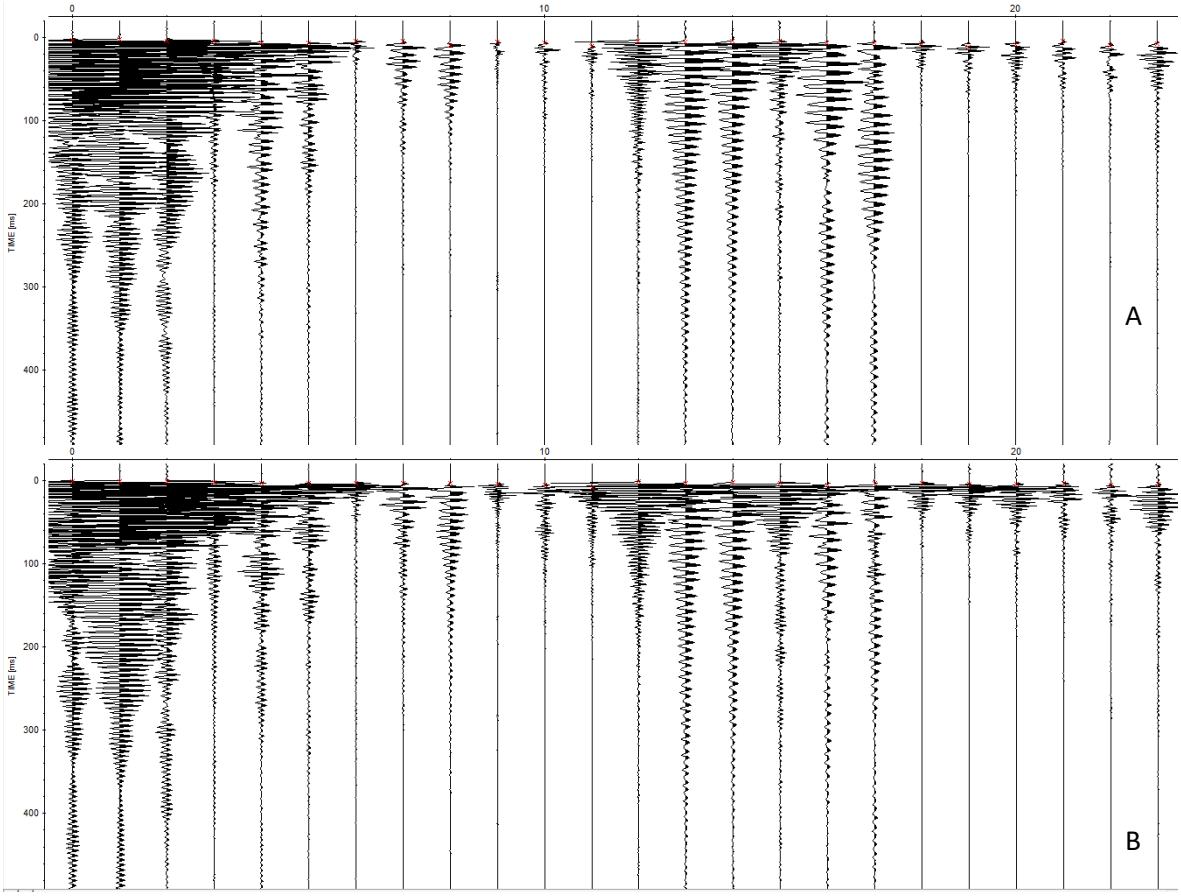

Figure 3.11: Geophone traces from South East Ridge Hits. A. Wooden Plank, B. direct rock hit. Red crosses mark manual picks of first significant arrival of energy. Direct rock hits have larger arrival amplitude for the same geophone array, seen in the wider horizontal range of the traces.

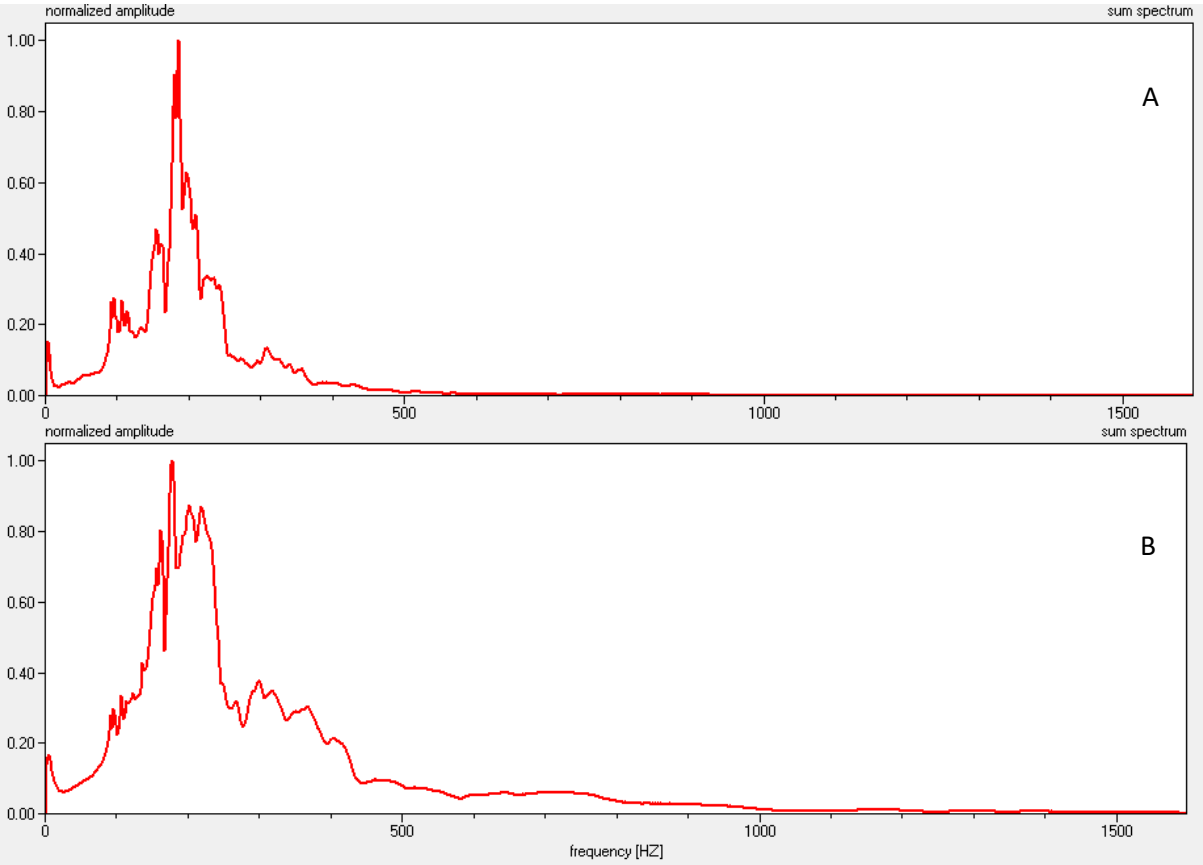

Figure 3.12: Frequency spectrum plots for South East Ridge shots. A. Wooden Plank hits 187.3 Hz, B. direct rock 198.6 Hz. This frequency is the average for all geophones from each shot type and is the frequency of the recorded wave.

As seen in the South East Ridge experiments, each of the source types at Cottage Rock have varying signatures of p wave arrival and different recorded frequencies at the geophones, summarised in Table 3.10. Both small sledge hammer and Estwing geologic hammers, hitting directly onto the rock surface resulted in a higher average frequency of recorded wave (185.5 Hz for small sledge and 128.5 Hz for Estwing). Comparing the wave signatures of both hammers the small sledge hammer gives a larger amplitude of recorded wave, resulting in less manual amplification of the traces to perform picks, and a higher frequency of recorded wave, enabling more accurate picking of first arrival.

Table 3.10: Summary table of recorded frequencies for different shot methods conducted at Cottage Rock. Direct rock hits by both small sledge hammer and Estwing are the highest frequency of the hammers, but the small sledge has significantly higher frequency and more significant energy signatures on the geophones, which makes for easier and more accurate manual picking. Average frequencies were calculated using 10 sets of frequency spectrum graphs for each shot type.

Shot Type	Average frequency of recorded wave (Hz)
Small sledge hammer rock	185.5
Small sledge hammer wood	113.5
Small sledge hammer metal	115.7
Estwing Rock	128.5
Estwing wood	117.5
Estwing metal	119.4

Using the frequency of the recorded wave of the direct rock hits from the small sledge hammer, 185.5 Hz, and the velocity ranges for the arriving p waves at each geophones, it is possible to calculate the wavelength of the arriving waveforms (wavelength = velocity / frequency). The lowest velocity for direct rock hits at Cottage Rock are 500 m/s, resulting in a wavelength of 2.7 m, average velocity of 2120 m/s results in wavelengths of 11.4 m and maximum velocities of the dense cluster (Figure 3.14) 2500 m/s results in a wavelength of 13.4 m.

Cross hole sonic logging

Cross-hole sonic logging techniques were used to measure p wave velocities in basaltic bedrock on Mt Pleasant, which is 6km from Sumner with comparable geology (Figure 1.6). The site was in a bench cut for a house which we drilled 30mm holes 0.5 m apart (Figure 1.3). The plan was to drill holes and measure velocity over 0.5m, 1m, 2m and 3m intervals but the high frequency source struggled to reach the receiver in distances over 0.5m. Measurements obtained ranged from 4629 to 5952 m/s using the piezometric cross hole logging kit. This is higher than measurements obtained at Sumner Beach, and although fractured, the rock chunks recovered from the drill holes had fewer pores than those at Sumner Beach.

Seismic velocity

The primary wave velocities of shots from South East Ridge (Figure 3.13) range from 1448 m/s to 4319 m/s for direct rock hits and 1200 m/s to 3207 m/s for hits onto a plank on the sand. The average velocity for direct rock hits is 160 m/s faster than the shots where the hammer hit a plank (2877 m/s vs. 2710 m/s) but overall the overlap between all of the velocity values is considerable and difficult to pick apart.

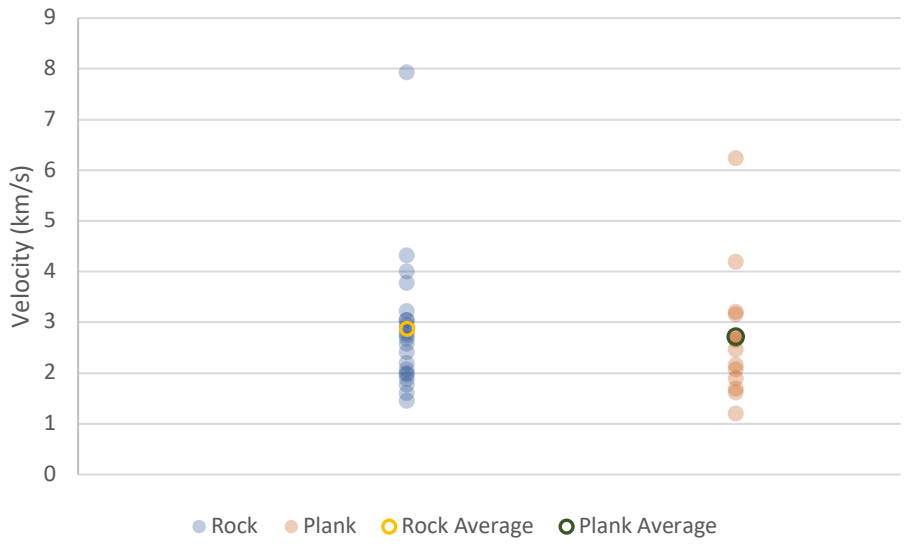

Figure 3.13: P wave velocities for rock hits vs plank hits for South East Ridge survey location. Data points have 70 % transparency applied to see density of clusters. Average p wave velocity is slightly less for plank hits than direct rock by 160 m/s.

The p wave velocity results from Cottage Rock show large variation from 527 m/s to 6007 m/s, but the majority of values fall between 904 and 4200 m/s (Table 3.11). Rock hit velocities on average are 600 m/s faster at Cottage Rock than hits on wood and metal plates on the sand (Figure 3.14) therefore direct rock hits were used only in future experiments. Direct rock hits also showed less variation in velocity, which meant the experiments were able to be more accurately reproduced.

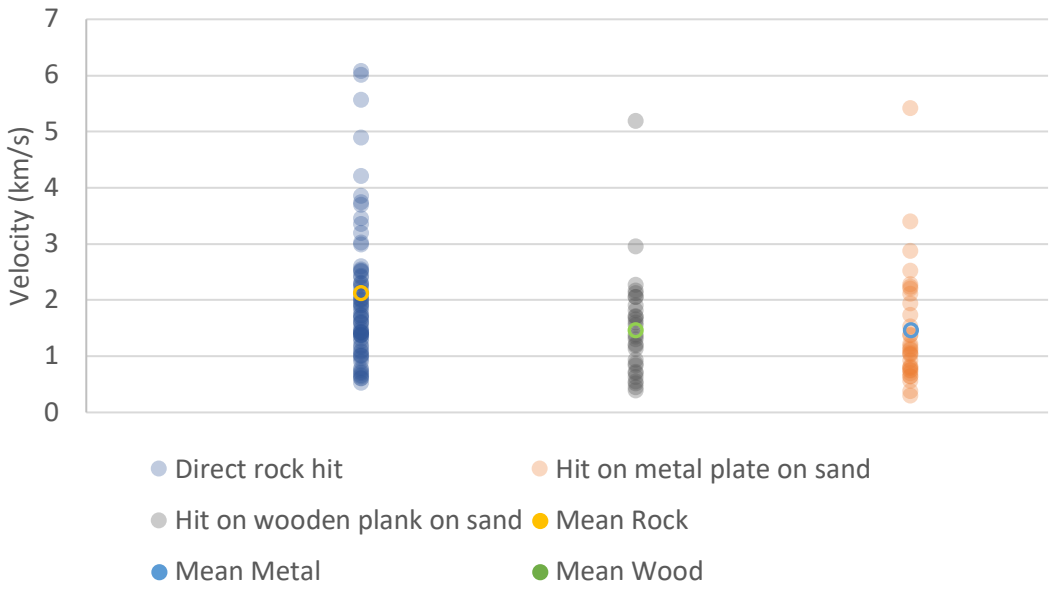

Figure 3.14: Scatter plot of p wave velocities comparing rock hits, wood hits and metal disc hits at Cottage Rock. Dots have 70% transparency applied to show cluster densities. Average rock hit velocities are on average 600 m/s faster than wood and metal hits.

P wave velocity results summarised in Table 3.11 displays upwards hits and sideways hits with both sledgehammer and Estwing geologic hammer. Initially, two different shot orientations were intended to be used to asses shear wave velocities from each shot but was beyond the scope of the project. However, the two different hit types, upwards and sideways, were both still included in further analysis of p wave velocities. Average p wave velocity for all sideways hits is 2270 m/s while upwards hits average is 2120 m/s, both values being similar, and it can be seen from Figure 3.15 there is significant overlap of p wave velocities between geophone across all direct shots performed at Cottage Rock.

Table 3.11: Summary table of rock hit p wave velocities from Cottage Rock shots. Geophone numbers are left hand side column while shot numbers and source types are on right. Up is upwards hit and side are sideways hits and an 'e' at the end of code indicates shot was performed with an Estwing geologic hammer.

	Velocity (m/s)										
Geophone	2001c up	2001d side	2002c up	2003ce up	2004ce up	2004de side	2006a side	2006b up	2007a side	2007b up	Average
1	739	527	2873	1907	698	609	955	1499	1587	1364	1276
2	2986	4394	3965	3691	1560	3603	1164	1852	1937	1595	2675
3	2012	3016	4200	1898	1606	2473	1672	0	999	720	2066
4	604	1424	740	780	754	1181	1375	1426	1428	1372	1108
5	3348	4252	2507	2178	1715	6181	1414	2138	1690	1678	2710
6	3850	6471	3266	2423	1728	2986	1337	2008	1473	1043	2659
7	3189	3942	4893	2594	2301	2523	1799	2285	2538	1308	2737
8	2502	2429	4164	2400	2252	1987	1091	1074	0	0	2237

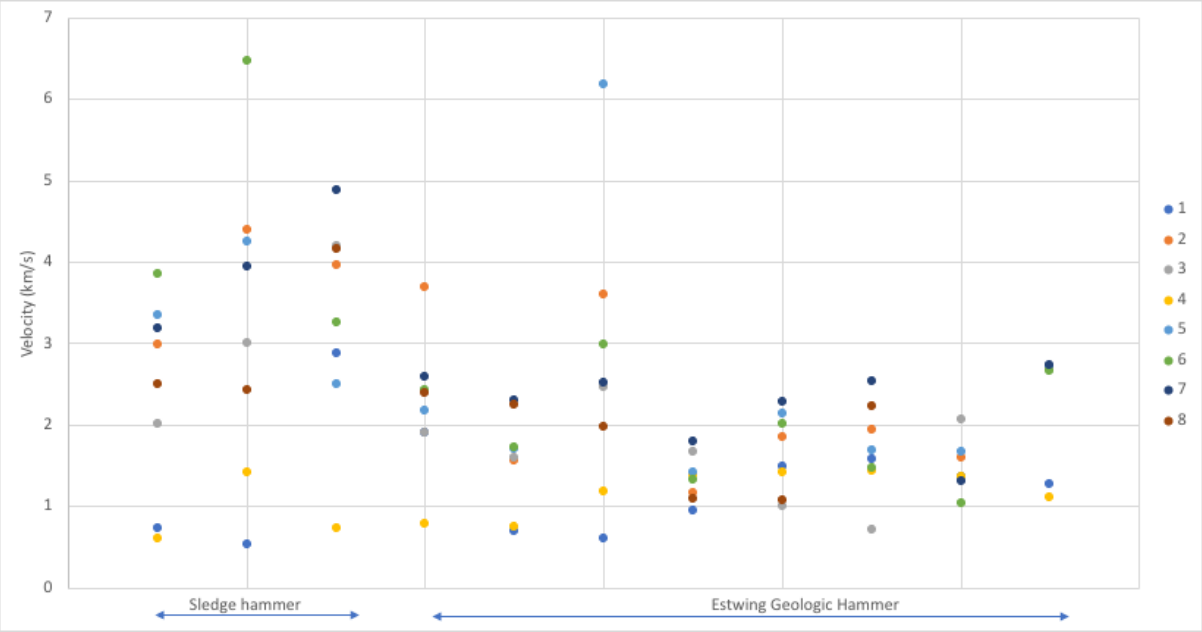

Figure 3.15: P wave velocity values for each geophone for each of the shots performed at Cottage Rock. Direct rock hits only are displayed with hits on plank and plate excluded. Sledge hammer hits have faster velocity and an overall greater range of velocity values compared to those shots from the Estwing geologic hammer.

Vp and lithology relationships in the field – Tuawera / Cave Rock

The purpose of using Cave Rock for a seismic survey was to analyse the influence of varying proportions of different lithologies and fracture densities on seismic velocity. Once the geologic model had been created, each shot path was sliced in the model and the amount of each rock type was measured as a percentage to plot on a ternary diagram (this process is outlined in Figure 3.16).

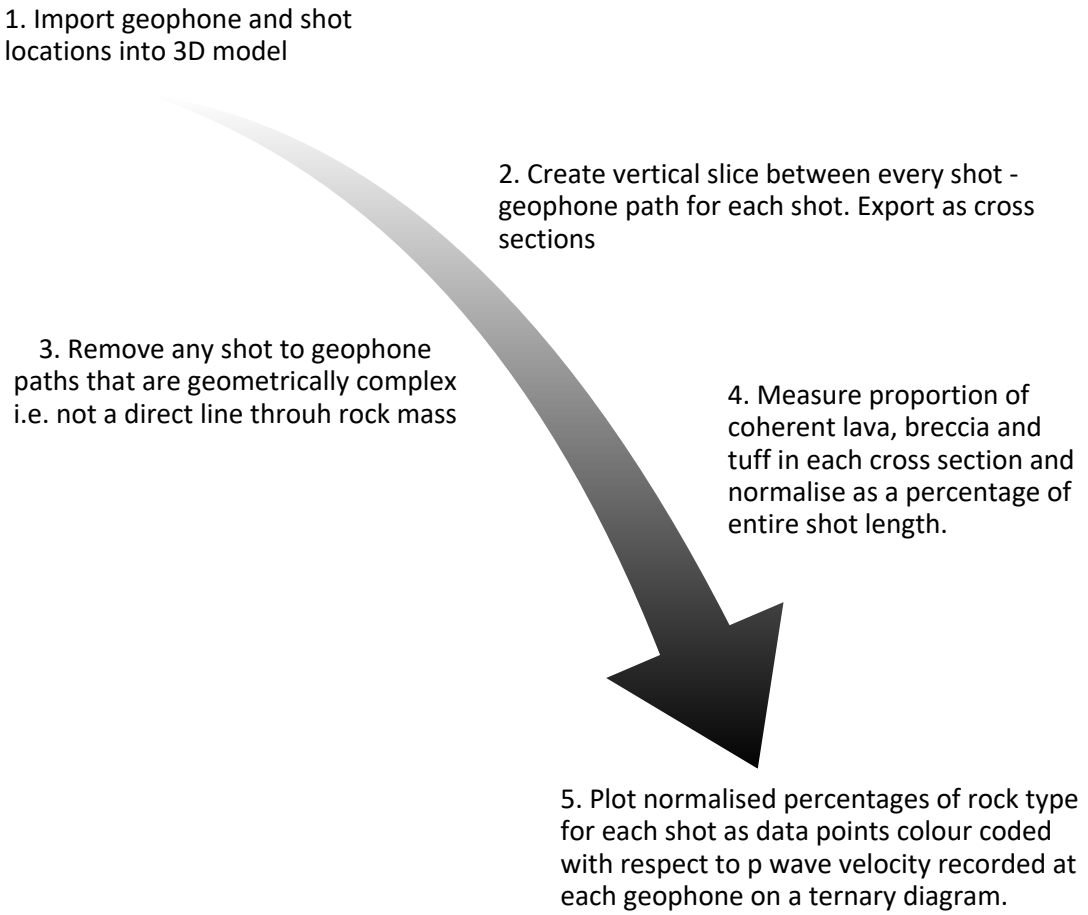

Figure 3.16: Flow process of creating ternary diagrams of the relationship between lithology type and p wave velocity.

The preliminary raw velocity results from the Cave Rock survey produced p wave velocities ranging from 761 m/s to 2805 m/s (absolute maximum of 4068 m/s) with all shots having similar p wave velocities throughout all geophones apart from shot 1e upwards, having an average velocity range between 1989 m/s to 4068 m/s.

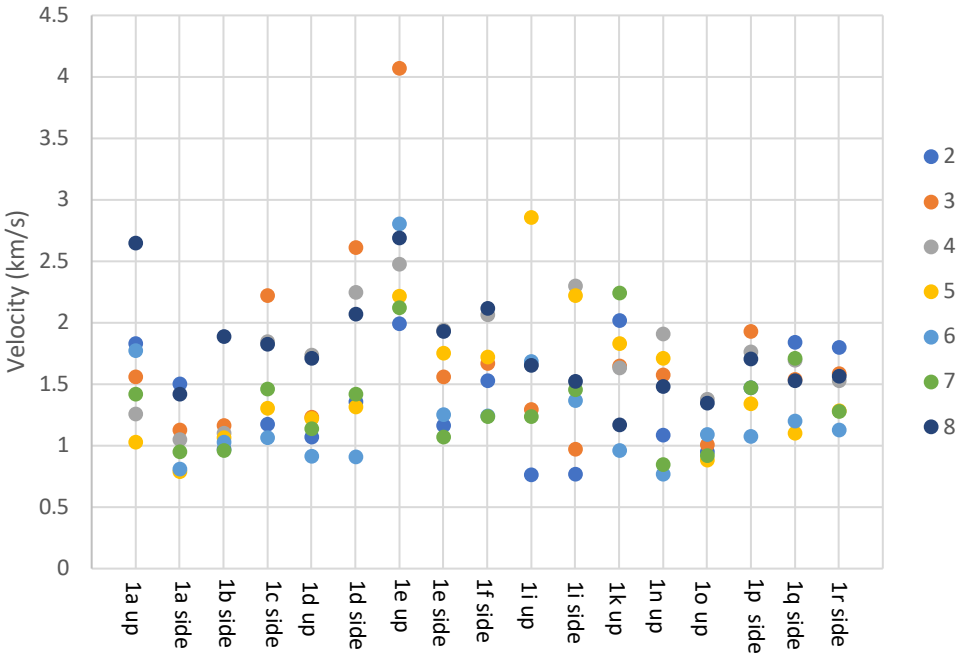

Figure 3.17: Scatter plot of average velocities from Cave Rock geophone survey. Points are colour coded for each geophone number and separated by shot numbers. Velocities range from 761 m/s to 2805 m/s and all shots have similar velocity ranges apart form 1e upwards, which ranges from 1989 m/s to 4068 m/s.

Correlating the results from the preliminary p wave velocity results and the proportion of each rock type in a table then plotting this on a ternary diagram shows few relationships between varying lithologies and p wave velocity. In Figure 3.18 and Figure 3.19 the sideways hits and upwards hits have been separated to show the different values in the cases where shots with two different directions at the same location can be plotted without overlap. Neither of the ternary diagrams show a clear increase or decrease in p wave velocity with increasing or decreasing coherent lava and breccia with significant overlap between dark purple dots (fast velocity) and pale orange dots (slower velocity). Tuff percentage stays relatively consistent between 0 – 10 %, breccia percentage falls between 40 – 95% (with the majority from 70% upwards) and coherent lava varies from 5 – 30%.

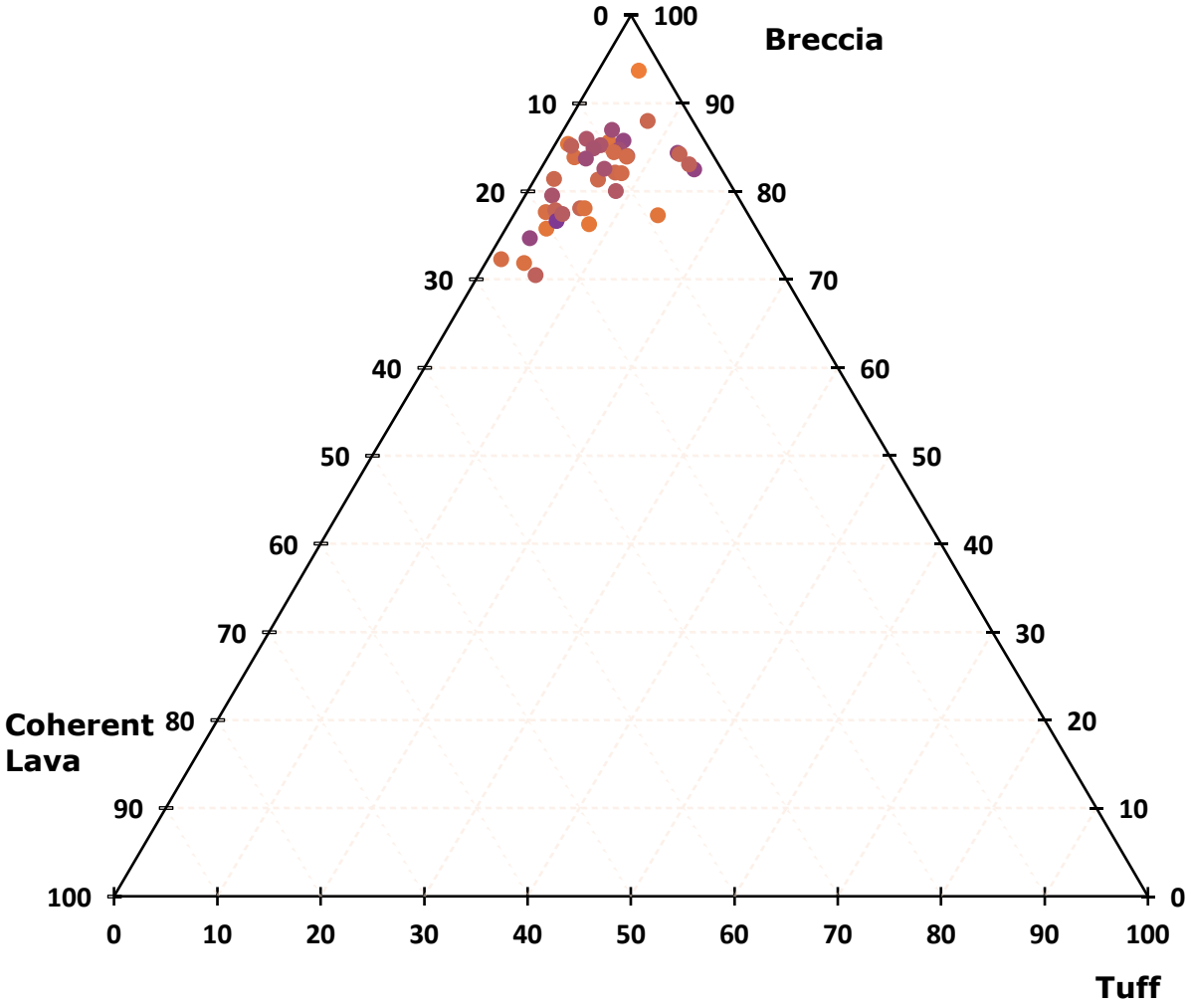

Figure 3.18: Triangular plot of sideways shot p wave velocities through varying percentages of breccia, lava and tuff from Cave Rock. Darker purple represents faster velocity and pale orange slower. There is no clear correlation between p wave velocity and percentage of breccia, coherent lava and tuff visible in this dataset.

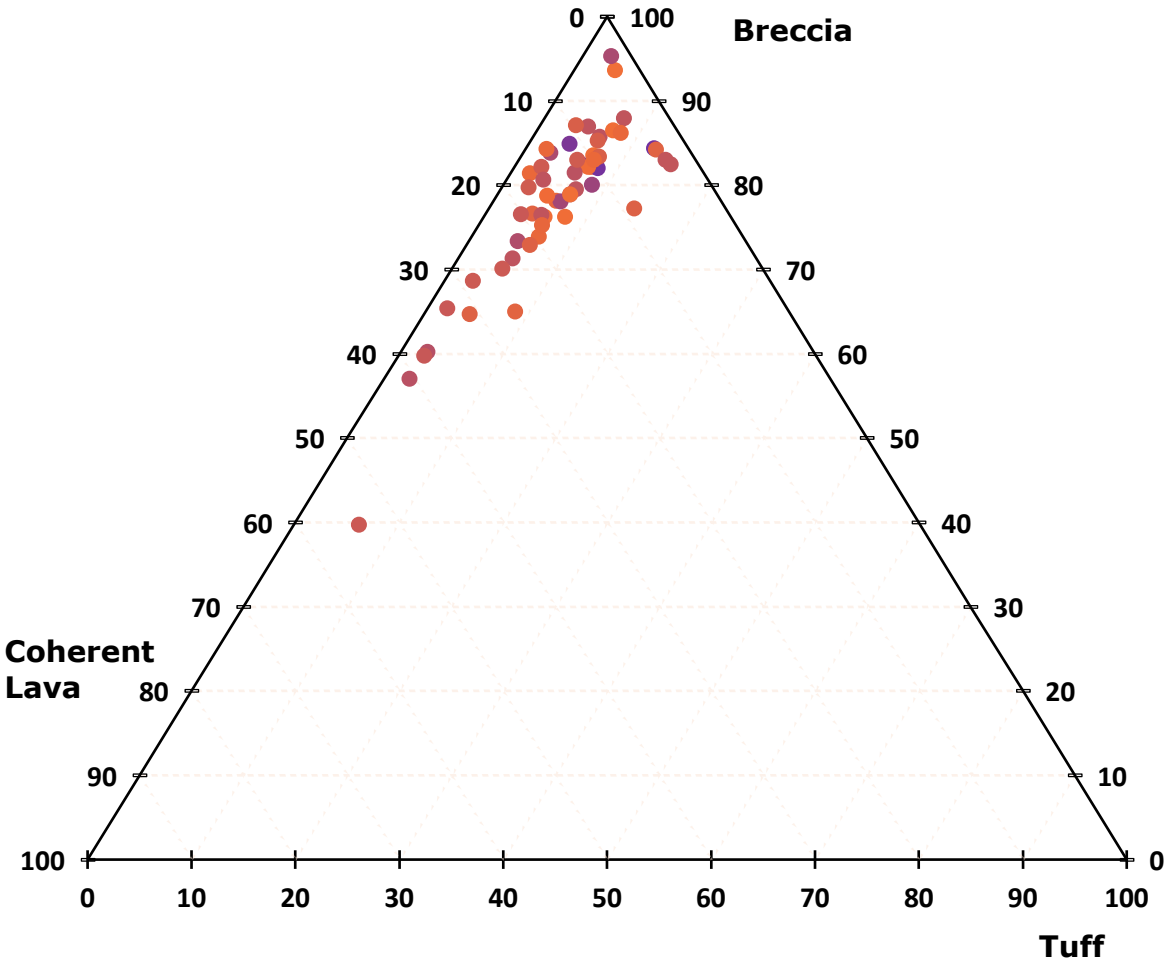

Figure 3.19: Triangular plot of upwards shot p wave velocities through varying percentages of breccia, lava and tuff from Cave Rock. Darker purple represents faster velocity and pale orange slower.

3.4 Results Summary

- Vp and Vs vary between lithologic samples collected at Sumner beach – coherent lava cores (Vp 2872 m/s and Vs 1257 m/s), breccia (Vp 2221 m/s and Vs 1104 m/s) and tuff (Vp 2080 m/s and Vs 1079 m/s) show different primary and shear wave velocities when measured in laboratory conditions.
- Fractures in core samples reduce velocity when perpendicular to energy direction but can have an increase or no influence if oriented parallel to energy propagation – P wave velocity decreases from 2979 m/s to 1136 m/s after three perpendicular fractures were introduced. S wave velocity has been shown to increase and P wave velocity increase or stay the same when parallel fractures are introduced.

- Coherent lava and breccia present at Sumner Beach have significantly different discontinuity densities – Scanlines undertaken at Cave Rock return 0.2 to 0.3 discontinuities/m for breccia coherent lava 1 to 3 discontinuities/m.
- Field Vp measurements show no distinct correlation between ray paths with varying lithology percentages – Increasing coherent lava or breccia shows no relationship to p wave velocity changes over shot lengths of 9 – 25 m.

Chapter 4: Discussion

This chapter discusses the results and relationships between laboratory experiments, field mapping findings and geophysical study p wave results. While the laboratory testing gathered data on both p and s wave velocities, the shot orientations in the field geophysics surveys did not enable straightforward s wave picking so only the influence of fractures and heterogeneity on p waves will be discussed.

4.1 Laboratory experiments

Analysing the results from the laboratory experiments conducted on rock samples from Cave Rock provides insight into understanding the results from the Cave Rock field experiments. When comparing the Vp and Vs of the intact rock cores for the different lithologies and the fracture and stack experiments on the same rock types there are distinct decreases with increasing fracture number. The coherent lava cores show both the highest density and p wave velocity of 2872 m/s (Table 3.1), however, it only takes one horizontal cut for the velocity through a core of coherent lava to drop to 2255 m/s, just above the average for breccia (2221 m/s) and tuff (2080 m/s). After two horizontal cuts, p wave velocity through coherent lava drops to 1621 m/s and after three cuts the p wave velocity dropped further to 1136 m/s. This velocity drop in the fracture experiment shows that initially in intact rock, lithology plays a role in p wave velocity but once fractures are introduced lithologic p wave variability can be overprinted by the dominant influence of fractures. Kahraman (2001) acknowledges that discontinuities play a role in sound wave velocities and document this relationship between discontinuity and p wave velocity in granite where after 3 'joints' simulated in the lab, p wave velocity reduces from 5500 m/s to 2000 – 3000 m/s, while Anderson et al. (1974), Castagna et al. (1985) and Savage (1999) also show that p wave velocity greatly reduces when fractures are oriented perpendicular to energy direction. Increasing fracture density in core samples of coal has also been shown to decrease p wave velocity (H. Wang et al., 2015).

The lab results from the Cave Rock samples show similar relationships to studies by others (Anderson et al., 1974; Dinçer et al., 2004; Kahraman, 2001) of decreasing wave velocities due to fracture orientations and lithology changes (Liberty et al., 2015). Relationships between p

wave velocity and lithology has also been well documented and shows similar relationships to my findings. P wave velocity in lavas from Mt Ruapehu, NZ, ranges from 3701 m/s to 4472 m/s for altered and unaltered coherent lava, 2390 m/s to 3112 m/s for unaltered and altered brecciated lava margins and 4767 m/s to 4118 m/s for unaltered and altered intrusions (Mordensky, Villeneuve, Kennedy, et al., 2018).P wave velocities from hydrothermal andesite lavas and breccia of around 4165 m/s from the Taupo Volcanic Zone, NZ (Wyering et al., 2014). Velocities of tuffs from central Italy range from 3100 m/s to 4200 m/s (Vinciguerra et al., 2009) and 2000 m/s to 3000 m/s from Campi Flegrei (Vanorio et al., 2002). The results from Cave Rock show similar p wave velocity relationships for tuff, coherent lava and breccia with the fastest p wave velocity typically in coherent lava while breccia is lower and tuff slightly lower again.

My studies also show that after simulating fractures parallel to energy direction, p wave velocity showed little to no decrease in velocity. Vp has been shown to decrease in the lab with fractures perpendicular to energy direction, but also show little change with fractures oriented parallel to energy direction. This has implications for shot paths in the field for sections of coherent lava with cracks perpendicular to energy propagation having a large influence on Vp where cracks parallel to energy may have little to no influence on p wave velocity.

4.2 Mapping

The geologic mapping and scanline fracture mapping at Cave Rock document relationships between geotechnical units and discontinuity densities between them. The orange – red tuff layer and the capping lava present at Cave Rock represent small portions of the seismic shot paths while the upper and lower breccia and central lava represent the dominant lithologies. From the scanlines at Cottage Rock and Cave Rock, coherent lava on Sumner beach has an average discontinuity density of 1 to 3 discontinuities/m and breccia 0.2 to 0.3 discontinuities/m. Although the coherent lava makes up only 5 – 30% of each shot path, it has been shown in the lab that three fractures introduced perpendicular to energy propagation into a coherent lava core can decrease Vp by over 1800 m/s from 2979 m/s to 1136 m/s, lower than cores of tuff and breccia. Initially it was hypothesised that the shots with the most coherent lava percentage in the ray path may be the fastest as it was the densest, highest

velocity lithology in the absence of fractures. However, the results from the scanlines suggest that the coherent lava was significantly more fractured. This, together with the laboratory data on the influence of fractures, suggests that both fractures and lithology need to be considered in the interpretation of seismic velocities. The scanlines also showed that discontinuity orientations varied significantly through the coherent lava unit, meaning that no shot – geophone path had significantly more or fewer parallel or perpendicular fractures compared to any of the other shots. This resulted in all shots having sections of coherent lava with numerous fractures and joints throughout, which will influence and reduce the seismic energy through attenuation of energy through scattering, dispersion and reflection of the waves due to the fracture component.

Another finding from the field results and cross sections sliced from the geologic model was that some of the shot points inside the cave did not have a direct line through the outcrop from shot to geophone. The advantage of using the tunnel through Cave Rock was that surface waves, travelling along the surface of the outcrop, would have to travel around to the end of the tunnel and back up over the top to each geophone, arriving later than the p waves directly through the rock mass which would make for clearer and easier first wave arrival picks. If the cross section between shot and geophone was not a direct line through rock mass, or had an unusual geometry relationship with the wall of the cave, it was not included in velocity calculations or plots.

Volcanic setting and history of Cave Rock

From the field measurements and observations at Sumner Beach, the volcanic history can be split into two different time intervals with two different possible interpretations. The volcanic deposits at Sumner Beach likely flowed from a source vent to the south east, forming the lower breccia and central coherent lava layers. This lower level deposition was followed by a period of erosion from valleys and radial drains which was followed by a second eruptive period, beginning with pyroclastic deposits (the orangey – red tuff layer) and then subsequently upper breccia and upper coherent lava layers.

Typical valleys on cone volcanoes form valleys that then erode along the directions of past flows, leaving flat surfaces with smaller radial drains (Figure 4.1) (Cotton, 1944; Hampton &

Cole, 2009). It is possible that due to the location of Sumner Beach being within two overlapping cones of the Lyttelton Volcanic Complex (Hampton & Cole, 2009), that different stages and orientations of lava flows may overlap with varying orientations. Another possible interpretation is that the two varying structures present at Cave Rock formed by initially being the sides of a valley flow followed by a period of erosion, after which Cave Rock was in the location of the bottom of a valley (Figure 4.2). Lava flows in eroded channels can have varying strikes and dips depending on channel orientation, with flows in the bottom of a pre-existing channel flowing parallel to long axis of channel, while on the side of the channel flows may dip more inwards (Figure 4.1). If two flows are separated by an unconformity, dips of flows above and below the unconformity surface would be expected to have different dips to each other.

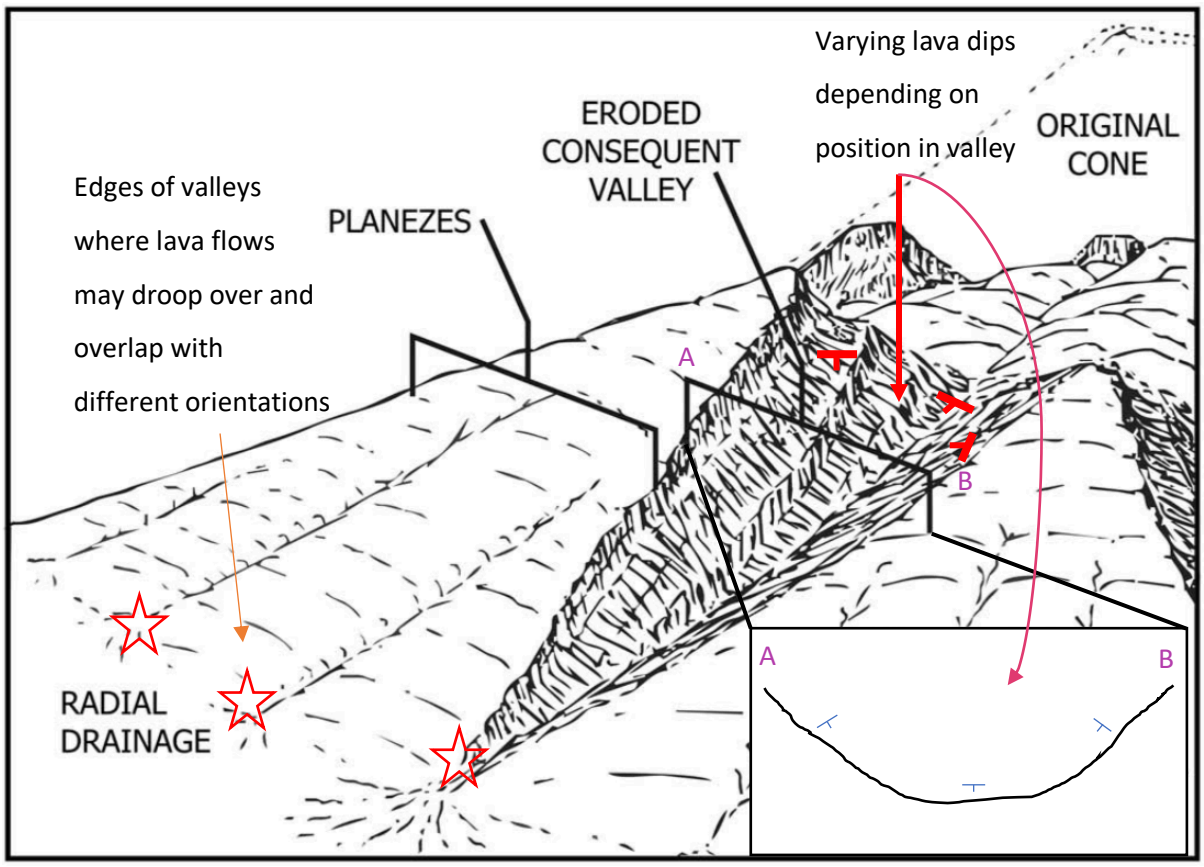

Figure 4.1: Model of typical volcanic planezes from erosion features and radial drainages (modified from Cotton (1944) and Hampton and Cole (2009). Small red stars locate possible areas where bottom unit of Cave Rock (underneath tuff) may have formed.

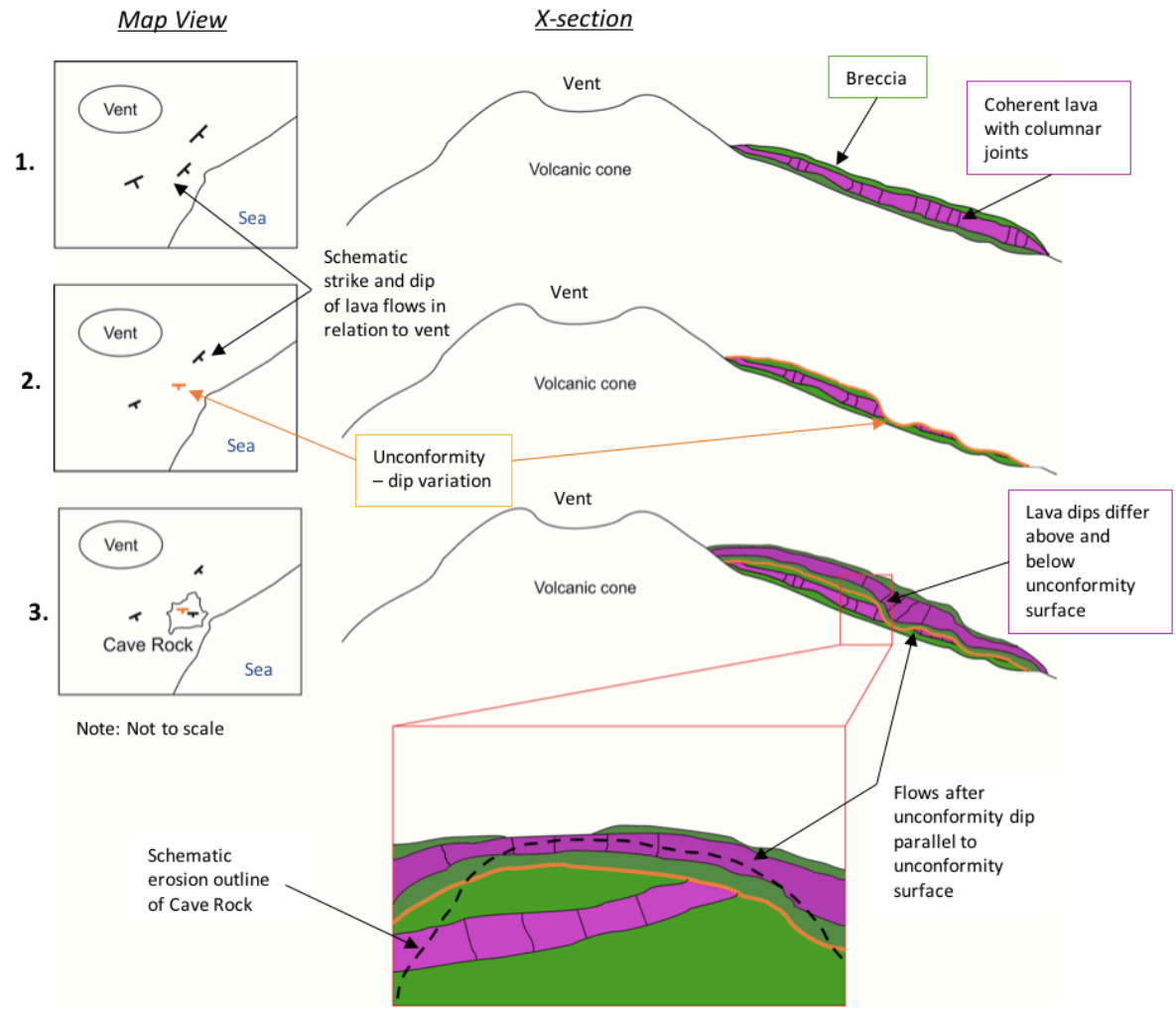

Figure 4.2: Schematic of coherent lava and breccia flows and their structural relationship to location of formation in lava flow channel.

4.3 Geophysical surveys

Cross hole sonic logging

The plan for the cross hole sonic logging experiment was to drill holes and measure velocity over 0.5m, 1m, 2m and 3m intervals but the high frequency source struggled to reach the receiver in distances over 0.5m. This is most likely due to the basalt being highly fractured and the energy being attenuated rapidly. To gather velocity measurements over a longer distance using this method it would require a material with less discontinuities or a source with a slightly lower frequency to penetrate the rock mass. The velocity results from Mt Pleasant were significantly higher than those at Sumner Beach (5290 m/s average Vp) which could be due to lower porosity and weathering at Mt Pleasant. Although it was difficult to retrieve

intact core from the Mt Pleasant site, fractured chunks of basalt had far fewer pores than those samples collected at Sumner Beach.

Influence of lithology and fractures on seismic velocities in the field

The shots from the initial geophone survey on South East Ridge and Cottage Rock showed that velocities through breccia, tuff and lava have p wave velocities that range from 1448 m/s to 4319 m/s (SE Ridge) and 527 m/s to 4200 m/s for coherent lava at Cottage Rock. While there is a slight (160 m/s) difference between direct rock hits and plank-on-sand hit velocities there is no significant difference between the two values at South East Ridge. However at Cottage Rock, there is a 600 m/s average velocity difference between direct rock hits and hits on the wooden plank and metal plate. Comparing hit types based on velocity, direct rock hits gave the fastest p wave velocity at Cottage Rock and South East Ridge.

Lesage et al. (2018) discuss the importance of frequency and wavelength, and that if a seismic source has a wavelength too long it will not accurately be able to determine volcanic structures. Using the equation wavelength = velocity / frequency, the wavelength that is the shortest will have the highest recorded frequency at the geophones. Therefore at the South East Ridge site the direct rock hits have the highest frequency and the shortest wavelength, 14 m using 2800 m/s velocity average and 198.7 Hz frequency. At Cottage Rock, the average velocity and recorded frequency results in an average wavelength of 13.4 m (2100 m/s / 185.5 Hz). A wavelength of 14 m is relatively large considering that the longest shot point to geophone distance is 11 m, but as the small sledge hammer paired with direct rock hits gives the highest frequency and shortest wavelength, this was the method used at the larger, Cave Rock survey.

At Cave Rock, the shot lengths were 9 – 25 m, and velocities ranged from 761 to 2805 m/s, with an average velocity through the outcrop of tuff, coherent lava and breccia of 1536 m/s which when compared to the frequency of arriving waves generated by the small sledge hammer (185.5 Hz from Cottage Rock and 198.6 Hz from South East Ridge), the wavelength issues discussed by Lesage et al. (2018) are minimised. Ideally, seismic sources with a higher frequencies would have also been experimented with but due to time constraints and equipment availability the small sledge hammer was used for the Cave Rock Survey.

The results from the Cave Rock ternary diagrams (Figure 3.18, Figure 3.19) show little or no relationship with varying lithology percentages and velocity of p wave arrivals through the shot paths around the cave. When comparing the data from the mapping and laboratory aspects of the project, this lack of relationship can be associated to the varying fracture densities of the units and the influence of fractures perpendicular to energy direction of seismic waves. If unfractured lithologies were present at Cave Rock, most importantly the coherent lava, upscaling the laboratory Vp to predict the velocity in the field would suggest that the fastest shots from the survey would be those that consisted of the most coherent lava. However, scanlines show that the discontinuity density of the coherent lava is 6 – 8 times larger than the breccia and I showed Vp decreases in the laboratory by simulating fractures perpendicular to energy propagation. Vp of coherent lava in the field is slower than under laboratory conditions.

Cottage Rock is an effective field analogue for the effect of fractures influencing Vp as it consists of fractured coherent lava, which in the lab measure an average of 2872 m/s but in the field produces a p wave velocity average 2127m/s, with 75 % of the measurements recording slower than 2592 m/s (for direct rock hits only). In the lab, fractures were simulated by cutting the core with a rock saw, resulting in a relatively planar smooth surfaces whereas in the field, coherent lava includes many fractures, discontinuities and bedding surfaces are undulating and rough or undulating and smooth. These discontinuities are non-parallel to the propagation of seismic energy which consequently reduces the velocity of seismic waves, especially when fractures are rougher (Kahraman, 2002). The lab data (Figure 3.3) shows that a single fracture in the coherent lava reduces the Vp of the coherent lava to values equivalent to the unfractured tuff and breccia. Similarly, the lab results with multiple lithologies shows that the interaction between fractures and lithologies can produce non-systematic relationships between lithology and Vp (Figure 3.5). Therefore, the fractured coherent lava in the field might be expected to have similar and variable Vp as the relatively unfractured breccia and tuff and this can explain the lack of correlation of Vp and lithological proportions in the field.

Chapter 5: Conclusions

Influence of lithology and fractures on seismic velocities in the field

This thesis aimed to evaluate the influence of lithology changes and discontinuities on p wave velocities by conducting a combined field and laboratory geophysical study of volcanic rocks from Sumner Beach, New Zealand. The specific aims for the project included:

Aim 1: Evaluate the influence of lithology and fractures on p and s wave velocity in the lab

Aim 2: Develop methodology for gathering seismic p wave arrivals, geological and geotechnical data in 3D volcanic outcrops.

Aim 3: Evaluate the influence of lithology and fractures on p wave velocity on outcrop scale.

Aim 4: Establish volcanological setting and interpretation for Tuawera / Cave Rock, Sumner

The results from the lab showed that p and s wave velocity varied between individual lithology samples, decreased when fractures were introduced perpendicular to energy propagation direction and either slightly increased or stayed the same when fractures parallel to energy propagation were introduced.

In the field surveys, the array of eight 3C geophones recording energy signals sent artificially from a small sledgehammer proved effective in recording clear energy signals in all survey locations on Sumner Beach over shot lengths of 5 to 25 metres. The geophone surveys combined with field geologic and scanline fracture mapping and 3D modelling of the layers enabled shot paths through varying proportions of units and their geotechnical properties to be compared to the p wave velocities for respective shots.

On the outcrop scale there was no distinct correlation between p wave velocity for various shot orientations at Tuawera / Cave Rock when plotted against proportion of fractured coherent lava and breccia on a ternary diagram. This lack of correlation between proportions of various lithology and p wave velocity can be evaluated by comparing the laboratory experiments and field mapping observations, as fractured coherent lava has been shown in the lab to display similar p wave velocities to unfractured samples of breccia and tuff.

As a part of the field mapping and structural observations at Sumner Beach, a volcanic interpretation of the beach outcrops has been included in the thesis to tie together the study sites volcanic history. The key observation is the identification of distinct flow units separated by an unconformity, indicating a period of erosion. Structural observations lead to two interpretations; two different flow directions from separate vents; or flows from the same vent but the side of a channel vs. the bottom of a channel. As lava flows have naturally undulating surfaces with varying dips over several metres (Bailey et al., 2006; Naranjo et al., 1992) it is likely that the structures at Cave Rock have formed from a similar vent, but the rock record has captured varying sections of lava flows i.e. side of flow vs middle low point of flow.

3D geologic modelling techniques proved extremely helpful in generating accurate cross sections through shot orientations in the field to then extrapolate the proportion of each lithology present in each shot.

Upscaling of velocities and implications for Engineering Geology

Differences between breccia and coherent lava are useful to understand tunnelling, quarrying, fluid flow/hydrology and geothermal purposes. Basaltic andesite with smectite clay alteration has been shown to be a semi-ductile cap for hydrothermal systems (Hulen & Lutz, 1999). Low porosity and permeability samples of andesitic lava from Volcán de Colima typically have prevalent microfractures, whereas samples with higher porosity typically have larger, connected pores (Farquharson et al., 2015) resulting in higher permeability – important for fluid flow modelling. Accurate mapping of lava flow lithologies and relationships with structural fabric in the crust - such as active fault lines - is important when modelling for slope stability and mass movement, as emplacement and rock type of lava flows can be among key controls on large scale volcanic slumps (Okubo, 2004). Breccia, having few discontinuities, has been identified as a semi intact massive weak rock mass with properties similar to weak concrete therefore it is important to fully understand the properties of the rockmass, especially for tunnelling purposes (Karzulovic & Díaz, 1994).

This study has shown that by using a combined lab and field study of p waves in volcanic rocks, Vp can vary between lithologic samples and is influenced negatively by the presence of discontinuities perpendicular to the propagating energy direction. Discontinuity density

differences per metre of 6 – 8 times have been recorded between fractured coherent lava and volcanic breccia, which can make it difficult to predict the proportions of lithology correlating to different Vp measurements in varying shot orientations on outcrop scale geophysical surveys over 5 to 25 metres. Implications for these findings is that coherent lava with a multitude of discontinuities has the possibly to be mistaken for breccia or tuff based on solely field surveys, although in the lab the coherent lava can show Vp and Vs ranges higher that the breccia and tuff respectively.

References

Anderson, D. L., Minster, B., & Cole, D. (1974). The effect of oriented cracks on seismic velocities. *Journal of Geophysical Research, 79*(26), 4011-4015.

Anderson, D. L., & Spetzler, H. (1970). Partial melting and the low-velocity zone. *Physics of the Earth and Planetary interiors, 4*(1), 62-64.

Aps, A. S. (2020). Free template for triangular diagram in ms excel. Retrieved from http://www.phasediagram.dk/download/TriangularExcelTemplate.htm

Arts, R. J., Rasolofosaon, P. N., & Zinszner, B. E. (1996). Experimental and theoretical tools for characterizing anisotropy due to mechanical defects in rocks under varying pore and confining pressures. In *Seismic anisotropy* (pp. 384-432): Society of Exploration Geophysicists.

Badley, M. E. (1985). Practical seismic interpretation.

Bailey, J. E., Harris, A. J., Dehn, J., Calvari, S., & Rowland, S. K. (2006). The changing morphology of an open lava channel on Mt. Etna. *Bulletin of volcanology, 68*(6), 497-515.

Barton, N. (2006). *Rock quality, seismic velocity, attenuation and anisotropy*: CRC press.

Borr, M. (1982). The Interior of the Earth: its Structure, Constitution and Evolution. *Edward Arnold, London*.

Brune, J. N. (1970). Tectonic stress and the spectra of seismic shear waves from earthquakes. *Journal of Geophysical Research, 75*(26), 4997-5009.

Bruno, P. P. G., & Castiello, A. (2009). High-resolution onshore seismic imaging of complex volcanic structures: An example from Vulcano Island, Italy. *Journal of Geophysical Research: Solid Earth, 114*(B12).

Castagna, J. P., Batzle, M. L., & Eastwood, R. L. (1985). Relationships between compressional-wave and shear-wave velocities in clastic silicate rocks. *Geophysics, 50*(4), 571-581.

Chaminé, H. I., Afonso, M. J., Ramos, L., & Pinheiro, R. (2015). Scanline sampling techniques for rock engineering surveys: insights from intrinsic geologic variability and uncertainty. In *Engineering Geology for Society and Territory-Volume 6* (pp. 357-361): Springer.

Chiarabba, C., Amato, A., Boschi, E., & Barberi, F. (2000). Recent seismicity and tomographic modeling of the Mount Etna plumbing system. *Journal of Geophysical Research: Solid Earth, 105*(B5), 10923-10938.

Christchurch City Libraries. (2019). Tuawera — Cave Rock. Retrieved from https://my.christchurchcitylibraries.com/ti-kouka-whenua/tuawera/

Çobanoğlu, İ., & Çelik, S. B. (2008). Estimation of uniaxial compressive strength from point load strength, Schmidt hardness and P-wave velocity. *Bulletin of Engineering Geology and the Environment, 67*(4), 491-498.

Cotton, C. A. (1944). *Volcanoes as landscape forms*: Whitcombe & Tombs limited.

Dankbaar, J. (1985). Separation of P-and S-waves. *Geophysical Prospecting, 33*(7), 970-986.

del Potro, R., & Hürlimann, M. (2008). Geotechnical classification and characterisation of materials for stability analyses of large volcanic slopes. *Engineering Geology, 98*(1-2), 1-17.

Dinçer, I., Acar, A., Çobanoğlu, I., & Uras, Y. (2004). Correlation between Schmidt hardness, uniaxial compressive strength and Young's modulus for andesites, basalts and tuffs. *Bulletin of Engineering Geology and the Environment, 63*(2), 141-148.

Farquharson, J., Heap, M. J., Varley, N. R., Baud, P., & Reuschlé, T. (2015). Permeability and porosity relationships of edifice-forming andesites: a combined field and laboratory study. *Journal of Volcanology and Geothermal Research, 297*, 52-68.

Ferrazzini, V., Aki, K., & Chouet, B. (1991). Characteristics of seismic waves composing Hawaiian volcanic tremor and gas-piston events observed by a near-source array. *Journal of Geophysical Research: Solid Earth, 96*(B4), 6199-6209.

Fortin, J., Stanchits, S., Vinciguerra, S., & Guéguen, Y. (2011). Influence of thermal and mechanical cracks on permeability and elastic wave velocities in a basalt from Mt. Etna volcano subjected to elevated pressure. *Tectonophysics, 503*(1-2), 60-74.

Hampton, S., & Cole, J. (2009). Lyttelton Volcano, Banks Peninsula, New Zealand: primary volcanic landforms and eruptive centre identification. *Geomorphology, 104*(3-4), 284-298.

Harris, J. M. (1988). Cross-well seismic measurements in sedimentary rocks. In *SEG Technical Program Expanded Abstracts 1988* (pp. 147-150): Society of Exploration Geophysicists.

Hayles, J., Serzu, M., Tomsons, D., Everitt, R., & Lodha, G. (1994). Cross-Hole Seismic and Single-Hole Geophysical Surveys for Characterizing an Area of Moderately Fractured Granite.

Heap, M. J., & Kennedy, B. M. (2016). Exploring the scale-dependent permeability of fractured andesite. *Earth and Planetary Science Letters, 447*, 139-150.

Helbig, K. (1984). Transverse isotropy in exploration seismics. *Geophysical Journal International, 76*(1), 79-88.

Herbst, R., Kapp, I., Krummel, H., & Lück, E. (1998). Seismic sources for shallow investigations: A field comparison from Northern Germany. *Journal of Applied Geophysics, 38*(4), 301-317.

Hoek, E. (2000). Practical rock engineering.

Hornby, B. E. (2001). Upscaling: elastic anisotropy from ultrasonic laboratory measurements of borehole seismic surveys. *Advances in anisotropy: selected theory, modeling, and case studies. Soc expl geophys, open file publ, 5*, 21-46.

Hulen, J. B., & Lutz, S. J. (1999). Altered volcanic rocks as hydrologic seals on the geothermal system of Medicine Lake volcano, California. *Geothermal Resources Council Bulletin, 28*(7), 217-222.

Jolly, A., Chardot, L., Neuberg, J., Fournier, N., Scott, B., & Sherburn, S. (2012). High impact mass drops from helicopter: a new active seismic source method applied in an active volcanic setting. *Geophysical Research Letters, 39*(12).

Jolly, A., Lokmer, I., Kennedy, B., Keys, H., Proctor, J., Lyons, J., & Jolly, G. (2014). Active seismic sources as a proxy for seismic surface processes: An example from the 2012 Tongariro volcanic eruptions, New Zealand. *Journal of Volcanology and Geothermal Research, 286*, 317-330.

Jones, L. E., & Wang, H. F. (1981). Ultrasonic velocities in Cretaceous shales from the Williston basin. *Geophysics, 46*(3), 288-297.

Kahraman, S. (2001). A correlation between P-wave velocity, number of joints and Schmidt hammer rebound number. *International Journal of Rock Mechanics and Mining Sciences, 38*(5), 729-733.

Kahraman, S. (2002). The effects of fracture roughness on P-wave velocity. *Engineering Geology, 63*(3-4), 347-350.

Karzulovic, A., & Díaz, A. (1994). *Evaluación de las Propiedades Geomacánicas de la Brecha Braden en Mina El Teniente.* Paper presented at the Proc. IV Congreso Sudamericano de Mecanica de Rocas, Santiago.

Keys, W. S. (1979). Borehole geophysics in igneous and metamorphic rocks. *The Log Analyst, 20*(04).

Klemperer, S. L. (1987). Seismic noise-reduction techniques for use with vertical stacking: An empirical comparison. *Geophysics, 52*(3), 322-334.

Krohn, C. E. (1984). Geophone ground coupling. *Geophysics, 49*(6), 722-731.

Kuster, G. T., & Toksöz, M. N. (1974). Velocity and attenuation of seismic waves in two-phase media: Part I. Theoretical formulations. *Geophysics, 39*(5), 587-606.

Lee, R. L., Bradley, B. A., Pettinga, J. R., Hughes, M., & Graves, R. W. (2013). A 3D seismic velocity model for Canterbury, New Zealand for broadband ground motion simulation.

Lengliné, O., Duputel, Z., & Ferrazzini, V. (2016). Uncovering the hidden signature of a magmatic recharge at Piton de la Fournaise volcano using small earthquakes. *Geophysical Research Letters, 43*(9), 4255-4262.

Lesage, P., Heap, M. J., & Kushnir, A. (2018). A generic model for the shallow velocity structure of volcanoes. *Journal of Volcanology and Geothermal Research, 356*, 114-126.

Li, D., Zhang, L., & Tang, W. (2005). Reliability evaluation of cross-hole sonic logging for bored pile integrity. *Journal of geotechnical and geoenvironmental engineering, 131*(9), 1130-1138.

Liberty, L. M., Schmitt, D. R., & Shervais, J. W. (2015). Seismic imaging through the volcanic rocks of the Snake River Plain: insights from Project Hotspot. *Geophysical Prospecting, 63*(4), 919-936.

Manghnani, M., & Woollard, G. P. (1965). Ultrasonic Velocities and Related Elastic Properties of Hawaiian Basaltic Rocks'. *RATIO, 10*, 10-11.

Mavko, G. (2005). Conceptual overview of rock and fluid factors that impact seismic velocity and impedance. *Retrieved, 11*(11), 2012.

McCann, D., Grainger, P., & McCann, C. (1975). Inter-borehole acoustic measurements and their use in engineering geology. *Geophysical Prospecting, 23*(1), 50-69.

McIntyre, D., Welday, E., & Baird, A. (1965). Geologic application of the air pycnometer: a study of the precision of measurement. *Geological Society of America Bulletin, 76*(9), 1055-1060.

Miller, R., Pullan, S., Waldner, J., & Haeni, F. (1986). Field comparison of shallow seismic sources. *Geophysics, 51*(11), 2067-2092.

Moon, V., Bradshaw, J., Smith, R., & de Lange, W. (2005). Geotechnical characterisation of stratocone crater wall sequences, White Island Volcano, New Zealand. *Engineering Geology, 81*(2), 146-178.

Moore, J. R., Geimer, P. R., Finnegan, R., & Thorne, M. S. (2018). Use of Seismic Resonance Measurements to Determine the Elastic Modulus of Freestanding Rock Masses. *Rock Mechanics and Rock Engineering, 51*(12), 3937-3944.

Mordensky, S., Villeneuve, M., Farquharson, J., Kennedy, B., Heap, M., & Gravley, D. (2018). Rock mass properties and edifice strength data from Pinnacle Ridge, Mt. Ruapehu, New Zealand. *Journal of Volcanology and Geothermal Research, 367*, 46-62.

Mordensky, S., Villeneuve, M., Kennedy, B., Heap, M., Gravley, D., Farquharson, J., & Reuschlé, T. (2018). Physical and mechanical property relationships of a shallow intrusion and volcanic host rock, Pinnacle Ridge, Mt. Ruapehu, New Zealand. *Journal of Volcanology and Geothermal Research, 359*, 1-20.

Nara, Y., Meredith, P. G., Yoneda, T., & Kaneko, K. (2011). Influence of macro-fractures and micro-fractures on permeability and elastic wave velocities in basalt at elevated pressure. *Tectonophysics, 503*(1-2), 52-59.

Naranjo, J., Sparks, R., Stasiuk, M., Moreno, H., & Ablay, G. (1992). Morphological, structural and textural variations in the 1988–1990 andesite lava of Lonquimay Volcano, Chile. *Geological Magazine, 129*(6), 657-678.

Nur, A. (1971). Effects of stress on velocity anisotropy in rocks with cracks. *Journal of Geophysical Research, 76*(8), 2022-2034.

Okubo, C. H. (2004). Rock mass strength and slope stability of the Hilina slump, Kīlauea volcano, Hawai'i. *Journal of Volcanology and Geothermal Research, 138*(1-2), 43-76.

Ring, U., & Hampton, S. (2012). Faulting in Banks Peninsula: tectonic setting and structural controls for late Miocene intraplate volcanism, New Zealand. *Journal of the Geological Society, 169*(6), 773-785.

Saubin, E., Kennedy, B., Tuffen, H., Villeneuve, M., Davidson, J., & Burchardt, S. (2019). Comparative field study of shallow rhyolite intrusions in Iceland: emplacement mechanisms and impact on country rocks. *Journal of Volcanology and Geothermal Research, 388*, 106691.

Savage, M. (1999). Seismic anisotropy and mantle deformation: what have we learned from shear wave splitting? *Reviews of Geophysics, 37*(1), 65-106.

Schubnel, A., & Guéguen, Y. (2003). Dispersion and anisotropy of elastic waves in cracked rocks. *Journal of Geophysical Research: Solid Earth, 108*(B2).

Sewell, R. (1988). Late Miocene volcanic stratigraphy of central Banks Peninsula, Canterbury, New Zealand. *New Zealand journal of geology and geophysics, 31*(1), 41-64.

Silver, P. G. (1996). Seismic anisotropy beneath the continents: Probing the depths of geology. *Annual review of earth and planetary sciences, 24*(1), 385-432.

Stein, S., & Wysession, M. (2009). *An introduction to seismology, earthquakes, and earth structure*: John Wiley & Sons.

Toksöz, M., Johnston, D. H., & Timur, A. (1979). Attenuation of seismic waves in dry and saturated rocks: I. Laboratory measurements. *Geophysics, 44*(4), 681-690.

Toksöz, M. N., Cheng, C. H., & Timur, A. (1976). Velocities of seismic waves in porous rocks. *Geophysics, 41*(4), 621-645.

Tolstoy, M., Cowen, J., Baker, E., Fornari, D., Rubin, K., Shank, T., . . . Holmes, R. (2006). A sea-floor spreading event captured by seismometers. *Science, 314*(5807), 1920-1922.

Tonn, R. (1989). Comparison of seven methods for the computation of Q. *Physics of the Earth and Planetary interiors, 55*(3-4), 259-268.

Ulusay, R. (2014). *The ISRM suggested methods for rock characterization, testing and monitoring: 2007-2014*: Springer.

Urosevic, M., Evans, B., Poole, G., Seman, M., & Basso, L. (1995). Using seismic data and cross-hole analysis to image fractures. *Exploration Geophysics, 26*(3), 340-346.

Vanorio, T., Prasad, M., Patella, D., & Nur, A. (2002). Ultrasonic velocity measurements in volcanic rocks: Correlation with microtexture. *Geophysical Journal International, 149*(1), 22-36.

Vilhelm, J., Rudajev, V., Živor, R., Lokajíček, T., & Pros, Z. (2010). Influence of crack distribution of rocks on P-wave velocity anisotropy–a laboratory and field scale study. *Geophysical Prospecting, 58*(6), 1099-1110.

Vinciguerra, S., Del Gaudio, P., Mariucci, M., Marra, F., Meredith, P., Montone, P., . . . Scarlato, P. (2009). Physical properties of tuffs from a scientific borehole at Alban hills volcanic district (central Italy). *Tectonophysics, 471*(1-2), 161-169.

Wang, H., Pan, J., Wang, S., & Zhu, H. (2015). Relationship between macro-fracture density, P-wave velocity, and permeability of coal. *Journal of Applied Geophysics, 117*, 111-117.

Wang, Z. (2001). Fundamentals of seismic rock physics. *Geophysics, 66*(2), 398-412.

Westoby, M. J., Brasington, J., Glasser, N. F., Hambrey, M. J., & Reynolds, J. M. (2012). 'Structure-from-Motion'photogrammetry: A low-cost, effective tool for geoscience applications. *Geomorphology, 179*, 300-314.

Wyering, L., Villeneuve, M., Wallis, I., Siratovich, P., Kennedy, B., Gravley, D., & Cant, J. (2014). Mechanical and physical properties of hydrothermally altered rocks, Taupo Volcanic Zone, New Zealand. *Journal of Volcanology and Geothermal Research, 288*, 76-93.

Zamora, M., Sartoris, G., & Chelini, W. (1994). Laboratory measurements of ultrasonic wave velocities in rocks from the Campi Flegrei volcanic system and their relation to other field data. *Journal of Geophysical Research: Solid Earth, 99*(B7), 13553-13561.

Zhao, D., Hasegawa, A., & Horiuchi, S. (1992). Tomographic imaging of P and S wave velocity structure beneath northeastern Japan. *Journal of Geophysical Research: Solid Earth, 97*(B13), 19909-19928.

Online Appendices

Online Appendix 1

Tables of lithology percentages in different shot types at Cave Rock and corresponding p wave velocities for each shot. https://ucliveac-my.sharepoint.com/:x:/g/personal/cmc250_uclive_ac_nz/EQswxgcUZHxLs9023WOx3r4BBIauL6Dke-bIBZqFXgbfww?e=rhPM6r

Online Appendix 2

Folder of .dat files recording all seismic wave arrival tests from Sumner Beach geophysical survey. https://ucliveac-my.sharepoint.com/:f:/g/personal/cmc250_uclive_ac_nz/EnPnPZH0CfxJrRE8kzuPLk4B5wFPu6WeG6PvqgkYe0QHEw?e=3mDSyN

Online Appendix 3

Table of corresponding .dat files and shot type information from Sumner Beach geophysical survey. https://ucliveac-my.sharepoint.com/:x:/g/personal/cmc250_uclive_ac_nz/ES2FCv9r3u9BiAlKvcGN-sYByM3UjfSvclTZrGddl6Nq4Q?e=2w6Zjj

Online Appendix 4

YouTube video of Leapfrog Geothermal model methods and slices through various angles of Cave Rock, Sumner. https://www.youtube.com/watch?v=LFVqDlcOlYA&t=41s